UNIVERSITY OF MINNESOTA
ST. ANTHONY FALLS HYDRAULIC LABORATORY

Project Report No. 240

POLLUTION OF GRAVEL SPAWNING GROUNDS DUE TO FINE SEDIMENT

by

Panayiotis Diplas and Gary Parker

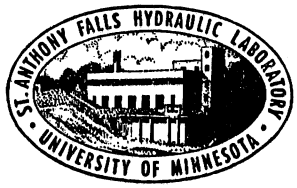

Prepared for:

OFFICE OF EXPLORATORY RESEARCH
OFFICE OF RESEARCH AND DEVELOPMENT
U. S. ENVIRONMENTAL PROTECTION AGENCY
WASHINGTON, D. C. 20406

EPA/R-808683-01-1

June, 1985
Minneapolis, Minnesota

ERRATA

Project Report No. 240

Pollution of Gravel Spawning Grounds Due to Fine Sediment

Page	Line	Reads	Should Read
30	15 bt	D_{90} represents the diameter that retains 10%	D_{80} represents the diameter that retains 20%
36	5 bt	geometric	arithmetic
83	1	$m'_1 = m'_2 = \ldots = m'$	$m_1 = m_2 = \ldots = m$
	5	$m_1 = m_2 = \ldots = 13.71$	$m'_1 = m'_2 = \ldots = 13.71$
97	7 bt	fines	fines (Sowers and Sowers, 1970)
119	8 bt	watersediment	water sediment
122	eq.(45)	log	$\log_{10}$
123	Fig. 65	LOG	LOG_{10}
108	Fig. 53	In the Fines Feed Rates instead of 2.0 gr/min, 4.3 gr/min, 2.7 gr/min	Should be: 2.0 gr/sec, 4.3 gr/sec, 2.7 gr/sec.

St. Anthony Falls Hydraulic Laboratory
University of Minnesota
Mississippi River at Third Avenue S.E.
Minneapolis, Minnesota 55414

Project Report No. 240

POLLUTION OF GRAVEL SPAWNING GROUNDS DUE TO FINE SEDIMENT

by

Panayiotis Diplas and Gary Parker

Prepared for:

OFFICE OF EXPLORATORY RESEARCH
OFFICE OF RESEARCH AND DEVELOPMENT
U. S. ENVIRONMENTAL PROTECTION AGENCY
WASHINGTON, D. C. 20406

Project Officer

Dr. Louis G. Swaby
Office of Exploratory Research
Office of Research and Development
Washington, D. C. 20406

EPA/R-808683-01-1

June, 1985

ABSTRACT

Laboratory experiments which model poorly sorted gravel-bed streams were conducted to examine certain phenomena associated with these streams. The existence and role of the pavement, sediment transport, the accumulation and retention of fines in the bed, and the effect of the fines accumulation in the stream behavior are the phenomena included in this study.

Two flumes were used. The first one operated as a recirculating system. It was 16.75 m long and 0.3 m wide with transparent walls. The narrow width of this channel suppressed any tendencies for the formation of bedforms. The second one operated as a feed system. It was 12 m long and 0.53 m wide with opaque walls. This flume allowed for the development of alternate bars. In total, seven series of experiments were performed. On the average, six experiments were conducted for each series. The first experiment of each series was conducted with a given mixture of bed material in the absence of fines. This mixture constitutes a scaled-down version of a rather typical bed material observed in natural gravel-bed streams. Fine material was introduced into the flume during the subsequent experiments. The amount of fines introduced was progressively increased, while the channel bed gradually changed from gravel to sand. At the end of each series the bed became completely covered with fines.

It was found that the pavement is a mobile bed phenomenon, which acts as a regulator that renders all available grain sizes to be of nearly equal mobility. This is accomplished by overrepresenting the percentage of large grains exposed to the flow. Flow visualization provided evidence of a correlation between grain motion and the turbulent bursting phenomena.

Field data, obtained from the literature, are used to study the bedload transport in paved gravel-bed streams. The stream examined in this case is Oak Creek, a small gravel-bed stream draining the east slope of the Coast Range, Oregon. The bed material of this stream is divided into ten ranges of grain size. The concept of a similarity transformation is used as a means of collapsing the individual bedload relations, developed empirically for each of the size ranges, into a single curve. The similarity parameter used here renders the bedload relations of nine out of ten size ranges almost perfectly similar. This parameter incorporates the variation in mobility as well as the hiding effects due to the difference in the size of the grains. A bedload relation is then developed which accounts for the effects of sediment grading. The same approach is used also for the data obtained from the present study, supporting the conclusions obtained from the analysis of the Oak Creek data.

The mechanics of fines infiltration into the bed is also described. While the fines accumulated into the bed did not affect the water surface slope or the channel depth, the amount of fines in the subpavement and pavement correlated well with the bedload transport rate. A model describing this process is in order. Initially, the fines collect in the immediate substrate, reducing the mobility of the grains in the pavement

and consequently reducing the bedload transport rate. This trend continues until the top of the subpavement becomes saturated with fines, and a significant quantity of fines appears in the pavement. At this point the bedload increases. This is due to the higher mobility of coarse particles moving over a surface which has been rendered smooth by fines filling in crevices between roughness elements. In this state the number of moving grains has been significantly reduced, but the rest periods between motions are much shorter. As the original gravel bed becomes buried below the sand bed, the bedload transport rate, as a result of the reduced availability of grains from the original bed, once again decreases.

As long as the subpavement is not saturated with fines and there are grains in the flow, these grains will eventually deposit into the bed. Whenever the fines appear in the pavement, then there is a semilogarithmic relationship between the amount of fines in the pavement and the mean flow concentration of fines.

The bedforms developed in the wider flume closely resembled those found in natural gravel bed streams. Details such as the variation of particle size along a bar were identical in both cases. Fines were deposited first and removed last from the downstream side of the bar and upstream side of the pool. The two flumes behaved similarly with regard to the amounts of fines in the substrate and pavement under similar flow conditions. It was clearly demonstrated that the most important factor affecting the depth of fines infiltration within the channel bed and the amount of fines accumulated in the bed is the relative size of the fines and the bed material.

Finally, the ability of the channel to purge itself of fines was tested. When there is no bed motion, the channel is capable of completely removing the fines from the pavement but not from the subpavement. When the bed is active, both pavement and subpavement can be cleaned. When the coarser tail of the fines size distribution curve overlaps, or is very close to the finer tail of the original bed material size distribution curve, as is the case of natural streams, then the fines do not infiltrate into the bed deeper than the subpavement. Most natural streams, therefore, are capable of purging themselves of fines when the bed is in motion, i.e. during floods. The duration and fines concentration of the flood, however, must be considered.

CONTENTS

FIGURES

Number

Number

Number

LIST OF TABLES

LIST OF SYMBOLS

ENGLISH SYMBOLS

a,b,c	-- the three axes that characterize the dimensions of a grain
B	-- channel width
C	-- a constant in eq. (1)
C	-- vertically averaged volumetric concentration of the flow in Section 8
c	-- local concentration averaged over turbulence in Section 8
c'	-- fluctuating local concentration in Section 8
$\overline{c}_i$	-- geometric mean value of the c-axes of the particles in the ith size range.
C_f	-- percent of fines by weight in the pavement
Dg	-- geometric mean diameter of the subpavement
$D_{\ell g}$	-- geometric mean diameter of the bedload
D_{50}	-- subpavement median grain size
D_{p50}	-- pavement median grain size
D_{b50}	-- bottom layer median grain size
$D_{\ell 50}$	-- bedload median grain size
D_{TV50}	-- median size of the volumetric top layer sample
D_{TA50}	-- median size of the areal top layer sample
D_{SV50}	-- median size of the volumetric substrate sample
D_{SA50}	-- median size of the aerial substrate sample
D_{90}	-- represents the diameter of the sieve that retains 10% of the material sieved by weight
D_i	-- representative diameter for the ith size range
$D_{\ell i}$	-- grain size representing the ith size of the bedload
$\overline{D}_i$	-- geometric mean size of the ith size fraction

$\overline{D}_{imin}$ -- geometric mean size of the smallest size fraction i

$\overline{D}_{imax}$ -- geometric mean size of the largest size fraction i

d -- flow depth

d' -- effective flow depth found by using Vanoni and Brooks method

E -- entrainment rate

E_s -- dimensionless entrainment rate

$E[\overline{D}_i]$ -- expected value of $\overline{D}_i$ based on the size distribution obtained from a volumetric sample

f_i -- fraction of the subpavment in the ith grain size range

$f_{\ell i}$ -- fraction of the bedload in the ith grain size range

$F = V/\sqrt{gd}$ -- Froude number

$p(A)_i$ -- percentage of the size fraction i obtained from an areal sample

$p(A_p)_i$ -- percentage of the size fraction i obtained from an areal sample whose particle placement resembles that of a pavement.

$p(V)_i$ -- percentage of the size fraction i obtained from a volumetric sample

Q -- water discharge

Q_s[gr/min] -- total bedload

Q_B -- volumetric total bedload

$q_B = \sum_i q_{Bi}$ -- volumetric total bedload per unit width

q_{Bi} -- volumetric bedload per unit width in the ith grain size range

$q^*_b = q_B/(\sqrt{Rg\ D_s}\ D_s)$ -- Einstein bedload parameter

$q^*_{Bi} = q_{Bi}/(\sqrt{Rg\ D_i}\ D_i)$ -- Einstein bedload parameter for the ith grain size range

$R = (\rho_s/\rho - 1)$ -- submerged specific gravity sediment

$Rp = \rho u_* D_g/\mu$ -- particle Reynolds number

r -- correlation coefficient

$(r_{ij})_s = \frac{q_{Bi}}{f_i}\left(\frac{q_{Bj}}{f_j}\right)^{-1}$ -- relative mobility of the bed material with respect to the subpavement

S -- water surface slope

U_∞ -- free stream velocity

u -- local flow velocity in x-direction averaged over turbulence

$u_* = \sqrt{\tau_o/\rho}$ -- shear velocity

v_s -- fall velocity of suspended material

w' -- fluctuating velocity component in the z-direction

$W_i^* = \frac{R\, q_{Bi}}{f_i\sqrt{g}(dS)^{1.5}} = \frac{q_{Bi}^*}{\tau_i^{*1.5}}$ -- dimensionless bedload in ith grain size range

W^*_r -- a reference value of the dimensionless bedload parameter W^*_i

x -- downstream direction along the channel

z -- direction upward normal to the channel bed

GREEK SYMBOLS

κ -- Von Karman's constant

λ -- alternate bar wavelength

μ, ν -- constants in eq. (5)

μ -- fluid viscosity

ρ -- fluid density

ρ_s -- density of the bed material

σ_g -- geometric standard deviation

$\sigma_{\ell g}$ -- geometric standard deviation of bedload

τ_o -- bottom shear stress

$\tau^*_i = \tau_o/(\rho\ Rg\ D_i)$ -- Shields stress for ith grain size range

$\tau^*_{50} = \tau_o/(\rho\ Rg\ D_{50})$ -- Shields stress for median diamter of subpavement

τ^*_{ri} -- reference value of τ^*_i at which $W^*_i = W^*_r$

τ^*_{r50} -- reference value of τ^*_{50}

$\phi_i = \tau^*/\tau^*_{ri}$

$\phi_{50} = \tau^*_{50}/\tau^*_{r50}$

ACKNOWLEDGEMENTS

This research was supported by the Environmental Protection Agency (contract number EPA/R-808683-01-1).

1. INTRODUCTION

As an ecological phenomenon, the process of fines input to and accumulation in gravel-bed streams falls in the category of non-point source pollution, and is considered to be one of the most significant pollution problems in this category. Non-point sources of pollution have been identified as a serious obstacle in attaining the 1983 goal of water quality adequate for fish and recreation, as specified in the Clean Water Act passed by Congress in 1972.

Salmon and related species of fish use the structure of natural gravel-bed rivers for the purpose of spawning. Natural gravel-bed rivers are typically characterized by a pool-and-riffle sequence which provides considerable variation in depth as a function of location at flows typically appropriate for spawning. Fish can explore the pool-and-riffle structure of a reach to locate areas suitable for spawning, often called "spawning riffles." There they excavate a pit, deposit the eggs, and in some species cover them with gravel relatively free of the fine sediment. The eggs are buried below the pavement, where they are protected against bedload motion and scour during floods. The eggs incubate in the gravel for a period of one to two months. After hatching, the alevins spend some 30 to 60 days in the intergravel environment before they emerge as fry. Spawning usually occurs from fall to spring. The juvenile fish also spend some time, up to two years, in the freshwater stream before migrating to the ocean.

Of all the factors that could adversely affect spawning success, fines accumulation in the gravel-bed streams is one of the most important. There is a voluminous body of research indicating the deleterious effects of fines on spawning activities, fish habitat, and the benthic population upon which fish feed (Shea and Mathers, 1978; Phillips, 1965; Koski, 1966).

The intergravel stage of life of the fish represent a critical phase of their life cycle. During this period they may be most susceptible to damages from high levels of fine sediments. Increased amounts of fines may injure the ova by adhering to or abrading the chorion of the incubating salmon eggs (Gibbons and Salo, 1973). In addition, intergravel flows must be sufficient to remove the toxic metabolic wastes produced by the eggs (Iwamoto et al., 1978). High levels of fines reduce the permeability of the gravel bed resulting in lower intergravel flows, as well as reduced interchange of water between the main stream flow and the intergravel flow (Vaux, 1968). Alevins and incubating salmon ova require certain levels of dissolved oxygen in the intergravel water for adequate survival and growth (Phillips and Campbell, 1961). The primary source of intergravel dissolved oxygen is the surface water of the stream (Sheridan, 1962). The eggs and alevins incubated at lower dissolved oxygen levels generally have lower survival rates, emerge later, and are usually less able to compete with other fish raised in higher levels of dissolved oxygen (Phillips, 1965). Finally, excessive amounts of fine sediments entrap the fry within the gravel as they try to escape.

In a field study conducted by Koski, it was found that the percentage of fines in a gravel-bed stream was the only variable to be significantly correlated with spawning success. Many methods have been reported attempting to quantify the effect of fines on the fry survival. An oft-quoted rule-of-thumb is that when substrate fines content exceeds 20 to 25 percent, fry survival is considerably reduced. However, this parameter seems to be site specific, such that spawning may occur successfully at a variety of ambient fines content, but an increase above the ambient values causes deleterious effects. Shirazi and Seim (1981) have attempted to remove some of the subjectiveness of this procedure by using substrate geometric mean diameter, D_g, instead of fines content as a parameter for gauging spawning success (Fig. 1). Beschta (discussion of Shirazi and Seims, 1982) argued that while D_g is strongly correlated with embryo survival, it is not an indicator sensitive to changes in spawning gravel composition as a result of land use activities. Hence its appropriateness in monitoring changes in the fish habitat quality due to human activities is rather questionable. He recommended the use of the freedle index, the quotient of the geometric mean and geometric standard deviation, in place of the geometric mean. A similar approach was introduced earlier by Lotspeich and Everest (1981).

High levels of fine sediment in stream beds threaten also the survival of the emergent fry. Juvenile fish often use the gravel bed interstices to escape from predators. Increased amounts of fines reduce the cover for escape (Phillips, 1971). Similarly they reduce the food resources for fish by decreasing the population and diversity of benthic community (Gibbons and Salo, 1973).

Natural as well as man-caused erosion processes introduce fine sediment into streams. In a mountainous terrain, the primary processes that deliver sediment to the channel are surface erosion, mass soil movements, and stream bank erosion (Anderson, 1971). Adams (1980), concluded from his field study that the amount of fine sediment in a stream bed seems to be determined mainly by the intrinsic characteristics of the watershed such as area, slope and relief.

The reason for the paramount importance of fines is that, of all factors deleterious to spawning likely to be exacerbated by the activities of man, it is one of the most prevalent. Forestry activities such as clear-cutting, and in particular road-building, can lead to the input of fine material into streams at rates that exceed the natural input by one or more orders of magnitude (Brown, 1974). Megahan and Kid (1972), reported that a dense network of roads associated with jammer logging increased the rate of erosion in the Idaho Batholith to 750 times that of the undisturbed rate, whereas logging caused only a sixty percent increase. The above-mentioned activities can be sources of increased rates of erosion for a number of years after the disturbance took place (Megahan and Kid, 1972). Swanston and Swanson (1976) found that roads in the H. J. Andrews Experimental Forest continued to be active sites for debris avalanche erosion 16 years after construction, while the duration of the clear-cutting impact was 8 years. The proper use of buffer strips along the banks of the river (Erman and Mahoney, 1983), and more importantly the careful design of the forest activities can significantly reduce the additional load of fines introduced into the streams. The above holds true for agricultural activities as well, which can also lead to high inputs of fine material.

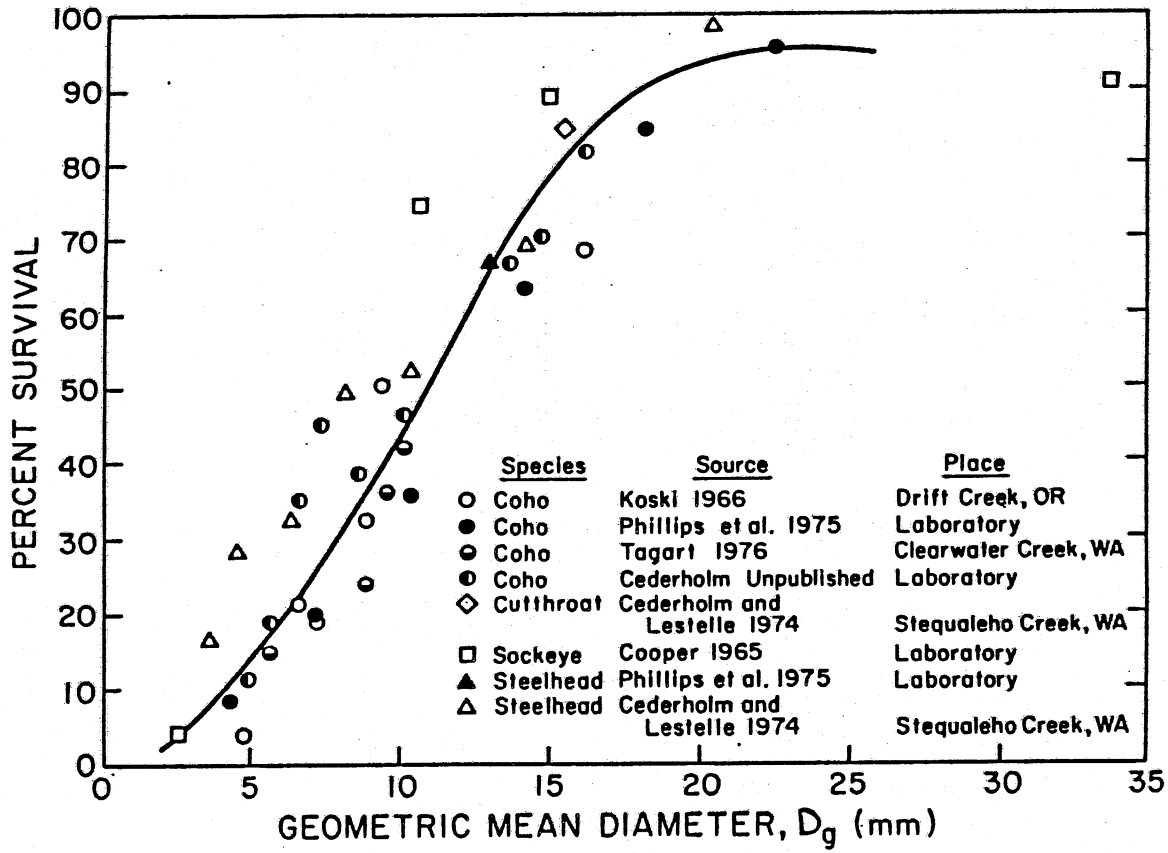

Figure 1. Relationship between percent embryo survival and substrate composition expressed in geometric mean diameter. (After Shirazi and Seim, 1981.)

It is therefore evident that stream sedimendation is a serious source of stream pollution. The percentage of fines in the stream bed has been suggested as a criterion for the stream quality (Bjorn, et al., 1977; Iwamoto et al., 1978). Alaska has adopted such a criterion (Alaska Department of Enviromental Conservation, 1979). In addition to this, high fines concentration in stream flows may result in different stream behavior, as has been found in laboratory experiments (Dhamotharan et.al., 1980).

In order to keep the pollution of a stream below dangerous levels, management criteria for the land use in the corresponding watershed should be developed. This requires the knowledge of three general relations, which are as follows:

1. A relation predicting the quantity and type of fines flowing into streams as a function of specific watershed activity, basin geological and vegetal structure, hydrological regime, etc.

2. A relation predicting the characteristics of retention of fines in the substrate as a function of fines input and other factors. For example, suppose fines delivery to a given stream is increased six-fold for a period of five years. During this period, what is the fines content in the bed? What is the substrate geometric mean diameter? To what extend, if it is possible at all, can the stream purge itself from the additional fines?

3. A relation indicating the effect of fines in the substrate on spawning success.

The present work is mainly devoted to the second relation, the mechanics of fines retention in the gravel bed streams.

2. RECOMMENDATIONS AND CONCLUSIONS

Laboratory experiments which model gravel-bed streams with poorly-sorted material were conducted in two parts: first, results were obtained from experiments during which no fine material was externally fed into the flume; and second, fine material was introduced into the channel and the experiments were repeated.

From the experiments performed in the absence of fines, the existence of a surface layer at the channel bed (pavement) significantly coarser than the subsurface material under mobile bed conditions, was demonstrated. The role of the pavement as a regulator that renders all available grain sizes of nearly equal mobility, by over-representing the percentage of large grains exposed to the flow, was verified. Flow visualization allowed for the observation that bedload motion correlates well with bursting phenomena that take place near the bed. From the experiments in the tilting flume, it was found that many bed features characteristic of natural gravel-bed streams can be simulated in the laboratory. Such features include the alternate bar bed configuration, and the grain size segregation observed along bars. The flow conditions at the head of the bar resemble those of a riffle. Thus, the observations made at the bar head can be used to predict the developments that would take place in a riffle under similar flow conditions.

Field data obtained from Oak Creek are used to study the bedload transport in poorly-sorted gravel-bed streams. A similarity approach is used to delineate a functional relationship obtained for the bedload transport rate. This functional relation is based on dimensional analysis. The bed material of Oak Creek is divided into ten grain size ranges. The concept of the similarity transformation is used as a means of collapsing the individual bedload relations, developed empirically for each of the size ranges, into a single curve. The similarity parameter used here renders the bedload relations of nine out of ten size ranges almost perfectly similar. This parameter incorporates the variation in mobility as well as the hiding effects due to the difference in the size of the grains. A bedload relation which allows for sediment grading effects is then developed. Statistical characteristics of the grains that participate in the bedload can be predicted reasonably well from the present analysis. The data obtained from the experiments conducted during this study are analyzed in the same manner as the Oak Creek data were. The latter results, while mostly qualitative in nature, support the conclusions obtained from the analysis based on the Oak Creek data.

From the experiments with fines, it was found that the flow did not interact with them for the mean flow concentrations encountered during the present study; the maximum mean flow concentration did not exceed 3,000 mgL^{-1}. On the other hand the bedload transport rate varied as a result of the fines that accumulated in the channel bed. The bedload variation as a result of the addition of fines correlates well with the amounts of fines in the subpavement and pavement.

A dimensional analysis, and results from other studies where the bed material was the same as the suspended material, are used to define the flow parameters that would possibly affect the amount of fines accumulated in the channel bed. From the present experiments it was found that the fines deposited below the surface bed layer do not interact with the flow. On the other hand, the percentage of fines by weight in the pavement correlates well with the mean flow concentration, given that the rest of the flow parameters do not vary significantly. This indicates that the amount of fines in the pavement is not very sensitive to small variations of the flow parameters. The correlation between the percentage of fines in the pavement and the mean flow concentration is semilogarithmic in nature.

The depth of infiltration depends predominantly upon the size of the infiltrating fines relative to the size of the grains composing the coarse bed matrix. For the matrix layers close to the surface of the bed framework flow parameters such as bed Shields stress and groundwater flow also affect the fines infiltration process into the bed. In nature, the coarser grains of the fines introduced into a stream are usually of a size comparable to the finer grains of the framework material. This condition encourages clogging of the framework pores within the subpavement layer, or the layer below it, and a seal is created that restricts the fines from infiltrating deeper into the bed. As a result, the fines fill the pore space from this seal toward the surface of the gravel bed.

When the channel bed was immobile, the flowing water could remove the fines from the pavement. Bed motion is required for the bed to be purged from the fines deeper than the pavement. Under mobile bed conditions, the fines could be removed up to a depth of 3.5 D_{90} from the surface of the bed. Only grains that can be suspended by the flow can be removed from the bed.

From the tilting flume experiments it was observed that fines first deposit in the pool and the bar tail, and later in the bar head. The cleaning process of the bed takes place in the reverse order. The fines are first removed from the bed at the bar head and later from the pool and bar tail.

3. OVERVIEW OF PREVIOUS RESEARCH

As early as 1923, observations on the effects of fines on the survival and emergence of salmonid fry have been reported (Harrison, 1923). Since then many studies have been devoted to the effects of fines content in the substrate of gravel-bed streams on spawning success (Iwamoto et al., 1978). On the other hand, the available body of research on the mechanisms of erosion and deposition of fines in gravel matrices under carefully monitored conditions is not large. A number of field studies are listed in a literature review undertaken by Iwamoto, Salo and Madej. Unfortunately most of them are lacking the field instrumentation necessary for making quantitative conclusions concerning the relation between input and retention.

Various facets of the mechanics of fines retention in gravel-bed streams have been examined in field studies performed with adequate instrumentation by Klingeman and Milhous (1970) and Milhous (1973) on Oak Creek, Lisle (1980) on Jacoby Creek, Adams (1980) and Adams and Beschta (1980) on five small streams, and by Frostick, Lukas and Reid (1984) on Turkey Brook tributary.

Oak Creek, a typical gravel stream, is located in the McDonald State Forest just west of Corvallis, Oregon. Extensive research has been carried out on this stream since 1969 by Klingeman and Milhous (1970) and Milhous (1973). Milhous' (1973) primary objective was to study the sediment transport in a gravel-bottomed stream. The existence and role of a single layer of coarser particles located at the surface of the bed material, characteristic of gravel-bed streams, was another aspect of his work. He also examined the role of fines in the bed.

Milhous verified the existence of a coarser surface layer, called pavement. The median size of the pavement was equal to 63 mm, and that of the material below the pavement, called subpavement, was 20 mm. The top layer appeared to consist of a well-sorted mixture of stones, while the material below the pavement layer was usually poorly sorted. He concluded that the pavement layer is the most important factor in limiting the availability of stream bed sediment and in controlling the relationship between stream flow and bedload discharge. At low flows the immobile pavement layer may have available pore space, allowing for the capacity to remove fines from suspension. At higher stages, when the pavement is set in motion, fines can be supplied from the bed, at rates determined by the pavement. Thus the pavement acts as a source and a sink of the suspended load depending on the flow rate. Fines tend to deposit in the interface between the bottom of the pavement and the top of the substrate, called the "silt reservoir," and from where they become available for suspension at high flow rates. The bedload measurements conducted during this study are considered to be the best available in the literature for gravel-bed streams. These measurements are utilized here, in a later chapter, to examine some characteristics of bedload transport in gravel-bed streams.

The sand (< 2 mm) fraction in the Oak Creek substrate takes a value near 12 percent. This value has been maintained over more than ten years,

suggesting that it is in some sense in balance with the stream and watershed on a long-term basis.

Jacoby Creek is located along the north coast of California and is used by anadromous salmonids for spawning. Lisle (1980) buried a number of cans, 17 cm in diameter and 22 cm deep, filled with well-sorted subrounded gravel, approximately 15 mm in diameter, below the pavement, in areas likely to be used by the fish for spawning. He measured the amounts of fines deposited into the cans, as well as the depth of their infiltration. The cans were placed along lines perpendicular to the flow in five spawning areas. They were recovered and replaced after each one of six consecutive flow events. He found that silts and very fine sands were concentrated on the bottoms of the cans, while sand and granules were caught in interstices near the top forming a seal. This seal penetrated deeper in areas of higher energy. The result of this seal is to limit further infiltration of fines. The suspended sediment comprised the bulk of the total sediment transport, but it constituted only one-fifth of the infiltrated material found in the cans. This happens because the finer particles of the bedload, being in contact with the bed, have better access to the pores of the pavement. He reported that the rate of infiltration of fines increased with total sediment transport, but the total amount of fines contained in the cans was reduced. This is probably due to the larger amount of grains in the sand range moving as bedload. These are the particles responsible for the seal formation, which might have been created in the early stages of bedload transport due to higher availability of these grains. Finally, Lisle found that the infiltration rates varied as much as three-fold along a line of cans placed perpendicular to the flow. This variation of fines infiltration across the stream was higher than the one taking place along the stream. The cross-channel variation of sediment transport was considered to be the major cause of this phenomenon.

The temporal and spatial variability of stream gravel-bed composition was monitored by Adams (1980) in five streams of the Oregon Coast Range. The objective of his work was to develop a better understanding of the parameters influencing this variability. Thirteen riffle areas were chosen as sampling plots in these five streams. Each sample was 25 cm deep and the percentage of fines was evaluated for the whole sample. He found that the percent fines within the stream bed varied between streams, between riffle areas in the same stream, and within the same riffle. He attributed this variation to differences in the size distribution of the gravel substrate and fines, the supply of fines available for intrusion into the bed, and the hydraulic condition of flow. For a single stream the amount of fine sediment in the bed was correlated to the stream sinuosity and bankfull stage. Sinuosity is the ratio of the length along the center line of the stream to the length along the valley. In a study conducted by Zimmer and Bachmann (1978) in a group of natural and channelized tributaries of the upper Des Moines River, it was concluded that channel sinuosity was significantly correlated with the variance of current velocity and depth between cross sections. This probably provides an explanation for the importance of channel sinuosity on the spatial variation of the amount of fines in a gravel-bed stream. The change in flow conditions across a single stream riffle is believed to be responsible for the variation in bed composition within the riffle. The variation of the sediment transport rate across the riffle and the variation of the composition

of the substrate is expected to contribute to the same phenomenon. It is also mentioned that the variation across the channel is typically more pronounced than it is along the channel.

Flushing of fines takes place most effectively during high flows, and is the main reason for the temporal variability of the fines in the substrate. Adams (1980) emphasized that the bed must move for fines to be flushed from the gravel. He also mentioned that flushing is a random event that occurs in localized areas of the stream. During the same study, Adams (1980) extracted a total of fifty-nine bed samples from twenty-one coast range streams in order to examine the fines stratification within the gravel bed. The depth of each sample was 40 cm, and the mean percent fines was determined for three depth ranges of 0 to 10 cm, 10 to 25 cm, and 25 to 40 cm. The corresponding mean values for all the samples of the percentage of fines for each range were 17.5%, 22.3% and 22.2%. Unfortunately the size distribution of the pavement and substrate material are not given.

Frostick, Lukas, and Reid (1984) conducted a study on Turkey Brook, a tributary of the River Lee located close to London, England, to determine how, where and why fine particles are likely to accumulate in gravel river beds. The bed of this tributary consists of rounded flint pebbles. It exhibits a coarser surface layer, i.e. a pavement, with fairly uniform material and median size of 27 mm, while the substrate has a median diameter of 16 mm. Six matrix traps were installed in the bed of Turkey Brook, each one of them with an opening of 0.5 m^2 and 0.33 m deep. Each trap was divided into sixteen compartments. The trap opening was closed by a lid of flint pebbles having a size distribution similar to that of the pavement layer, which conformed with the surrounding gravel surface. Ten compartments in each trap were left empty of substrate material, while the remaining six compartments were filled with materials of 48, 24, and 12 mm median diameters, two compartments per material. Three of the traps cut across a channel bar, and the other three were placed across a riffle. In each trap eight of the empty compartments were emptied weekly. Four compartments, three with different subsurface material and one without any subsurface material, were emptied monthly. The last four compartments, with the same subsurface material as the previous four, were emptied every three months. The empty compartments were used as reference for the infiltrated amounts of fines. For the three month period the amount of fines accumulated in the compartments with subsurface material was from 10 to 87% less than the fines accumulated in the empty compartment for the same period. Once more, it was found that the percent of fines that infiltrated into the substrate varies across the stream. Generally areas of higher velocity, and by influence of higher bedload rate, show higher amounts of intruded fines. Again there was a variation in the infiltration of fines along the stream, but it was of a lesser extent than the variation across the channel. The amount of fines that infiltrated in each compartment of a single trap is basically controlled by the material used as subsurface material. It was found that a coarse surface layer superimposed on a finer substrate, which is the case encountered in gravel-bed rivers, encourages the clogging of the near-surface pores with matrix fines. On the contrary, bed material of uniform size in the vertical direction can accumulate higher amounts of fines. When the bed material becomes finer towards the bed surface, an unrealistic situation for a natural stream, the infiltrated amount of fines is even higher.

The number of the laboratory studies conducted on the characteristics of fines intrusion and retention into gravel bed matrices is roughly the same as the field studies. The pioneer of this field is Einstein (1968). Flume experiments have also been performed by Beschta and Jackson (1977), Dhamotharan et al. (1980), and Carling (1984).

Einstein conducted his experiments in 1967. He studied the intrusion of silica flour (3.5 microns to 30 microns) into a gravel bed. He used two flumes, both of them of the recirculating type. Two gravel mixtures were used as bed material. The size of the grains in the first one ranged from 2.5 cm to 15 cm, and for the second one ranged from 6.4 mm to 38 mm. The gravel was inserted into the flume, clean water was introduced and recirculated at flows not large enough to move the gravel, and then a specified quantity of fines was introduced.

Einstein noted that at first the water was cloudy, but in time it clarified completely. As fines settled into the gravel, they slowly filtered through the pores to the flume bottom and gradually filled the pores from the bottom up. Once a particle was deposited in the gravel matrix, it was never re-eroded. Einstein observed that the decision between deposition and continued suspension was made at the very surface of the bed. As long as there was still empty pore space below this layer, no fines were observed to deposit there. Consequently the probability of deposition in the bed did not change until the entire volume of the bed pores was filled, after which no more deposition could take place. The probabilistic behavior thus resembles a step function.

The picture that Einstein gives of the problem of fines retention is a rather simple one. The gravel bed is like a bucket with pore space available for fines. The bucket fills from the bottom up. No fines can come out from the bucket until it is completely filled.

This description contradicts field evidence. In particular, it indicates that if a stream has any fines loading at all, then its pores must eventually fill completely with fines, as the only way fines can be removed is if they overflow the top of the gravel.

The experiments of Einstein are quoted often, and thus deserve special attention. They represent an important contribution in terms of the capacity of gravel to absorb fines from suspension, as well as the siltation rate of gravel matrices when almost all the sediment moves in suspension, and the bed material is considerably coarser and immovable. They are probably misleading in the light of field data, however, for the following reasons:

1. The gravel in the surface layer did not move.

2. No self-formed pavement was formed.

3. No pool-and-riffle structure was present.

4. The coarse and fine sediment phases were greatly removed from each other in terms of sizes.

5. A recirculating flume was used.

Of these five factors, the fourth is probably the most significant. Natural gravel substrates contain a wide range of sizes, usually ranging at least as fine as the fine sand range. Grains interlock to form a sand-gravel matrix. In most natural streams the fine end of the natural substrate overlaps with the fines being introduced from silvicultural or agricultural activities. When fines are fed into this matrix, they cannot settle to the bottom unimpeded. In a natural situation, fines are most likely to accumulate just below the pavement where they are most easily poised for re-entrainment when the pavement is broken. This indicates the importance of the first and second factors. In addition, because of their small size, the fines introduced into the flume were probably moving mostly in suspension. So, the siltation rates obtained apply only for suspended material with very coarse bed material that is not moving. In natural streams, however, small grains moving as part of the bedload also infiltrate into the subpavement, and actually account for most of the infiltrated material. These cannot be accounted for by Einstein's formulation. Einstein correlated the siltation rate with mean flow concentration of fines and found good agreement between experiment and his theory. This probably implies that the siltation rate depends only on mean flow concentration when the fines infiltrating below the surface layer are derived exclusively from suspended material.

The pool-and-riffle structure is important because it sets up intergravel flows (Vaux, 1968). This may provide an important local cleaning mechanism even at flows too small to move the gravel.

The fifth factor is that of flume type. In a recirculating flume, no outside loading of fines is present. A single grain passes through the system many times until it finally reaches a place where it will not be eroded again. Such locations will be abundant if the gravel never moves. A more realistic experimental set-up is a sediment feed flume, so that the fines loading is imposed. A recirculating flume can be used if the gravel is allowed to move, ensuring the formation of a pavement to control the capture and release of fines as described by Milhous.

Beschta and Jackson (1977) also performed a set of experiments on intrusion. Their objective was to determine and evaluate the factors influencing the intrusion of fine sediment into gravel bed streams. These experiments represent an improvement over those of Einstein in that a feed system was used. Two uniform sands were used as fines. The first one, which was used for the bulk of the experiments, had a median diameter of 0.5 mm, and the second 0.2 mm. The well-sorted gravel used as bed material had a median size D_{50} of 15 mm, and a geometric standard deviation σ_g of 1.6; it was very porous, with minimum sizes in excess of the maximum size of the fines present. Gravel bedload was essentially absent, and only a jiggling motion of the gravel was observed. Two fines feed rates were used, the higher one being five times the lower one. The Froude number was used to classify the flow conditions. Three ranges were identified; one for Froude numbers smaller than 0.8, the second for Froude numbers between 0.8 and 1.2, and the last for values larger than 1.2.

The bed samples extracted were 15 cm deep, and the amount of fines found in the sample was expressed as a percentage of the total material on this sample. This percentage of fines was correlated with the Froude number. When the fines with 0.2 mm median size were fed into the channel, the gravel pores filled from the bottom up in the Einsteinian mode. When the coarser fines were used, the largest sand grains were impeded as they worked their way downward because they became jammed in the gravel pores, creating a seal that did not allow any further infiltration of fines. For the low Froude numbers the sand seal was established within the upper 5 cm of the gravel. For moderate and high Froude numbers a jiggling motion of the surface gravel forced this seal deeper, i.e. 5 to 10 cm from the surface of the gravel.

Beschta and Jackson (1977) report that for the experiments with low fines input rates, the amount of fines accumulated in the bed was the lowest for the experiments with moderate Froude number and highest for the experiments with large Froude number. It seems that this is not an accurate statement. During the experiments with moderate Froude number, the concentration of fines at a distance of 1.0 cm above the gravel bed was considerably higher than the corresponding values for the experiments with low Froude numbers. These concentrations did not increase appreciably for the experiments with high Froude numbers. The increased concentration of fines at moderate to high Froude number experiments reduced the amount on the bed available to move as bedload. As it is mentioned earlier (Lisle, 1980), the smaller grains of the bedload, being in contact with the bed and its pores, have a higher probability of ingressing the bed than their counterparts that are suspended. Lisle actually notes that in a stream where the bulk of the total sediment transport was moving in suspension, 80% of the total amount of fines infiltrated into the gravel bed consisted of those grains that were moving as bedload. The reduced availability of fines in the bedload reduced their rate of intrusion. The slight jiggling motion of the gravel, absent for the low Froude numbers, encourages higher intrusion rates for those grains moving as bedload that can infiltrate below the surface layer. The mean percentages of the fines in the gravel bed after infiltration were 6.5, 4.7, 6.9% for the low, moderate and high Froude numbers, respectively. The duration of each run in these experiments was 60 min. During an additional experiment with Fr = 0.93, which was left to run for 120 min, the amount of fines that infiltrated into the gravel bed accounted for 6.5% of the sample. One then can conclude that the jiggling motion was not enough to counteract the reduced availability of grains in the bedload. The intrusion rate is thus seen to be lower for the moderate Froude numbers. A time span of 60 min is not enough to saturate the gravel bed with fines for this case. For high Froude numbers, the increased jiggling motion was probably able to compensate for the reduced number of grains in the bedload. An additional supporting factor is the depth of the seal. When the framework gravel is not moving, Einstein found that the fines keep infiltrating until the stored fines overflow the gravel surface. By increasing the depth of the seal, the pore space available for the deposition of fines increases. The depth of the seal seems to be influenced by the degree of mobility of the surface grains until it reaches a maximum depth, beyond which it is not affected by the mobility of the grains any more. On the other hand, the Shields stress indicates the mobility of the coarse surface layer grains, and thus seems to be a more appropriate parameter to be correlated with the amount of fines into the bed for given bed and suspended materials.

For the experiments with the high input rates of fines, Beschta and Jackson noted that the amount of fines collected at the end of the experiments in the gravel bed increased with Froude number. Here the same characteristics as in the low feed rate experiments were observed. There are two possible explanations for the more reasonable results obtained in this case. Either the duration of the experiments was sufficiently long, or the increased input rates of fines were high enough to provide a sufficient number of grains in the bedload; even though the concentrations of fines for the moderate and high Froude number experiments at a distance 1.0 cm above the bed followed the same trends as in the experiments with low input rates of fines, that is, they were tripled compared with the concentrations in the low Froude number experiments.

More recently Dhamotharan, Wood, Parker, and Stefan (1980) examined whether phenomena characteristic of natural gravel bed streams with poorly sorted material can be reproduced in a laboratory flume. Oak Creek, a fairly typical small gravel stream, was selected as the prototype because extensive research on this stream has been carried out both by Oregon State University and the U.S. Environmental Protection Agency. A physical model with an undistorded geometrical scale ratio of 1:8 based on Froude similarity was used at the St. Anthony Falls Hydraulic Laboratory (SAFHL). The median size and the geometric standard deviation of the bed material used in this study were 2.25 mm and 2.5, respectively. A similar study was conducted concurrently by Parker at the University of Alberta (1980). The SAFHL study used a sediment recirculating flume, while in the Alberta study a sediment feed system was employed. The flow rates in both studies were capable of moving even the coarser grains present at the bed. Both studies concluded that gravel stream phenomena, such as the formation of pavement, can be simulated in the laboratory. They also found that the bedload in the models follows a relationship similar to that of several field streams, including Oak Creek. A weak pool-and-riffle structure similar to that observed in the field was also present in the SAFHL model. In one of the experiments performed at SAFHL, fines were fed into the flume. The first part of the experiment was performed in the absence of fines. After the equilibrium stage was reached fines feeding commenced, everything else being kept the same. The fines used had a median of 0.12 mm, and their size was very close to the finer part of the size distribution of the original bed mixture. At the new equilibrium state the bedload rate was reduced by 36% compared to the bedload rate at the equilibrium state without any fines. It was found that the fines collect predominantly between the subpavement and pavement, in the manner described by Milhous (1973). Clogging of the pores of the gravel matrix hindered the bottom-up filling of pores observed by Einstein. This approach seems to be more realistic.

The armoring process in a gravel stream was also examined in both studies by interrupting the bedload recirculation or supply. The experiments were left to run until the bedload was near vanishing. It was found that the median size of the armor layer was at the most 10% coarser than the median of the pavement created at the same discharge.

Finally Carling (1984) in his flume experiments examined the influence of gross flow parameters on the siltation rates of sand into a gravel bed. The flow parameters that he considered included the bottom shear

stress, water depth, particle size of the introduced fines, Froude number, particle Reynolds number, and mean suspended sediment concentration. He used three different grades of fines (D_{50} = 0.15 mm, 0.19 mm, 1.4 mm). The two finer grains could be transported either as bedload or in suspension, while the third one could not be suspended. The gravel used for the bed was well sorted (σ_g = 1.7), with median size of 15.6 mm. The flow was not capable of moving the gravel, so no self-formed pavement was present. The grain size distribution of the coarsest sand was the only one to partially overlap with the gravel size distribution.

Carling concluded that the gross hydraulic parameters do not affect the siltation rate. He reasoned that if the sedimentation rate is governed by the hydrodynamics of a layer adjacent to the gravel bed, then only parameters describing the mechanics of this layer should correlate with the deposition of fines. Mean hydraulic parameters cannot provide any information about the hydrodynamic characteristics of this layer. In this fashion he justified his experimental results. He found that the initial concentration of sand was a mean flow parameter that correlated very well with the siltation rate. It is also mentioned that "even at low concentrations siltation is rapid regardless of the gross hydraulic properties of the flow or of the grain size of the sand". The coarsest sand was the only one to form a seal, which was of a patchy nature. Carling also observed that the surface layer of the gravel bed remained free of sand.

DISCUSSION

Phenomena associated with gravel streams are complicated. Some of them are better understood than others, but most of the available knowledge is qualitative in nature. Conflicting observations are rife concerning some of the phenomena. Nevertheless, one can draw some conclusions from the studies mentioned here. These are:

1. The existence of a surface layer coarser than the substrate at gravel streams is rather well documented.

2. The manner in which fines fill the pores of gravel matrices varies. Either a gravel matrix can be filled from the bottom-up, or a seal that hinders any infiltration below it may be created. The substrate, as well as the relation of the size of the infiltrating fines to the size of the particles in the gravel matrix play a decisive role in the infiltration process of the fines.

3. Infiltration rates vary across as well as along a stream, with the first variation being higher than the second. Flow characteristics are considered to be responsible for this.

4. Under certain conditions the stream can purge itself from the fines to a certain degree.

5. On a long term basis, when there is no human interference with the drainage area, the amount of fines in the stream is in equilibrium with the characteristics of the environment.

6. Gravel stream phenomena can be successfully simulated in the laboratory.

4. EXPERIMENTAL PROCEDURES

EXPERIMENTAL FACILITY

Dhamotharan et al. (1980) and Parker (1980) provided convincing evidence that many phenomena associated with gravel streams can be simulated in the laboratory. In the present study, no attempt was made to model any specific gravel stream. Instead a survey on the available information about the characteristics of gravel-bed streams was undertaken, so that the model would be a scaled-down version of a representative gravel stream. Unfortunately, no single flume at the St. Anthony Falls Hydraulic Laboratory satisfied all the requirements set forth for such a model. As a result, two flumes were used for this study. The first flume was 16.75 m long, 0.3 m wide, and 0.61 m deep (55 x 1 x 2 ft), and the second one was a tilting flume 12 m long and 0.91 m wide (40 x 3 ft). From now on these flumes will be termed the long and the tilting flume, respectively.

Most of the experimental work was carried out in the long flume, which recirculated both sediment and water. A view of the long flume is shown in Fig. 2 ; a schematic of the facility is shown in Fig. 3. One pipe, 4 cm in diameter, is used to recirculate the bedload with a small percentage of the flowing water, and another pipe, 10.2 cm in diameter, is used to recirculate the rest of the water. Both pipes discharge into the channel through an entrance box located at the head of the channel (Fig. 4). A Jaeger centrifugal pump is used to recirculate the water, and a Warren Rupp Sandpiper model air-powered diaphragm pump is used to recirculate the sediment slurry (Fig. 5). Originally the flume was inconveniently deep, so a false bottom with a slope of 0.003 was placed inside the flume to facilitate the experiments. This false bottom can be seen in Figs. 2 and 3. On the flume bed after the entrance box there was first a stretch of 1.6 m of riprap, and then a 14 m stretch of the mixture used for the experiments, two consecutive slots extending over the entire channel width, and a tailgate. The first slot is used to trap the bedload at the channel exit and recirculate it through the diaphragm pump. It was 15 cm wide and was located 60 cm upstream of the tailgate. The second slot collected the water which, through the recirculating pump and the 10.2 cm pipe, was returned to the entrance box. This slot was 20 cm wide and was located 10 cm upstream of the tailgate.

From the diaphragm pump the water-sediment mixture is either returned directly to the entrance of the flume, or diverted into a large cylindrical sediment separator. Within this device the sediment settles to the bottom, while the water leaves from the top and returns to the pipeline leading to the channel head. At the bottom of the separator the sediment falls into a graduated cylinder, where the bedload transport rate at the exit can be measured. By means of two fully enclosed air-operated flex valves, one on the bottom of the graduated cylinder and one on the main line, the sediment collected in the graduated cylinder can be flushed back into the system instantaneously. A set of two more valves was installed at the junction of

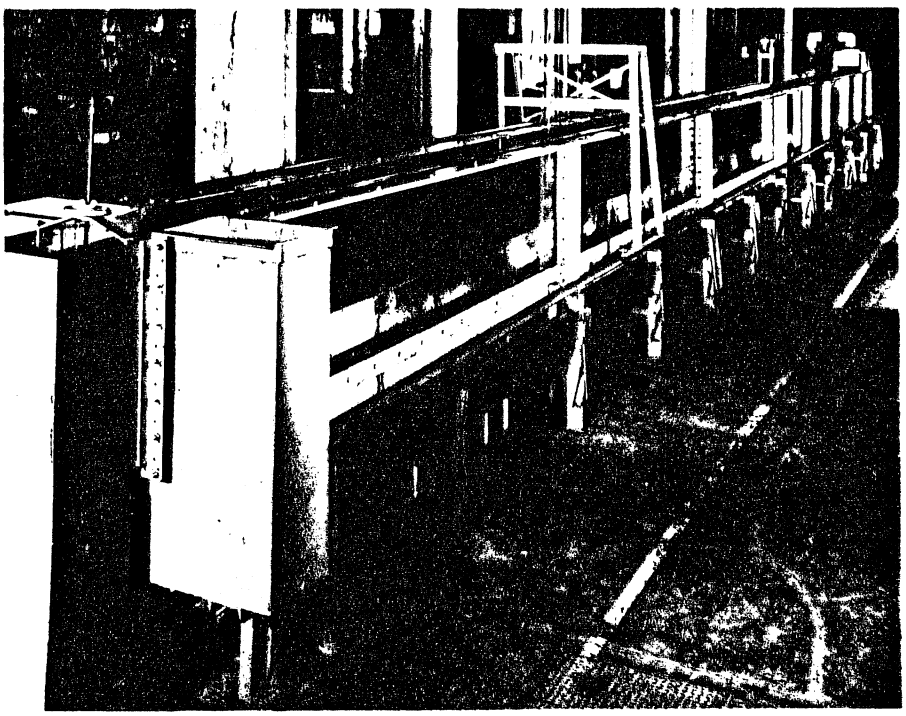

Figure 2. Side view of the long flume. Flow direction is from right to left.

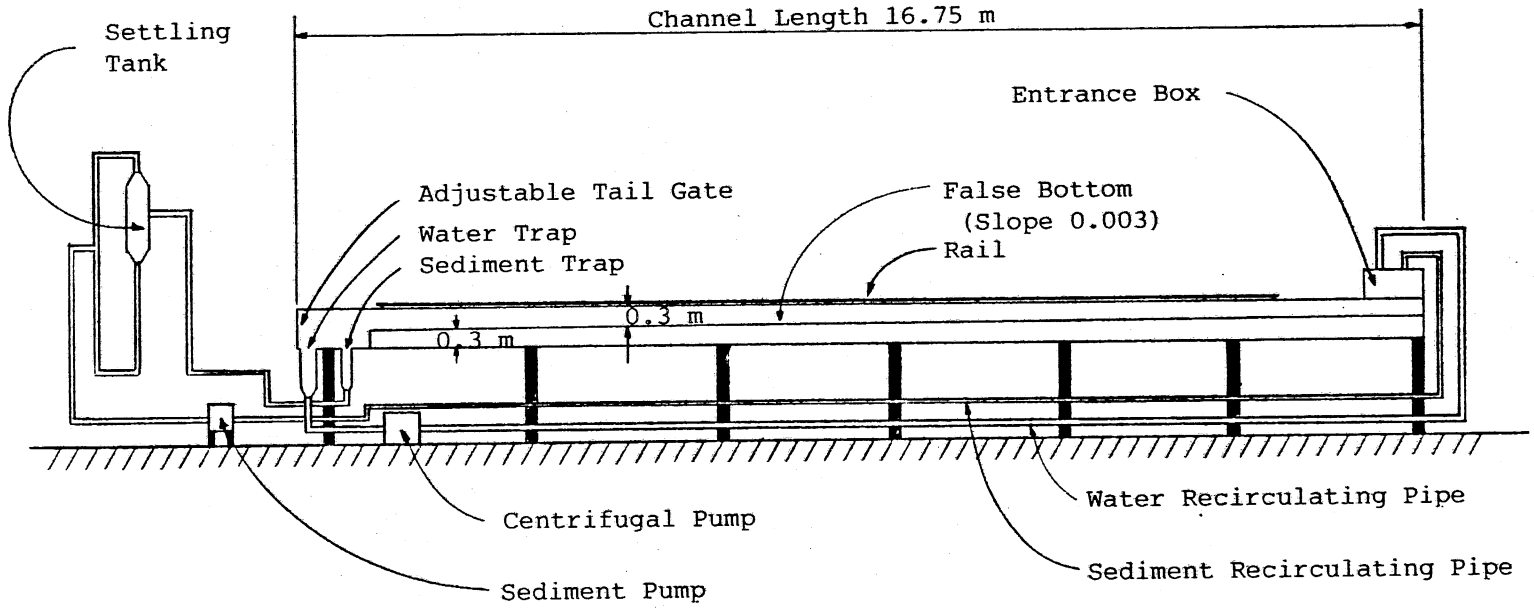

Figure 3. Schematic of the long flume facility. Flow is from right to left.

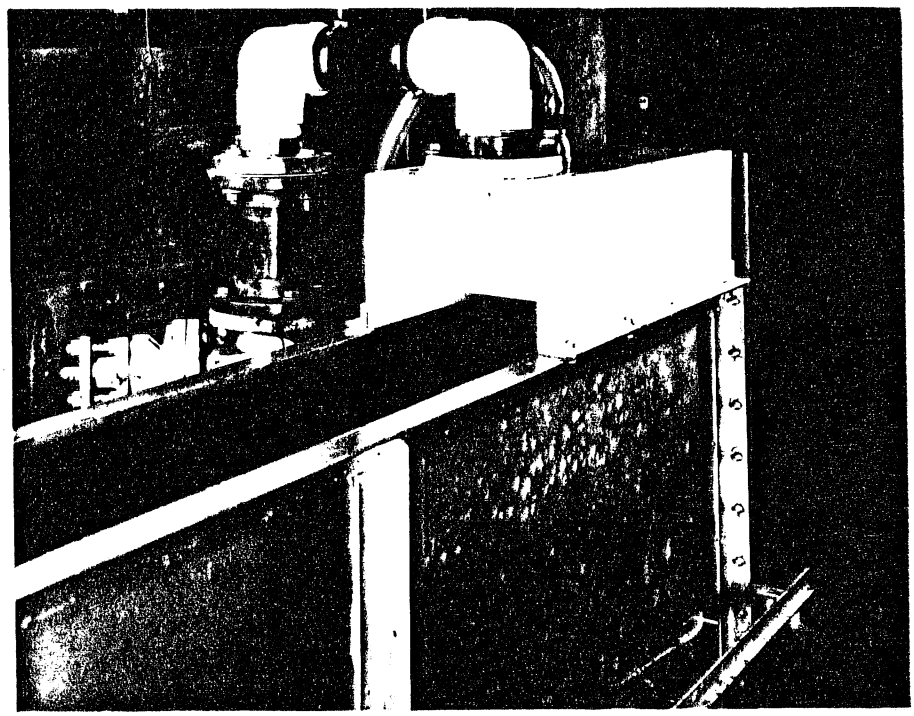

Figure 4. Long flume, view of the entrance box.

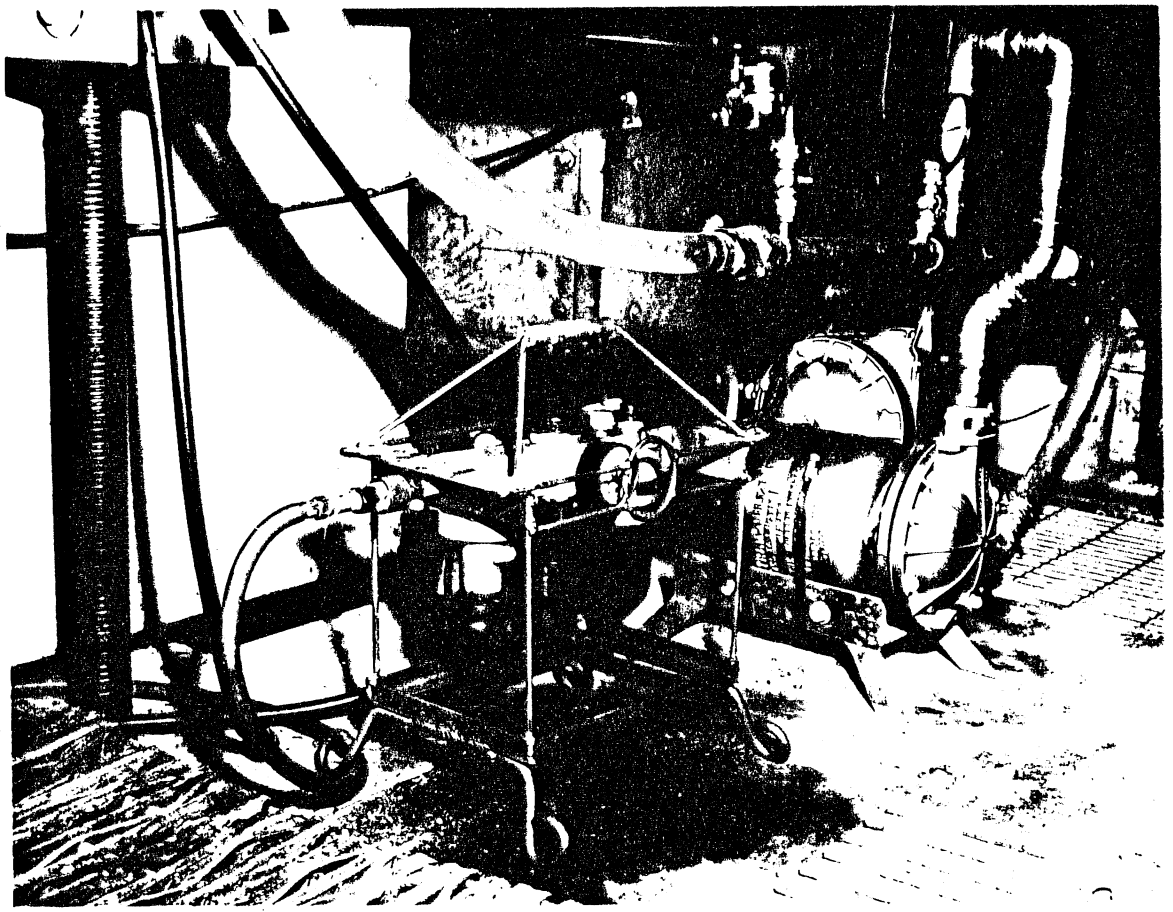

Figure 5. The diaphragm pump used to recirculate the sediment slurry.

the return sediment line with the sediment separator. These valves provided the option to remove the material collected in the graduated cylinder, when it was desirable, in order to examine the bedload characteristics. A schematic of the sediment separator and bedload measuring device is shown in Fig. 6. Two pictures of the installation are shown in Fig. 7.

The flow rate through the centrifugal pump was measured with an orifice meter attached to the line connecting the centrifugal pump and the entrance box. The flow rate through the diaphragm pump was measured by means of an elbow meter at the top of the sediment separator, through which the water was returned to the line carrying the sediment to the channel entrance. Both pipes are oriented against the wall of the entrance box at the point where they discharge into the channel. Just upstream of the rip-rap stretch, exactly at the point where the pipes discharge into the flume, a 40 cm long portion of the channel is devoid of any bed material, creating a local pool of water. The small pool of water and the rip-rap immediately downstream helped to dampen the excessive energy of the incoming water and provide a unidirectional flow.

Stainless steel rails mounted on the top of the channel walls support a travelling carriage. A manually-operated point gauge, and instruments used to measure velocity and concentration profiles, are mounted on this carriage. A screeding template is mounted on a carriage travelling on a separate set of rails attached to the flume floor. By adjusting the slope of the latter set of rails, the surface of the bed material was screeded to a desirable initial slope. A view of the long flume with the bed material in it is shown in Fig. 8.

The major advantages of this flume are its length and its transparent glass walls. The bedload motion, and the infiltration of fines into the bed can be observed closely through the walls; video pictures can also be taken. The narrow width of the channel, which suppressed any tendencies for the formation of bars, was its major disadvantage.

The tilting flume facility operated as a feed system in both water and sediment. A pipeline at the head of the channel supplied the water from the Mississippi River. The discharge is measured by means of an orifice meter. Two feeding systems at the upstream end of the channel introduce the sediment into the channel. One of them is used to introduce into the flume material identical to the original bed mixture. The second feeds the flume with fines. Each feeding system consists of three parts: an Accu-Rate Company screw feeder, a DC power supply unit, and a servo motor. The feeder can be adjusted with a dial to provide the desired feed rate of the material. The feeder was very consistent in keeping the feed rate close to the desired value throughout the duration of each experiment. Its feeding mechanism avoided any size segregation of the material stored within. The power supply is used to drive the servo motor, which rotates a metallic rod. A round tin plate 7.6 cm in diameter is attached at the end of this rod. Four tin dividers, each one of them 0.85 cm high, are placed radially on the tin plate. Through a dial in the power supply the desired rotation rate of the rod can be given. From the feeder the material passes through a funnel and a plastic tube, and is directed to the rotating tin plate. The rate of rotation of the plate is adjusted so that the material is

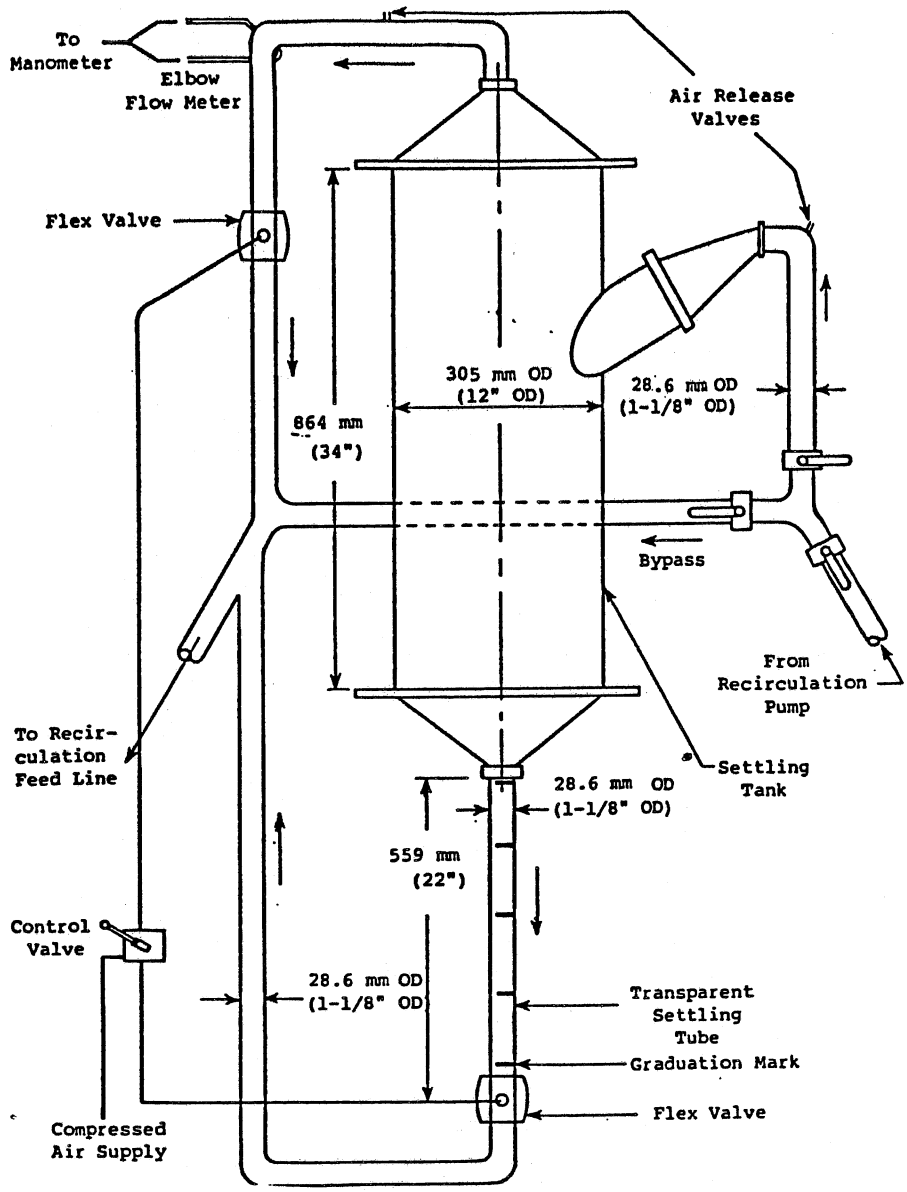

Figure 6. A schematic of the sediment separator and bedload measuring device.

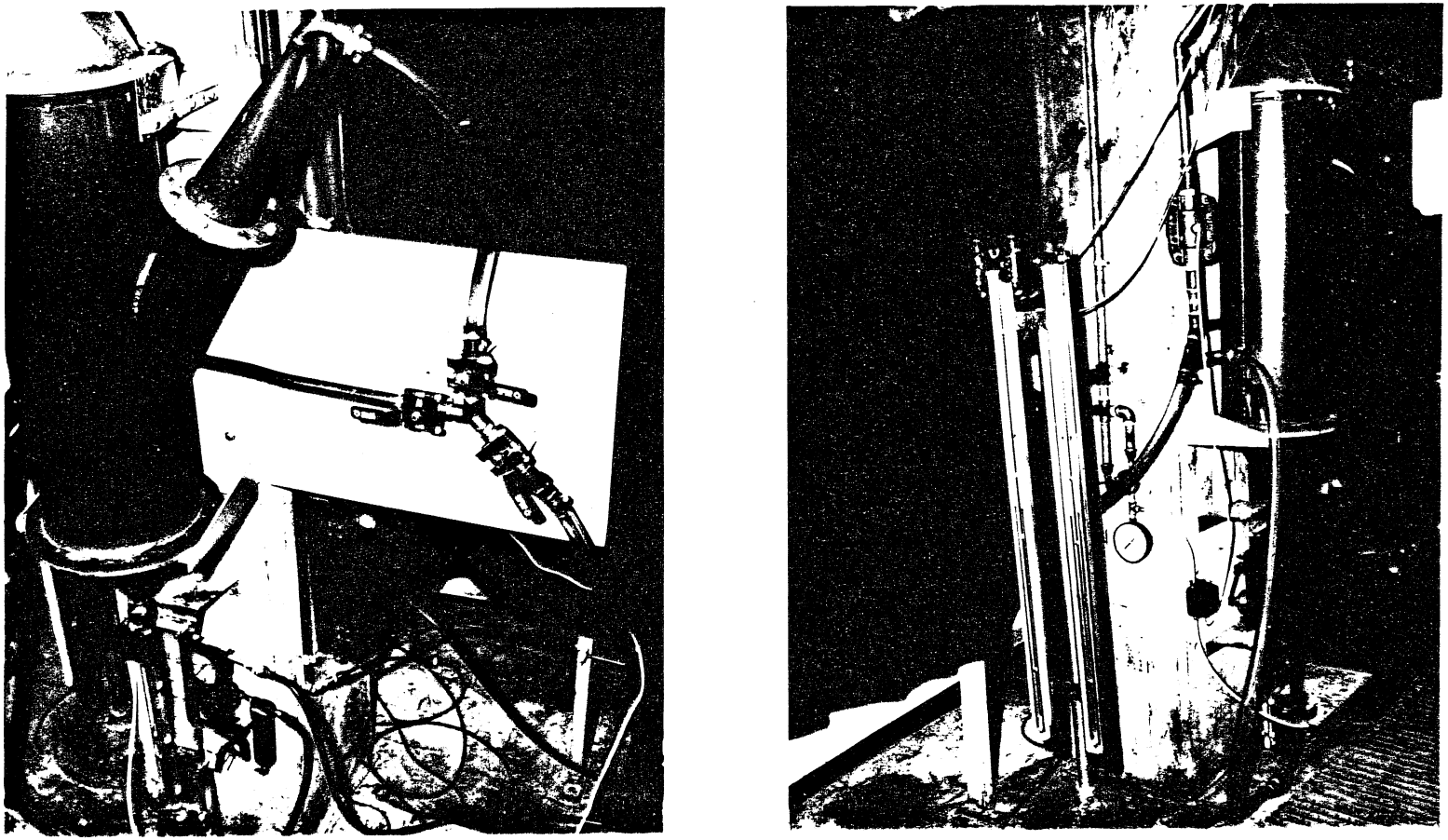

(a) (b)

Figure 7. Sediment trap (left) and bedload measuring installation (right).

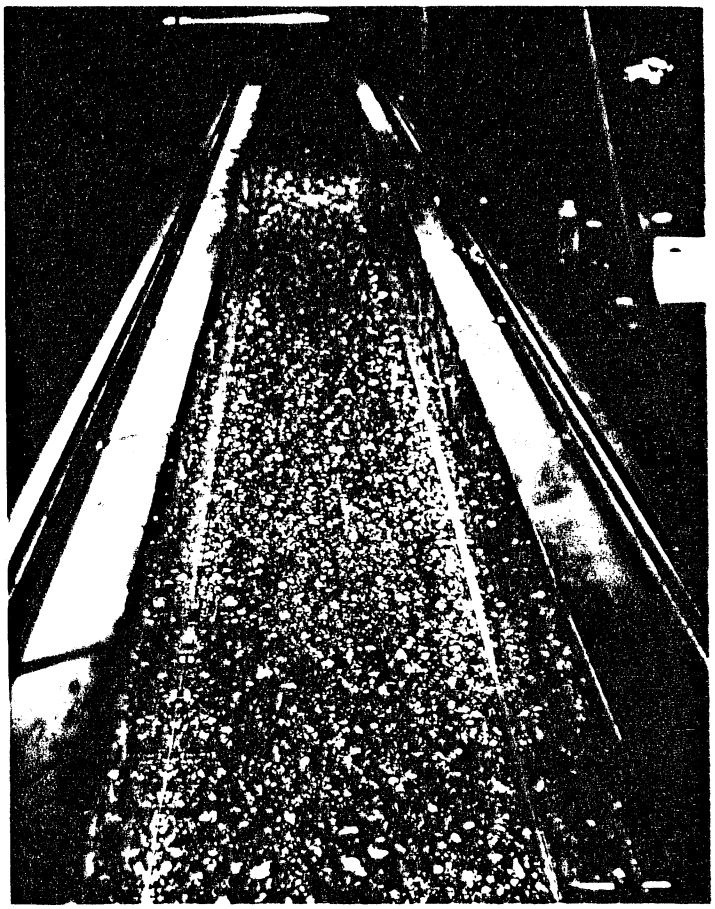

Figure 8. View of the long flume from upstream.

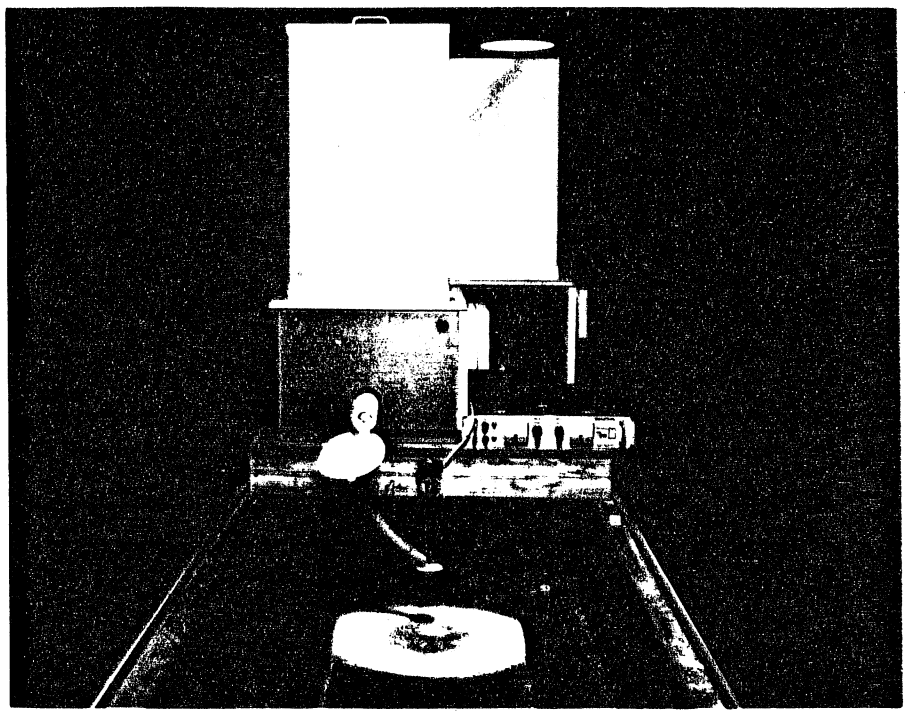

Figure 9. The two sediment feeding systems. The front feeder introduces the fine material into the tilting flume.

uniformly distributed across the channel. The feeder with the fines is shown in Fig. 9. Immediately behind it, in the same photograph, the feeder for the coarse material is partially visible.

The slope of the tilting flume can be adjusted mechanically from 0 to 2 percent. Stainless steel rails mounted on the top of the channel walls support a travelling carriage, which in turn is used to mount the screeding template, and the point gauge. False walls were placed in the main flume symmetrical to the center to obtain the desired width of 0.53 cm. A schematic of the tilting flume facility is shown in Fig. 10.

Again, a rip-rap reach 1.5 m long is placed at the upstream end of this channel. The next 9.6 m comprise the useful length of the channel, its bed covered with the bed material used for the experiments. At the downstream end of the bed material there is a slot 14 cm wide, extending over the entire channel width. This slot is used to trap the total outflow of the transported bed material. From there the sediment slurry is pumped out by means of a diaphragm pump, and is then either directly discharged into the sump or is diverted to the cylindrical sediment separator first, where bedload measurements are taken and bedload samples are extracted when desired, after which it is again directed to the sump. The water depth in the channel is controlled by means of an adjustable tailgate, located 60 cm downstream of the sediment trap.

The important feature of the tilting flume is its width, which was sufficient to allow for bars to develop. The short length of the channel and its opaque walls are its major drawbacks.

A Prandtl tube supported by a vernier meter, attached on the rolling carriage, was used to measure velocity profiles. Velocity measurements were taken only in the long flume. The Prandtl tube was mounted on the top of the carriage so as to allow for measurements across the whole channel width. Depending on the size of the fines introduced into the flume, a different Prandtl tube size was used. When the fines with median size of 0.11 mm were used, the external diameter of the Prandtl tube was chosen to be 0.3 cm, and when the fines with median size of 0.08 mm were used, a Prandtl tube with an external diameter of 0.16 cm was used. The Prandtl tube was connected to a Validyne diaphragm differential pressure transducer model DP7. The diaphragm used could measure maximum differential pressure up to 7.6 cm of water. The transducer was connected to a Validyne digital transducer indicator model CD 23, and this to a Heath Servo-Recorder model EU-208, and an Apple IIC microcomputer. From the recorder, a plot of the indication of the pressure transducer was obtained. The Apple computer, with a sampling rate of 500 readings per second, was used to store the data and compute the mean value of the readings of differential pressure at a point inside the flowing water. The transducer was calibrated before the beginning of each experiment, over a range from 0 to 5.1 cm of differential pressure of water, with a balancing device shown in Fig. 11. The other instruments used for the velocity profile measurements are also shown in the same figure.

The concentration of suspended sediment in the flowing water was also measured. Originally a turbidity meter using a light beam was utilized for concentration profile measurements. The turbidity measurements with this

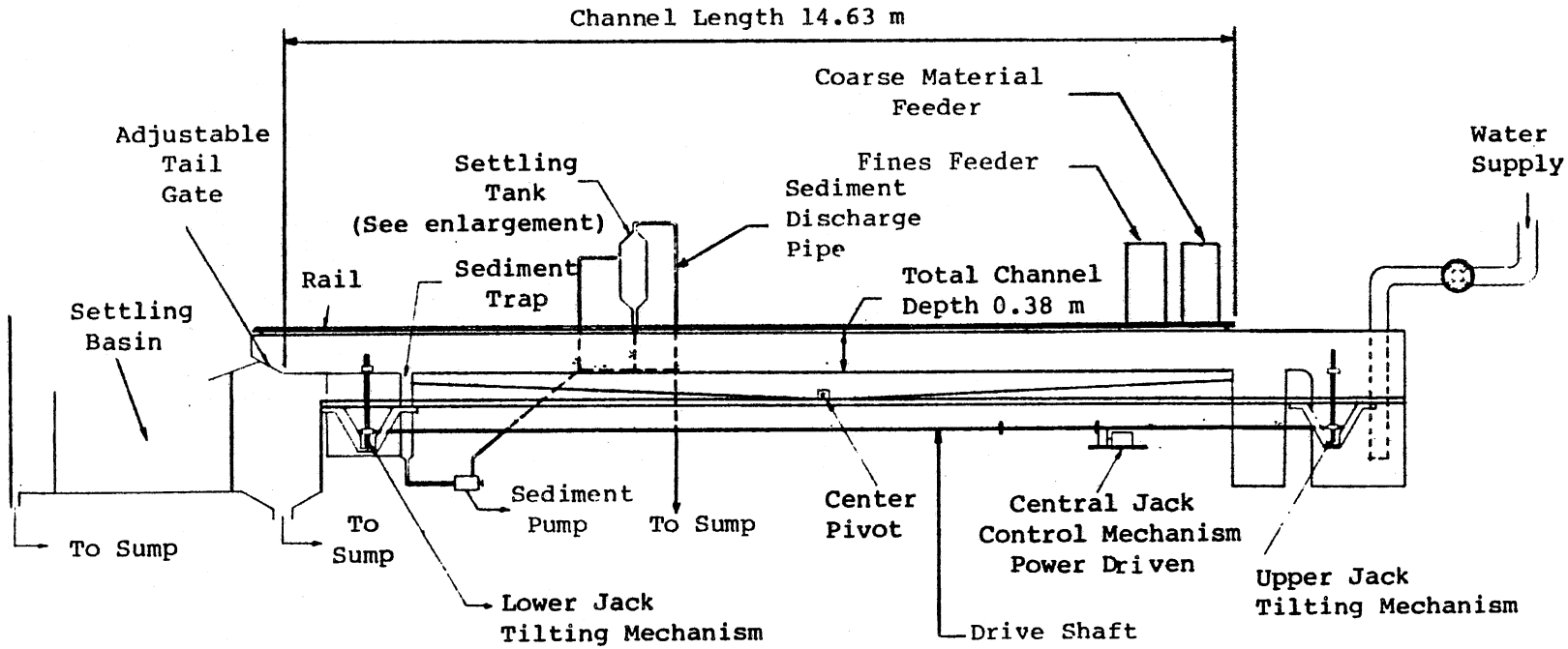

Figure 10. A schematic of the tilting flume.

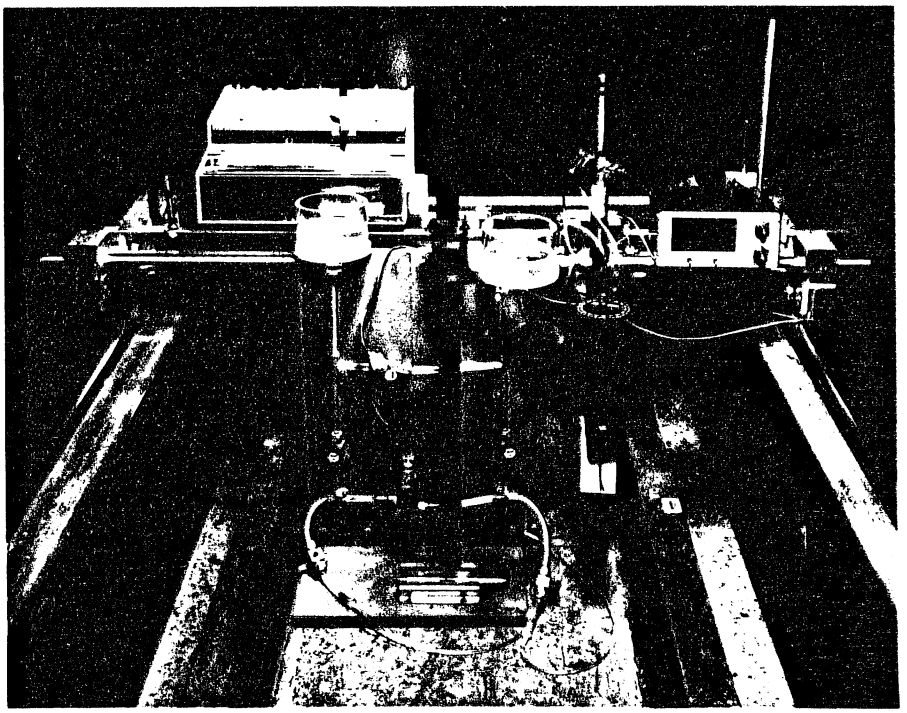

Figure 11. Instrumentation used for velocity measurements.

device were very sensitive to the color and size of the suspended material. A small amount of fines, either obtained from the coarse bed mixture or resulting from abrasion of the bedload particles in the return sediment line, became suspended, resulting in erroneous concentration measurements. In addition, the fines introduced into the flume which are recirculated exhibit a slight coloration as time progresses, which distorts the turbidity measurements. After recognizing these problems it was decided to use a simple siphon to withdraw samples of the flowing water. With the new system emphasis was shifted to mean flow concentration measurements.

The two different types of flumes used here, recirculating and feeding systems, provide the opportunity for comparing their behavior and discerning any similarities or differences. The ability of one type to model some phenomena associated with gravel streams better than the other can be also examined.

OVERVIEW OF EXPERIMENTS

Some of the main features that distinguish gravel streams from sand streams are: the presence of a bed surface layer coarser than the substrate, the poorly-sorted bed material, and the low bed shear stresses, which usually exceed the critical stress only moderately (Parker et al., 1982a). The present experiments were designed with these features in mind.

Four of the main parameters of the problem attacked in this study include the shear stress at the bed of the channel, channel slope, amount of fines introduced into the channel, and size of fines introduced. An appropriate choice of these parameters allowed for six series of experiments in the long flume and a single series in the tilting flume. The initial bed slope for the long flume ranged from 0.003 to 0.008. The initial slope for the tilting flume was 0.012. The dimensionless design Shields stress varied from 0.10 to 0.15, based on the mean size of the original mixture. On the average, six experiments were conducted for each series. Table 1 provides some information about the experiments.

Before the beginning of each series, a fresh mixture of bed material was introduced into the channel and was screeded with a template to the desired initial slope. A hand trowel was used to smooth any small irregularities after screeding. The process of vigorous screeding tended to winnow some fine material below the surface, creating an ersatz pavement. The thickness of the bed material initially placed in the long flume ranged from 6 cm to 15 cm in the downstream direction depending on the bed surface slope. In the tilting flume the thickness was 5 cm everywhere.

The first experiment of each series in the long flume was performed without any fines being added into the flume. During the rest of the experiments in each series, fines were introduced into the flume. Their amount was progressively increased with each experiment in the series (Table 1). Three cross-sections were designated for measuring bed and water surface profiles. A point gauge was used for these measurements. The distance between consecutive cross-sections was 2.0 m. The cross-section farthest downstream was located 2.5 m upstream from the tailgate. Water surface slope and bed surface measurements were taken every hour at

TABLE 1. SOME CHARACTERISTICS OF THE EXPERIMENTS

	Discharge Q	Flow Depth d	Initial Slope	Equil. Slope	Coarse Feed Rate	System (feed) Concen.	D_{50} of fines	Equil. Concentr.	Design τ_o	Equil. τ_o	Q_s	Pavement D_{50}	Subpavement D_{50}	Duration
	(ℓt/sec)	(cm)			gr/min	mgL^{-1}	(mm)	Mg_L^{-1}	(gr/cm sec^2)		gr/min	(mm)	(mm)	(hrs)
(1)	(2)	(3)	(4)	(5)	(6)	(7)	(8)	(9)	(10)	(11)	(12)	(13)	(14)	(15)
S1:E1	13.9	6.65	0.008	0.0053		0.0	0.08		46.62	29.82	150	4.44	1.8	26.75
E2	13.08	7.21		0.004		500				24.19	55	4.97	2.06	8.5
E3	13.35	7.15		0.0044		500				26.49	45	5.0	1.85	7.5
E4						1,000						5.02	2.02	9.3
E5	13.33	7.3		0.005		3,000				31.37	82	5.0	1.88	13.35
E6	13.33	7.55		0.0041		5,000				26.17	56.8	5.2	1.78	24.65
E7	13.33	7.7		0.0044		10,000				28.42	36.4			29.67
E8						30,000								63.54
S2:E1	19.25	9.76	0.008	0.0039		0.0	0.08		58.28	31.06	162	5.88	2.26	47.0
E2	19.25	10.01		0.0035		2,000				27.83	84.1	5.46	2.6	20.75
E3	19.25	10.13		0.0037		3,000				30.71	78.7	3.63	2.45	23.5
E4	19.25	10.39		0.0038		5,000				32.02	73.4	4.7	2.05	22.0
S3:E1	17.53	9.4	0.005	0.005		0.0	0.08		38.85	40.1	86	4.99	3.06	53.5
E2	17.53	8.8		0.005		2,000				37.08	122	5.33	2.41	27.0
E3	17.53	9.2		0.0041		3,000				31.25	86.0	5.53	2.05	27.5
E4	17.53	9.1		0.0045		5,000				34.35	105	5.5	2.17	46.5
E5	17.53	9.45		0.0043		10,000				34.12	80	5.23	2.15	37.75
E6	17.53	9.7									85			13.45
S4:E1	22.8	13.79	0.005	0.0032		0.0	0.11		46.62	36.0	30.5	4.64	2.46	39.0
E2	22.9	11.88		0.0028		2,000				25.7	24.0			24.0
E3	22.9	12.13		0.0029		3,000				27.58	8.0	5.08	2.45	24.0
E4	22.8	12.14		0.0029		5,000				27.11	7.3	4.84	2.21	27.25
E5	22.8	11.98		0.0026		10,000		164		23.76	25.0	3.8	2.17	26.5
E6	22.8	11.96		0.0028		10,000		1010		25.37	50.0	3.39	2.31	36.8
S5:E1	29.76	13.15	0.003	0.0024		0.0	0.11		38.85	20.57	103	4.92	1.98	53.5
E2	29.76	13.4		0.0026		2,000		21		24.5	95			24.0
E3	29.82	13.6		0.0024		3,000		22.5		22.72	150	3.98	2.46	25.75
E4	29.76	14.0		0.0028		5,000		23.5		28.48	60	4.61	2.49	23.16
E5	29.76	13.8		0.0028		10,000		302		27.77	101			20.5
E6	29.76	13.85		0.0018		10,000		2,200		16.25	125	4.59	2.24	4.0
S6:E1	32.7	14.7	0.003	0.0027		0.0	0.08		42.73	27.71	120	6.05	2.18	49.3
E2	32.7	14.7		0.0023		10,000				24.16	115			9.4
	32.7	14.7		0.0023		5,000				24.16	72			7.0
	32.7	14.7		0.0024		5,000				25.21	75			8.5
E3	32.7	14.8		0.0024		5,000				24.43	115			9.4
	32.7	14.8		0.0025		5,000		11,733		25.61	108			3.2
	32.7	14.8		0.0024		10,000				24.43	85	2.78	2.39	3.6
S7:E1	12.8	4.12	0.012	0.015	270	0.0			46.62	60.62	190	5.53	2.58	34.0
E2	12.8	3.88		0.016	270	156		170		60.90	210	6.13	2.17	25.0
E3	12.8	3.94		0.017	270	350		390		65.7	293	5.91	2.14	14.5
E4	6.3	2.42		0.017	0.0	430		500		40.36	0.0	6.18	2.27	9.0
E5	6.3	2.43		0.017	0.0	0.0				40.53	0.0	6.27	2.18	19.0
E6	12.8	4.0		0.015	270	0.0				58.86	205	6.52	2.38	11.0
E7	15.4	4.4		0.017	750	0.0				73.4	560	6.2	2.21	10.0

In Column (6), the feed rate at which the coarse material was fed into the tilting flume is listed.
Column (7) includes the amounts of fines that were introduced into the flume; these values represent system concentrations for the long flume experiments and feed rate concentrations for the tilting flume experiments.
The effect of the channel sidewalls has not been considered in column (10), while it has been accounted for using the Vanoni Brooks method, in Column (11) for the long flume experiments.

the beginning of the experiment, and every three hours toward the end. Bedload measurements were taken every 20 min. The experiment was stopped when it reached equilibrium. The conditions indicating equilibrium were chosen to be: temporal constancy of the water surface slope, bedload rate, and suspended sediment concentration in the flow. When the experiment was considered to be in equilibrium, velocity measurements were taken at the most upstream cross-section. These measurements were taken along three verticals to the bed, one at the center of the cross-section and the other two symmetrically located about the center, 7.5 cm on either side. Siphon samples were also taken with a Pitot tube at this stage to estimate the mean flow concentration. One or two bedload samples were extracted toward the end of the experiment.

In the tilting flume the number of experiments performed was seven. The first run was without fines infeed. During the rest of the experiments, the impregnation of fines into gravel bed was examined, as well as the ability of the flume to purge itself of the fines accumulated in the bed. The equilibrium criteria are somewhat different for this flume. The rate of coarse feed should be equal to the bedload transport rate at the exit of the channel, and the two size distributions should be identical. The concentration computed from the feed rate of fines divided by the water discharge should be the same as the measured mean flow concentration. Finally, as in the case of the long flume, the water surface slope should remain constant. Bed and water surface profile measurements were taken at three cross-sections, each 1.5 m apart. The cross-section farthest downstream was located 1.5 m upstream from the sediment trap. Water surface, bed surface, and bedload measurements were taken as often as for the long flume experiments. Bedload and siphoning samples were obtained when the run had reached equilibrium.

Before the beginning of each series, and at the end of each experiment, a number of sets of bed samples were obtained. Each one of these sets is composed of a sample of the bed surface layer, removed with the use of wet clay, and two volumetric samples taken immediately below the surface layer. The thickness of the surface layer sample was roughly equal to the D_{80} of the pavement, the values of which ranged from 6.0 to 8.2 mm with a mean value of 7.0 mm; D_{90} represents the diameter of the sieve that retains 10% of the material sieved by weight. The first volumetric layer is termed subpavement sample; the one below that constitutes a bottom layer sample. Each volumetric sample is obtained by extracting a layer of bed material with a spoon, about 1.5 cm thick.

In order to verify that the sediment in the flume was essentially identical to the original mix, a large volumetric sample was extracted from the channel bed before the commencement of each series.

A video camera was used to capture the motion of the moving grains from the sidewalls of the long flume. This camera was also used for the flow visualization performed in the long flume.

Each experiment was assigned a symbol, e.g. S2:E3, where the letter S stands for series, and E for experiment. The above symbol thus refers to the third experiment of the second series. The tilting flume experiments belong to the seventh series (S7).

SEDIMENT CHARACTERISTICS

The mixture used as bed material in the channel was obtained by mixing six different well-graded sediments in specified proportions. Starting from the finer component their median diameters were 0.46 mm, 0.66 mm, 1.6 mm, 1.9 mm, 3.1 mm, 6.25 mm. Their respective geometric standard deviations (σ_g) were 1.4, 1.9, 1.7, 1.4, 1.3, 1.3. The corresponding specific gravities were around 2.65. The size distributions of sediment components used to derive the final mix are shown in Fig. 12. The size gradation of the sediment mix so obtained is shown in Fig. 13. Grain size statistics are given in Table 2. The median grain size is 2.44 mm, and the standard deviation is 2.75. The specific gravity of the mixture was 2.63. The shape of the grains ranged from well rounded to subangular. Most of them were subrounded, while a small percentage of plate-like particles was present. Extra care was taken to insure repeatability of the size distribution of the mixture. Particles with diameters smaller than 0.2 mm were excluded from the mixture in order to minimize suspension from the bed material. The bed mixture so obtained constitutes a scaled-down version of a rather typical bed material observed in natural gravel-bed streams.

Two sizes of silica flour were used as fines, one with D_{50} = 0.080 mm and the other with D_{50} = 0.11 mm, both being well sorted. Their size distributions are shown in Fig. 14. Table 2 gives information about some characteristics of their size distributions. The white color of the fines was very helpful for the purpose of observation. The specific gravity of both sediments was 2.65.

PAVEMENT VERSUS ARMOR

One of the characteristics of gravel-bed streams is the existence of a surficial layer coarser than the substrate material. When this surface layer is mobilized during floods, it is called pavement. In this case bed activation is a regular phenomenon that takes place several days a year, during which most of the grains, small and large, participate in the motion. When this surface layer is so coarse that it never moves, it is called an armor layer. This terminology is used in the present work. Some researchers favor this terminology, while others prefer the name armor for the first case and pavement for the second. The interested reader can find the arguments of both sides in the literature (Bray and Church, 1980; Carling, 1981; Milhous, 1981; Parker, 1981).

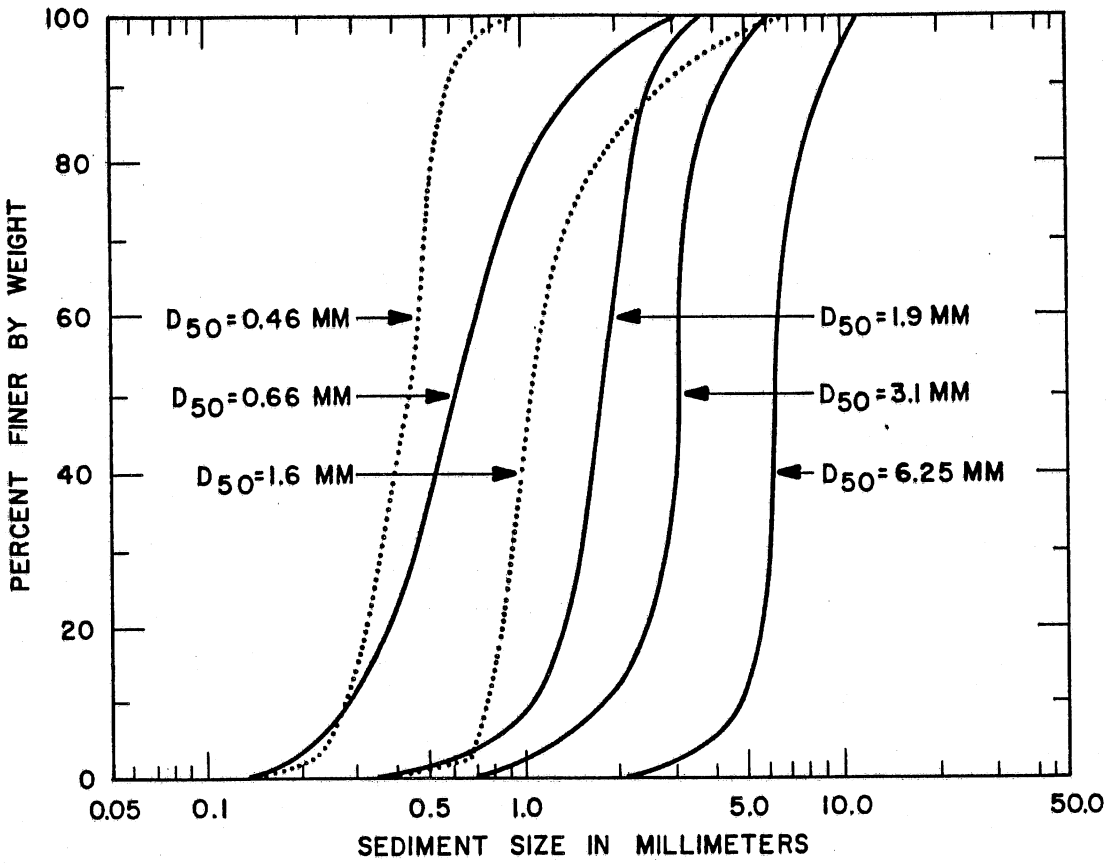

Figure 12. Size distributions of the sediment components used to derive the sediment mix.

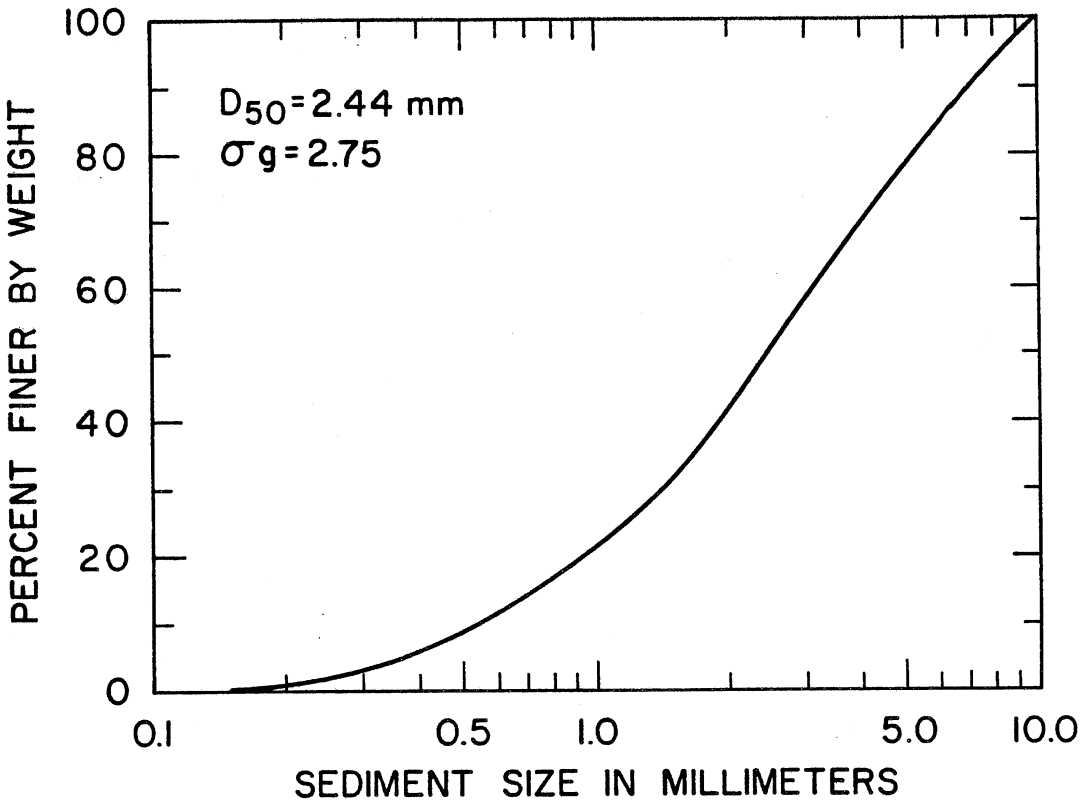

Figure 13. Size distribution of the bed material used in the experiments.

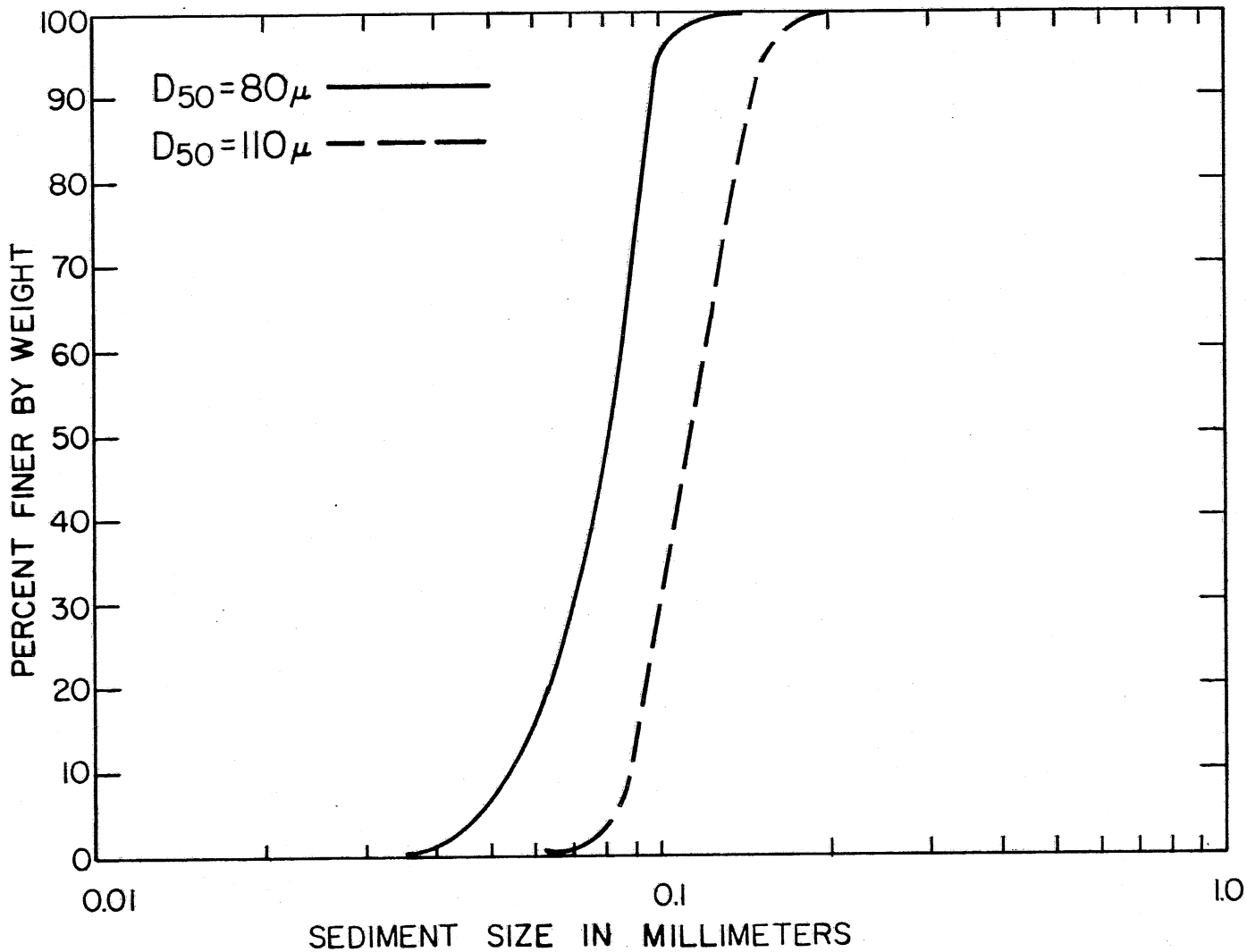

Figure 14. Size distributions of the sediments used as fines.

TABLE 2

CHARACTERISTICS OF THE INITIAL BED MIXTURE AND OF THE MATERIALS USED AS FINES

	Bed Mixture	Fines I	Fines II
D_{50}	2.44 mm	0.08 mm	0.11 mm
D_{90}	7.00 mm	0.098 mm	0.15 mm
D_{10}	0.54 mm	0.054 mm	0.089 mm
σ_g	2.75	1.27	1.24
R	1.63	1.65	1.65

5. SAMPLING METHODS

Two sampling methods are examined here, i.e. the areal and the volumetric (bulk) methods. The areal sample consists of all the grains of the bed that are exposed to the channel flow within a selected area. In this case the volume of the sample depends on the height of the exposed particles. A volumetric sample is obtained by removing a predetermined volume of bed material. The volume of the sample in this case is independent of the dimensions of the individual particles. Kellerhals and Bray (1971) give three rules that should be followed for sampling: a) the correct population should be sampled; b) the resulting grain size distribution should be comparable with bulk sampling, which is commonly used for fluvial sediments; and c) the method used should be efficient.

When the pavement of a gravel bed stream is to be sampled, areal sampling is one of the appropriate methods that can be used. If a model in the laboratory is used, then areal sampling is the only suitable sampling technique for the pavement. Procedures for converting areal samples to equivalent volumetric samples should be devised. In the same paper Kellerhals and Bray derive a conversion formula based on an ideal model that consists of tightly packed cubes of various sizes randomly arranged to represent a gravel mixture. This formula, which converts an areal size distribution to a volumetric size distribution, can be stated as follows:

$$p(V)_i = C\, p(A)_i\, \overline{D}_i^{-1} \tag{1}$$

where $p(V)_i$ and $p(A)_i$ represent percentages of the size fraction i obtained from volumetric and areal samples respectively, $\overline{D}_i$ is the arithmetic mean size for the same size fraction, and C is a constant. By integrating (1) over the whole range of sizes available in the sample one can get

$$E[\overline{D}_i] = \int_{\overline{D}_{imin}}^{\overline{D}_{imax}} p(V)_i\, \overline{D}_i\, d\overline{D}_i = C \int_{\overline{D}_{imin}}^{\overline{D}_{imax}} p(A)_i\, d\overline{D}_i = C \tag{2}$$

where $E[\overline{D}_i]$ is the expected value of $\overline{D}_i$, based on the size distribution obtained from a volumetric sample. In this case the expected value coincides with the geometric mean diameter of the volumetric sample.

Areal sampling is biased in favor of the coarser grains. Formula (1) attempts to correct for this problem by adjusting toward a finer size distribution, equivalent to the corresponding volumetric size distribution. From experiments conducted by Proffitt (1980) with sediments of different

mean sizes and standard deviations, it was found that formula (1) over-corrects an areal sample. Instead Proffitt empirically derived the following conversion formula

$$p(V)_i = C\ p(A)_i\ \overline{D}_i^{-0.47} \tag{3}$$

Three axes, vertical to each other, are usually used to characterize the dimensions of a grain. These axes are: a,b,c, where a is the largest and c is the smallest. The intermediate b-axis coincides most nearly with the sieve opening D. In his experiments, Proffitt tried to obtain a nearly homogeneous mixture. As one can discern by observing the surface layer of a gravel river bed, the orientation of the grains, especially of the larger ones, is not arbitrary. These grains always try to establish a placement on the bed surface that provides the maximum resistance to their dislocation by the flow; i.e. the bed is typically imbricated. The axis that can be considered as representative for the height of these particles is thus the c-axis. There was no preferred orientation mentioned for the surface grains in Proffitt's experiments. As such, the sieve diameter D seems to be the representative height for the surface stones in this case. Since $c < D$, one can conclude that the areal sample of a pavement layer exhibits a smaller bias toward the coarser grains than an areal sample of a surface layer with arbitrarily oriented grains. Assuming that a formula similar to (3) holds in the case of the presence of a pavement, then (3) should be modified as follows:

$$p(V)_i = C\ p(A_p)_i\ \overline{c}_i^{-0.47} \tag{4}$$

where $p(A_p)_i$ is the percentage of the size fraction i obtained from an areal sample, whose particle placement resembles that of a pavement. One can further assume that the axes of the grains of a given stream are related as follows:

$$\overline{c}_i = \mu\ \overline{D}_i^{\nu} \tag{5}$$

with $\nu < 1$. Then (4) becomes

$$p(V)_i = \left(C\ \mu^{-0.47}\right)\ p(A_p)_i\ \overline{D}_i^{-0.47\nu} \tag{6}$$

It is not one of the objectives of the present work to solve the sampling problem. Some qualitative conclusions are drawn here instead.

An adhesive material is usually used to remove an areal sample. The properties of adhesives vary. Proffitt used wax in his experiments. In

the present study custer feldspar clay, commonly used for pottery, was used. Wet clay was attached to one side of a plastic coffee can cover, and this was forced against the bed surface to obtain an aerial sample of approximately 57 cm^2. Each sample was then washed through a 0.053 mm sieve and dried. A typical dried areal sample mass was about 55 grams. Under the applied pressure, the clay tended to penetrate somewhat deeper than the bed surface. From observations it was concluded that the areal sample was crudely equivalent to a volumetric sample of the material present in the surface layer to a thickness approximately equal to the coarsest grain of this layer. Justification for this is provided below.

During the present study it was considered important to find the infiltration depth of the fines, as well as the amount infiltrated. Two layers of substrate material, both being about 1.5 cm thick, were extracted with a spoon to yield volumetric samples. The volumetric samples were taken from the substrate material exposed after the removal of the pavement. The surface area of the sampled substrate material was 57 cm^2. Typical dried volumetric sample mass was about 140 grams. All the samples were sieved mechanically after drying. The method used for removing the pavement is not a true areal sample. Similarly the method used for the substrate does not provide a fully volumetric sample, as the thickness of the sample is not many times larger than the D_{90} of the mixture. Both are intermediate in nature.

In order to examine the possible variation in the grain size distribution due to the sampling methods used, at the end of each one of 6 experiments two sets of samples, one areal and one volumetric, were obtained. Each volumetric set consists of four consecutive samples, sequential in the vertical, of about 1.5 cm vertical thickness. Each areal set consists of six consecutive samples, also sequential in the vertical. The thickness of the areal sample is about 0.65 cm. The first layer in both cases is the bed surface layer. The median size of each sample is shown in Table 3. The ratio of the median size of the volumetric top layer sample D_{TV50}, is compared with the median of the corresponding areal top layer sample D_{TA50}. As can be seen from Table 2, the ratio D_{TA50}/D_{TV50} is larger than 1.5 and smaller than 2.7, with a mean value of 1.95. The average of the medians of the substrate layers for each set is used to compare the two methods for the substrate material. Where D_{SV50} is the median size for the substrate material sampled volumetrically, and D_{SA50} is the corresponding median size for the substrate material obtained with the areal method, it was found that the ratio D_{SV50}/D_{SA50} varied between 0.95 and 1.38, with a mean value of 1.1.

It is known that the finer grains concentrate between the bottom of the surface layer and top of the subpavement (Milhous, 1973). This material is not included in an areal sample of the top layer, but it does appear in a volumetric sample of the same layer. The top layer, then, is not appropriate for a comparison of the two different sampling techniques, since it is not uniform in the vertical direction. The substrate material was found to be typically uniform with depth, so that it is more suitable for such a comparison. The comparison indicates that for the present study, both methods give similar results. A better indication of the comparison is given in Fig. 15, where the size distributions of four samples, two volumetric and two areal all taken at the end of the same experiment, are plotted.

TABLE 3. COMPARISON OF SAMPLING TECHNIQUES

	S5:E1	S5:E1	S6:E1	S7:E1	S7:E6	S7:E7	$\overline{D}_{TV50}$ (mm)	$\overline{D}_{SV50}$ (mm)	$\overline{D}_{TV50}/\overline{D}_{SV50}$
Volumetric Samples									
1st (top) layer D_{TV50} (mm)	2.6	2.0	3.55	3.25	4.15	3.5	3.18		
2nd layer D_{SV50} (mm)	1.6	1.5	1.9	2.65	2.75	2.28			1.43
3rd layer D_{SV50} (mm)	1.9	1.87	2.1	2.59	2.1	2.7		2.22	
4th (bottom) layer D_{SV50} (mm)	1.98	3.0	2.6			3.27			
Areal Samples							$\overline{D}_{TA50}$ (mm)	$\overline{D}_{SA50}$ (mm)	$\overline{D}_{TA50}/\overline{D}_{SA50}$
1st (top) layer D_{TA50} (mm)	5.62	5.3	5.75	6.2	6.15	6.6	5.94		
2nd layer D_{SA50} (mm)	2.7	2.3	1.63	2.63	2.15	2.2			
3rd layer D_{SA50} (mm)	1.85	1.78	1.5	3.9	2.43	1.7		1.99	2.98
4th layer D_{SA50} (mm)	1.7	1.6	1.48	2.2	1.7	2.2			
5th layer D_{SA50} (mm)	1.5	1.56	1.43		2.3	2.2			
6th (bottom) layer D_{SA50} (mm)	1.27	1.4	1.95		3.4	2.8			
$\frac{\overline{D}_{TV50}}{\overline{D}_{TA50}}$							0.54		
$\frac{\overline{D}_{SV50}}{\overline{D}_{SA50}}$								1.12	

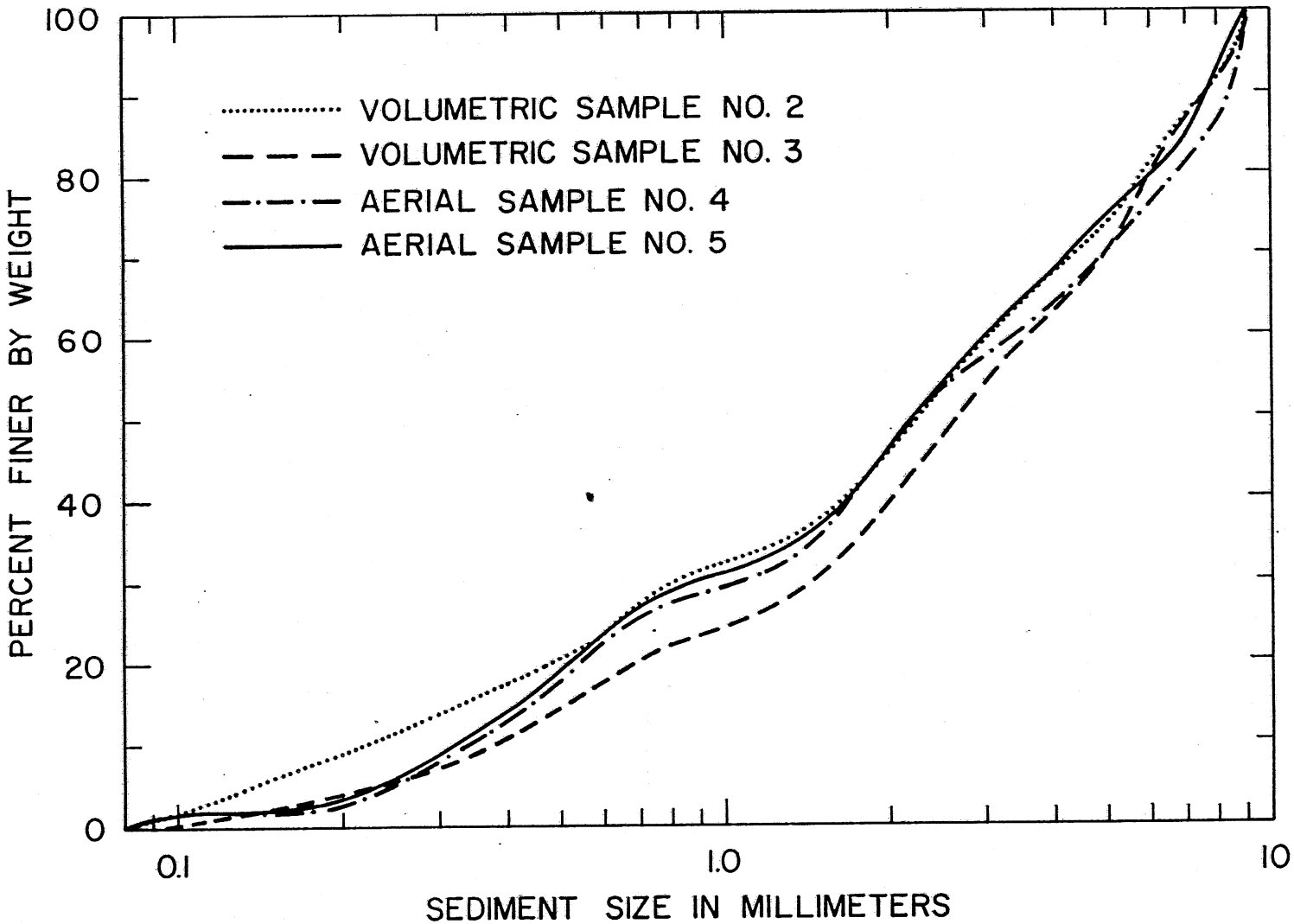

Figure 15. Comparison of volumetric and areal samples. The samples were removed at the end of run S7:E7.

It is thus concluded that for the present study grain size distribution obtained from areal samples can be directly compared with volumetric samples. Some error is so introduced, but at an acceptable level.

6. VELOCITY MEASUREMENTS AND SHEAR STRESS DISTRIBUTION

The instrumentation used to measure velocity profiles has been described in Section 4. Only mean velocity measurements were measured in the present study. The Prandtl tube has been proven to be a suitable instrument for such measurements. In a previous study (Diplas, 1983) the same system was used for velocity measurements under similar flow conditions. The accuracy of the system was examined and found to be very good.

In the long flume velocity profiles were taken along three normals to the bed, all at the same cross-section. One velocity profile was taken at the center of the channel and the other two 7.5 cm on each side of the center. The first velocity measurement of each velocity profile was taken at the channel bed, the next five 0.13 cm apart, the next four 0.25 cm apart, and the rest of them 0.51 cm apart up to the water surface. The middle velocity profile was unaffected by flow asymmetry due to presence of the channel sidewalls. In most of the experiments the other two velocity profiles were slightly affected by the sidewalls. A few of them were strongly affected.

The velocity measurements were used to estimate the bed shear stress distribution. Leighly's (1932) method is employed here to calculate bottom shear stresses. Leighly assumed that the lines orthogonal to the isovels are lines of zero shear because the mean velocity gradient normal to them vanishes. An isovel is defined as a line in the flow field along which the value of the velocity is constant. This assumption is a very good approximation in regions of weak secondary currents. In present experiments the effect of the secondary currents was neglected, because even though they were present they were expected to be rather weak. The following procedure is used to estimate the bottom shear stress; first the isovels of a cross-section are drawn, then orthogonals to the isovels are plotted, and finally the momentum balance of the flowing water confined by two orthogonals, the channel bottom, and the water surface, is considered. An example of a bottom shear stress distribution derived in this way is shown in Fig. 16. This method was used to calculate the bottom shear stress distribution for all the experiments of series four and five.

The bed shear stresses are used in the present study for bedload calculations, for which only a knowledge of the bottom stress averaged over the channel width suffices. Because the long flume is relatively narrow, the bed shear stresses are expected to be smaller than in the case of a wide flume with the same surface slope, bed material, and channel depth. A procedure that accounts for side-wall correction was introduced by Johnson (1942) and modified later by Vanoni and Brooks (1957). This method was used here. The isovel method is used to test whether or not the Vanoni and Brooks method accurately estimates the average bottom stress. From the glass walls of the long flume it was observed that minimal grain motion was taking place very close to these walls. As a result, the central region of

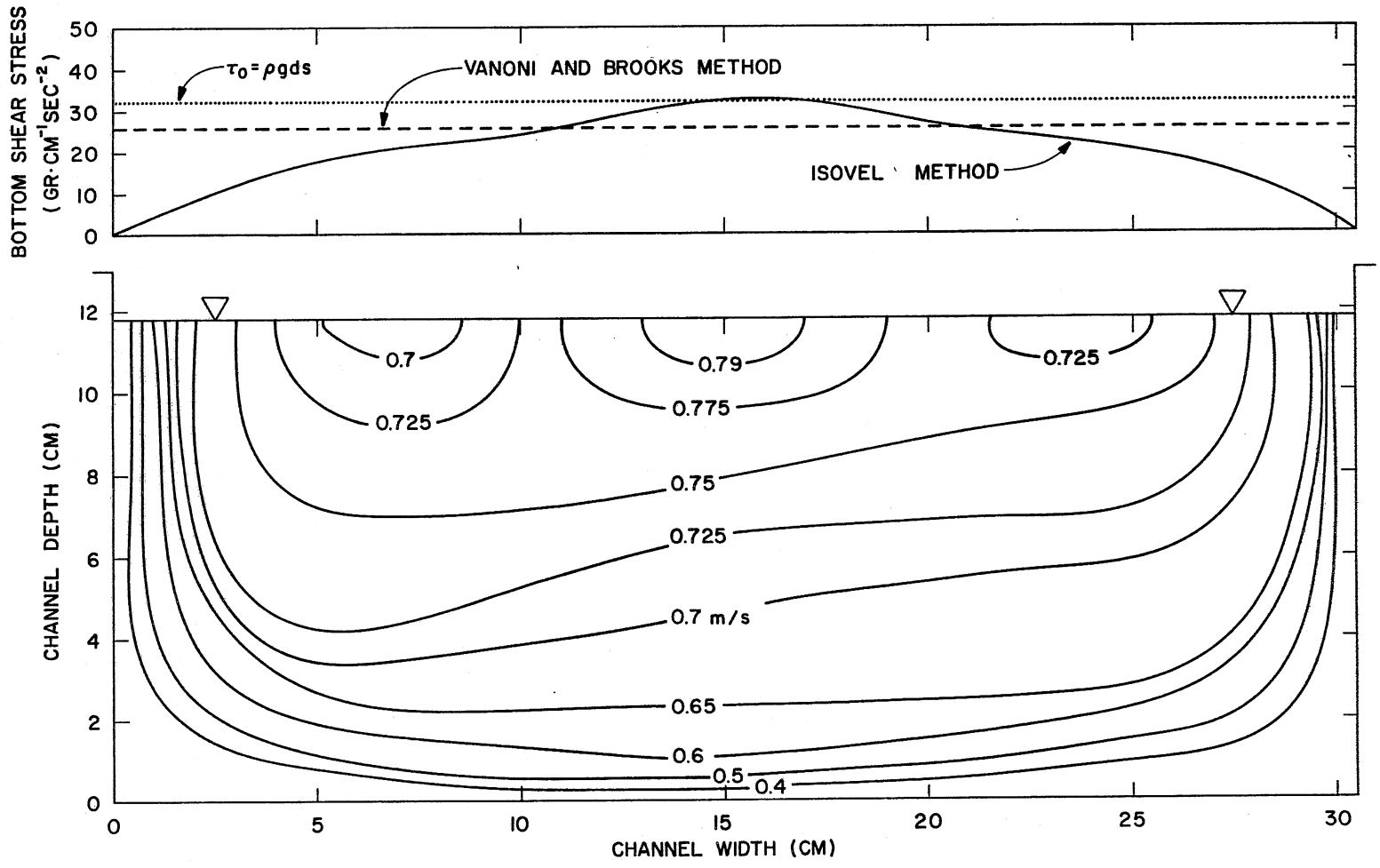

Figure 16. Plot of isovels and shear stress distributions derived from different methods, for run S4:E2.

the channel, 24 cm wide, was considered to be the active part of the bed. The absence of bedload in the regions next to the side-walls, each of them approximately 3.2 cm wide, was attributed to the presence of these walls.

In Table 4 the average bottom shear stresses, obtained for the experiments of series four and five from different methods, are compared. These methods include: the Vanoni and Brooks method, the values obtained from the isovel method averaged over the whole channel width, the values obtained from the isovel method averaged over the central 24 cm of the channel width, and the method that neglects the side-walls. The first and third methods give similar values. The Vanoni and Brooks method was thus considered to predict fairly accurately the average bottom stress for the central 24 cm of the channel width. The values calculated by this method were used to quantify the average bed shear stress of the channel.

TABLE 4. COMPARISON OF DIFFERENT METHODS USED TO CALCULATE THE MEAN BED SHEAR STRESS

	Vanoni and Brooks Method	Isovel Methods Averaged over the Whole Channel Width	Isovel Method Averaged over the Central 24 cm of the Channel Width	Effect of Sidewalls is Neglected $\tau = \rho gds$
	$gr/(cm\ sec^2)$	$gr/(cm\ sec^2)$	$gr/(cm\ sec^2)$	$gr/(cm\ sec^2)$
S4:E1	36.0	28.33	33.2	42.4
S4:E2	25.7	21.88	24.3	32.47
S4:E3	27.58	25.32	25.0	34.34
S4:E4	27.11	23.82	26.4	33.77
S4:E5	23.76	20.91	23.5	30.40
S4:E6	25.37	23.8	26.4	32.1
S5:E1	24.5	22.98	26.0	33.35
S5:E3	22.72	19.38	20.8	31.86
S5:E4	28.48	26.96	29.6	37.58
S5:E5	27.77	25.44	27.2	37.04
S5:E6	16.25	16.32	17.0	24.94

7. RESULTS FROM THE EXPERIMENTS WITHOUT FINES

LONG FLUME

The Approach to Equilibrium without Fines

The first experiment of each series is conducted without any fines being fed into the flume. The purpose of this experiment is to allow for the formation of the surface pavement present in gravel streams. It is expected that in this way the conditions encountered in natural streams are closely simulated in the flume. The existence of such a pavement plays an important role with respect to the bedload transport as well as the process of fines intrusion into the bed (Parker et. al., 1982a, 1982b, 1982c; Frostick et.al., 1984).

The channel was screeded at the beginning of each series to provide the desired initial flume slope. The process of vigorous screeding tended to winnow some fine material below the surface, creating an ersatz pavement. This can be seen in Fig. 17. On the average the relation between pavement median size D_{p50} and subpavement median size D_{50} after the screeding was $D_{p50} = 1.7\ D_{50}$.

The most significant changes in the state of the channel bed, the water surface slope, and bedload transport rate took place during the first few hours of the experiment. The sediment transport rate at the beginning of the experiment was significantly higher than the ultimate equilibrium value. During this period the bed is very active, and the bedload is basically composed of material with sizes near the median grain size of the original mixture and smaller. A significant part of the bedload moves in discrete linguoid waves of sediment, each one of which consists of well-sorted material. Each wave moved through the channel as a discrete unit, fading with time as the channel approached the equilibrium state. During this process a significant part of the finer material ($D < 0.5$ mm) that moves with these waves of sediment infiltrates below the surface layer. At the end of the experiment when pavement, subpavement, and bottom layer samples were extracted from the channel bed it was observed that the subpavement collects most of these finer particles ($D < 0.5$ mm). At the equilibrium state, one, or at most two, weak waves of sediment appeared occasionally. In some series these waves disappear during some experiments to appear in some later experiment. The existence of such waves have also been reported from field observations (Milhous, 1973). These waves were predominately composed of particles with diameter $D < 3.0$ mm. As an example, at the equilibrium state of run S3:E1, two waves of sediment were observed, one composed of material near 0.8 mm in diameter, and the other with material around 2.5 mm in diameter. The bedload that was not moving in waves was made up of all sizes available in the surface layer, with a higher percentage in the smaller diameters, but not biased toward a specific particle size. During the experiments an attempt was made to avoid measuring the bedload rate when a wave of sediment was exiting the channel. The variation of bedload rate with time during experiment S3:E1 is shown in

Fig. 18. In two experiments a winding ridge appeared at the center of the channel bed. This ridge was present in about half of the length of the channel and was mainly composed of uniform material with diameter around 2.0 mm.

Movement of the Grains

The transparent channel side-walls facilitated the observation of the motion of grains. At the equilibrium state of S3:E1 dye was utilized to visualize the bursting phenomenon near the bed, and to explore its possible relation with the motion of the grains. The needle of a syringe was placed inside the bed, with the tip of the needle within the surface layer of bed material. A plastic tube 0.8 mm in diameter, attached on the channel side-wall, connected the needle with the body of the syringe, from where the dye was pumped into the flume. A video camera was used to record both the motion of the grains and to follow the injected dye.

It was observed that the initiation of the motion of the bedload grains correlates closely with the bursting that takes place close to the channel bed. It was thus assumed that the motion of the grains could be used as a means of visualizing those turbulence bursts that are capable of moving the grains on the flume bed. The boundary shear stress in the present experiments was fairly high so as to render the grains at the surface of the channel bed very close to the threshold of motion. Under such conditions even a burst that is small in strength is expected to mobilize some grains of the pavement. If this is true, then most of the bursts that take place near the bed can be accounted for by observing the motion of the particles at the channel bed.

A video camera was used to record the action at the bed of the channel. Then, the so obtained videotape was repeatedly played on a monitor. Most of the monitor screen was covered with paper leaving only an opening at the center of the monitor that depicted an area at the center of the channel bed of approximately 5 x 5 cm^2. Then 20 series of observations were made, lasting 20 sec each. During this 20 sec period, the number of times that the pavement grains were mobilized was counted. Usually not only an isolated particle was mobilized, but rather many particles were mobilized at the same time. Sometimes the particles mobilized during a burst were larger or smaller than those set in motion in another burst. This may be due to the different strength of the individual bursts. From these observations it was found that the dimensionless bursting period, $U_\infty T/\delta$, where U_∞ is the velocity at the outside part of the boundary layer, T_∞ is the bursting period, and δ is the boundary layer thickness, took a mean value around 6.2, with a standard deviation of 1.0.

Measurements of the bursting period in bounded turbulent flows have been done mainly in experiments with smooth walls. There is some controversy regarding the variables that should be used to scale the bursting period. Initially, it was thought that wall variables are more appropriate for such scaling. Later, outer variables were used to obtain a dimensionless bursting period that was constant independent of Reynolds number (Cantwell, 1981). A mean value around six is suggested for TU_∞/δ (Cantwell, 1981). More recently Blackwelder and Haritonidis (1983) conducted some detailed measurements in a boundary layer and found that the bursting period when scaled with outer variables decreases with Reynolds

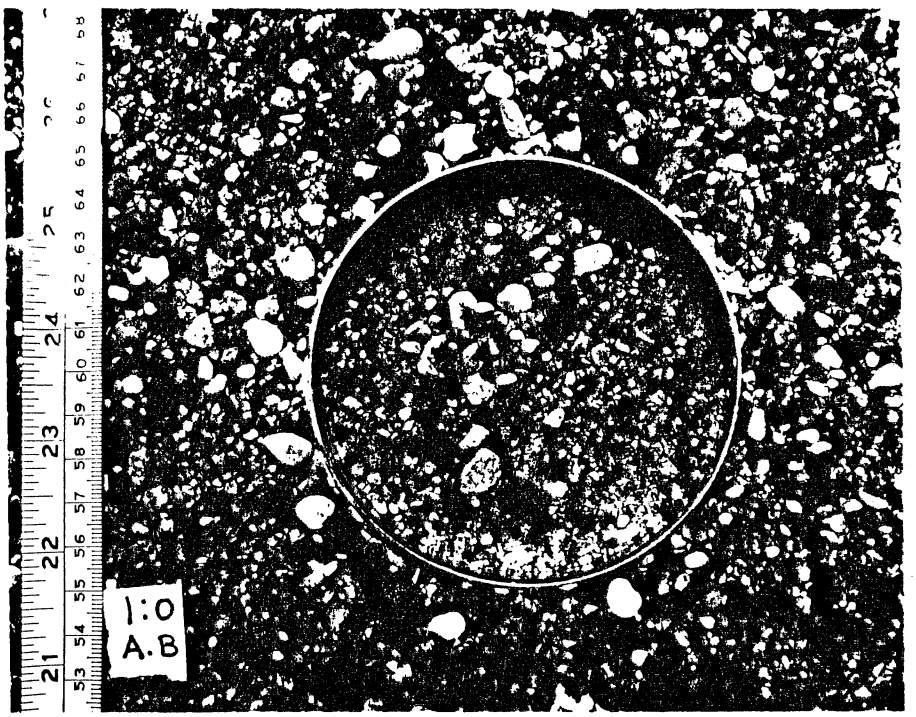

Figure 17. Comparison of surface bed material and substrate material after screeding before the beginning of run S1:E1.

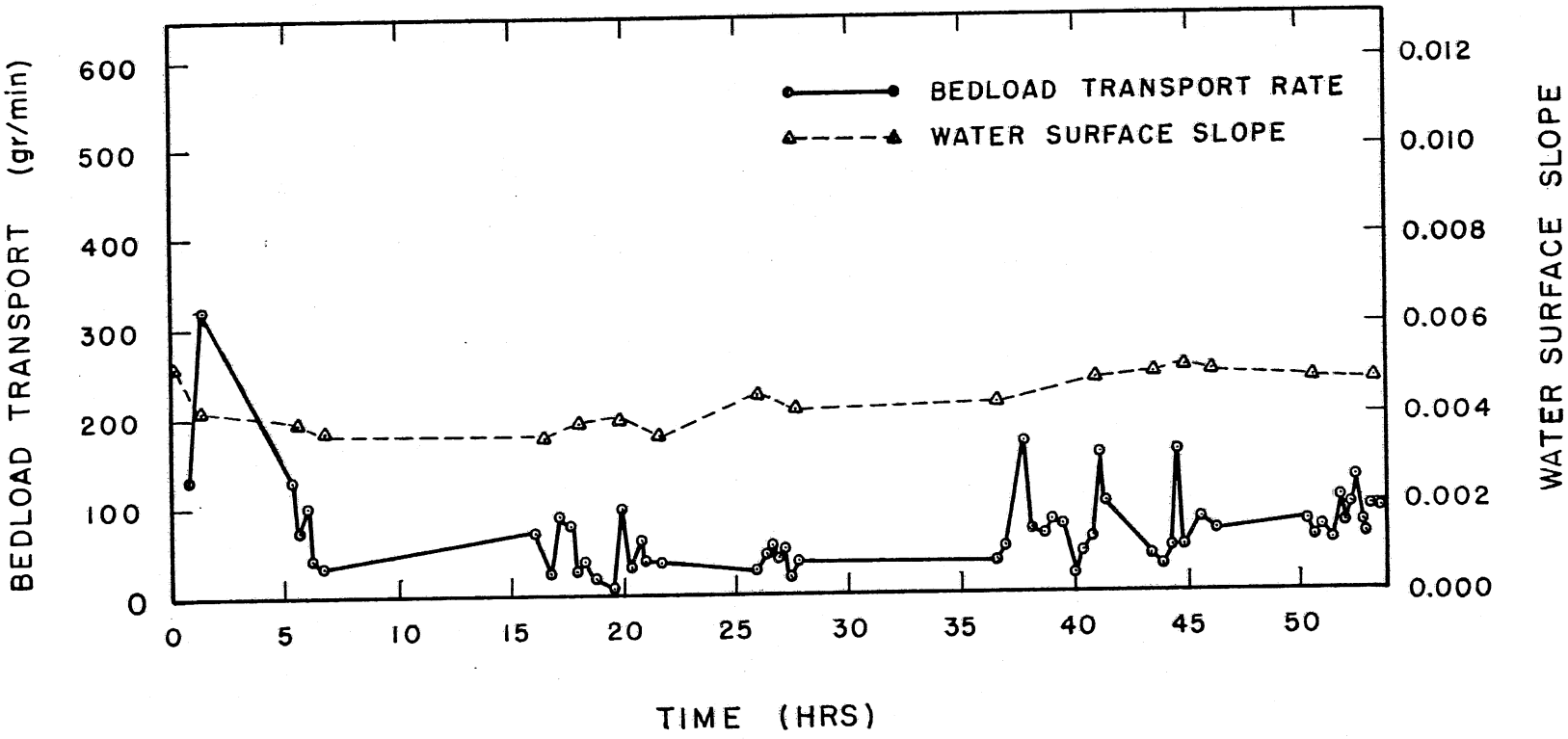

Figure 18. The variation of bedload transport rate and water surface slope with time during run S3:E1.

number, while when it is scaled with wall variables, e.g. ν and u_*, is constant independent of Reynolds number. The value that TU_∞/δ reached for the maximum Reynolds number attained during the latter study was about 3.7. Luchnik and Tiederman (1983) examined the bursting period in a two-dimensional channel flow. They found that the bursting period, when normalized with outer variables, initially decreases with Reynolds number to attain a constant value of about 3.2 for large Reynolds numbers.

Nowadays, it is believed that the mean bursting period for bounded turbulent flows with smooth walls scales with inner variables (Blackwelder and Haritonidis, 1983). The results mentioned in the previous paragraph suggest that the bursting period scaled with outer variables becomes independent of Reynolds number for high Reynolds numbers.

In the case of a rough wall the kinematic viscosity does not play an important role in the mechanics of the flow adjacent to the wall. It thus seems that for such flows the use of outer variables to scale the bursting period might be appropriate. If the bursting period scaled with outer variables becomes constant for high Reynolds number in the case of smooth walls, then one might expect that for rough walls this will be true even for moderate Reynolds numbers.

When outer variables, e.g. U_∞ and δ , are used to normalize the bursting period, the mean value obtained from the present study is close to the values obtained by Blackwelder and Haritonidis (1983), and Luchnik and Tiederman (1983); these values are 6.2, 3.7 and 3.2, respectively. Instead when ν and u_* are used to normalize the bursting period, the mean value obtained from the present study is an order of magnitude larger than the mean value reported by Blackwelder and Haritonidis; that is, 4,100 and 300, respectively.

Sutherland (1967) and Grass (1971) have also indicated that the turbulent bursts are largely responsible for the initiation of movement of bedload grains. A simple argument can support this observation. It was observed many times that the same particles were moving as bedload. A specific grain on the bed was mobilized and moved a few centimeters downstream, where it rested for a while, to be mobilized again some time later. It is known that the static friction coefficient has a higher value than the corresponding dynamic friction coefficient. This means that a particle requires a greater force to commence motion, than it does to continue motion. From this observation, it is rather clear that the shear stress due to the mean flow is unable to keep a grain moving, much less to initiate its motion. Thus turbulent bursting seems to be a likely mechanism capable of providing the additional force required to set a bed particle in motion near critical conditions.

The Role of the Pavement

When the bottom shear stress is very low, such that the pavement is stable, the flow can transport only the finest particles found in the pavement. At this stage the material being transported depends on availability in the pavement layer, since the stable pavement protects the small particles in the substrate from being exposed to the fluid forces. When the flow is strong enough to set some of the larger pavement particles in motion, the underlying material is no longer protected and becomes

available for entrainment. At this stage the bed material becomes the source of the bedload. Thus, hydraulic parameters become more important than availability in describing the bedload transport. The shear stress that "breaks" the pavement is called the critical stress for the pavement. Milhous (1973) gives a complete account of this phenomenon. During the experiments of the present study, the shear stress was always higher than the critical stress for the pavement. It has been found by several researchers that the material of an armor layer and the bedload in paved streams become coarser as the bottom stress increases (Proffitt, 1980; Milhous, 1973). During the present experiments it was observed that the average D_{p50} for a series was increasing with the average value of the bed shear stress for a series; to wit for the fifth series the average bed stress was 25 gr/(cm sec^2), for the fourth series 27 gr/(cm sec^2), for the first 28 gr/(cm sec^2), for the second 30.5 gr/(cm sec^2) and for the third series 35 gr/(cm sec^2), while their corresponding D_{p50} values were 4.5 mm, 4.85 mm, 4.89 mm, 5.34 mm, and 5.34 mm.

Milhous (1973) described the pavement formation as a process of segregation of material. The initial bed mixture should be nonuniform, while the applied shear stress should be between the critical stress of the smallest particles and the largest particles for the pavement to occur. A mixture is considered to be nonuniform when its geometric standard deviation is larger than 1.5. Parker (1980, 1982b, 1982c) and Milhous (1973) have described the features and the role of the pavement. The results from this study agree with their conclusions. The bed was always active, but a closer look would reveal that there are long rest periods between movements of a particle. Parker et al. (1982c) describe this as follows: "motion on the bed was continuous in the macroscopic sense, but sporadic in the microscopic sense." The bedload grains continually interchange with pavement grains. Although the bed is active, only a very small number of grains are in motion at a given instant. This is what Parker et al. described as sporadicity of the motion. This sporadicity allows for the coexistence of the pavement with the motion of the particles in it. From the present experiments it was demonstrated once more (Parker, 1980) that the pavement is a mobile bed phenomenon that is in place even during floods capable of mobilizing even the coarsest particles of the pavement.

Fenton and Abbot (1977), Paintal (1971), Ettema (1980), and Egiazaroff (1965) have all indicated the importance of the protrusion of a grain into the flow to its resistance. It was found (Fenton and Abbot) that for a particle completely exposed into the flow the critical Shields stress was 0.01. When the particle did not protrude into the flow at all, its critical shields stress was 0.15, and was even higher when the top of the particle was placed below the surface of the surrounding bed.

The pavement is considered to be one of the most important features of gravel-bed streams. Parker and Klingeman (1982b) advanced the thesis that the pavement acts as a regulator that renders all the available grain sizes of nearly equal mobility. This is accomplished by over-representing the coarser grains that are intrinsically less mobile in the pavement. In this way the increased availability of the coarser particles, combined with their increased protrusion into the flow, balances their larger weight which reduces their mobility. The pavement protects the smaller particles of the bed material, which are stored below the pavement, from being washed

away. If this theory of approximate equal mobility is true, the bedload size distribution should be close to that of the subpavement, which represents the bulk of the bed material.

Typical relations among surface layer median size D_{p50}, subpavement median size D_{50}, and bottom layer median size D_{b50} at the equilibrium state are $D_{p50} = 2.4\ D_{50}$ and $D_{b50} = D_{50}$. The major difference between bedload and subpavement material was in the amount of finer grains contained in each one of them. The finer grains ($D < 0.5$ mm) were much fewer in the bedload. The ratio of the pavement median size to subpavement median sizes for natural gravel streams ranges from 1.5 to 3.0 with values between 2.0 to 2.5 encountered more often (Parker, 1980). Thus the present results are representative of the field case. Analysis of the bedload samples indicates that the bedload becomes slightly coarser as equilibrium is approached. The bedload median size, $D_{\ell 50}$, was much closer to the subpavement median size than the pavement median size; to wit $D_{\ell 50} = 1.14\ D_{50}$, $D_{\ell 50} = 0.5\ D_{p50}$. A view of the pavement and the subpavement material is shown in Fig. 19. The size distributions of the pavement, subpavement, bottom layer, and bedload material for experiment S4:E3 are shown in Fig. 20.

At the equilibrium state, the composition of the surface bed material usually varied along the flume, that is parts of the flume bed were coarser or finer than others. Field observations have also indicated considerable variation of the material in the surface layer along and across the channel. The narrow width of the long flume did not allow for significant lateral variation.

From the glass side walls it was also observed that only the grains exposed to the flow could be mobilized. Thus grain motion was basically confined to the surface layer. Parker (1980), and Dhamotharan et al. (1980) reported similar observations from their own experiments. More specifically Dhamotharan et al. used paint to spray the grains. They found that the thickness of the layer from which grains are entrained by the flow is about equal to the D_{65} of the pavement layer.

Excluding the occasional appearance of a ridge, the channel bed was always flat. The narrow width of the flume suppresses any tendencies of the bed to develop bars.

TILTING FLUME

The purpose of the experiments in the tilting flume was to examine the effect of channel bedforms on the mechanics of fines retention in the channel bed. The first task here is to simulate in the laboratory flume the bed features commonly encountered in gravel-bed streams. A pool-and-riffle sequence in conjunction with an alternate bar formation, is the most important bedform characteristic of single-thread gravel streams. As mentioned earlier, the first experiment was performed in the absence of fines. The initial channel slope was 0.012, and the Shields stress based on the D_{50} of the original mixture was $\tau^*_{50} = 0.12$. The total duration of the first experiment was 34 hours. The coarse material feed rate was 270 gr min during the first 23 hours, and 324 gr/min for the subsequent 11 hours. The bedload variation with time for the experiment S7:E1 is shown in Fig. 21. In Fig. 22 the water surface slope variation is shown for the same

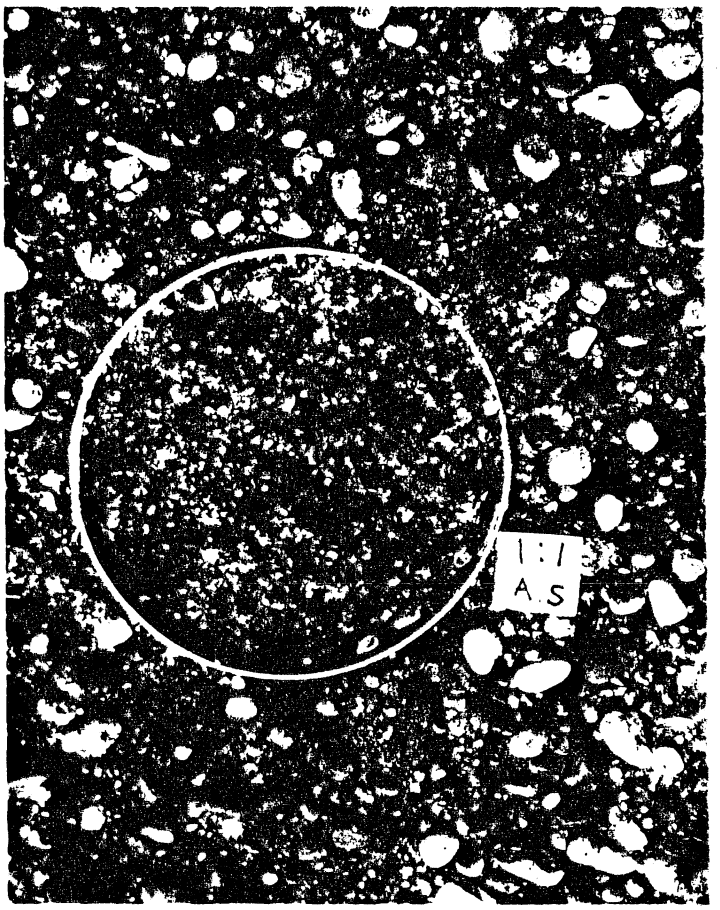

Figure 19. Pavement and subpavement material at the end of experiment S1:E1.

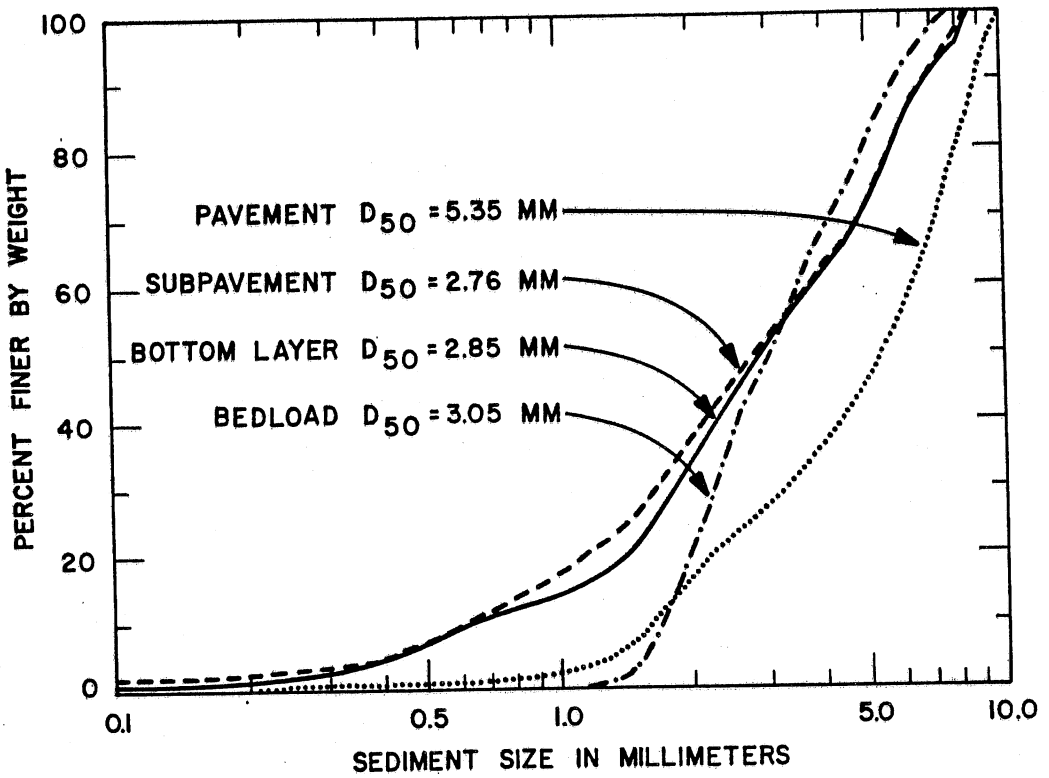

Figure 20. The size distributions of pavement, subpavement, bottom layer, and bedload material at the end of experiment S4:E3.

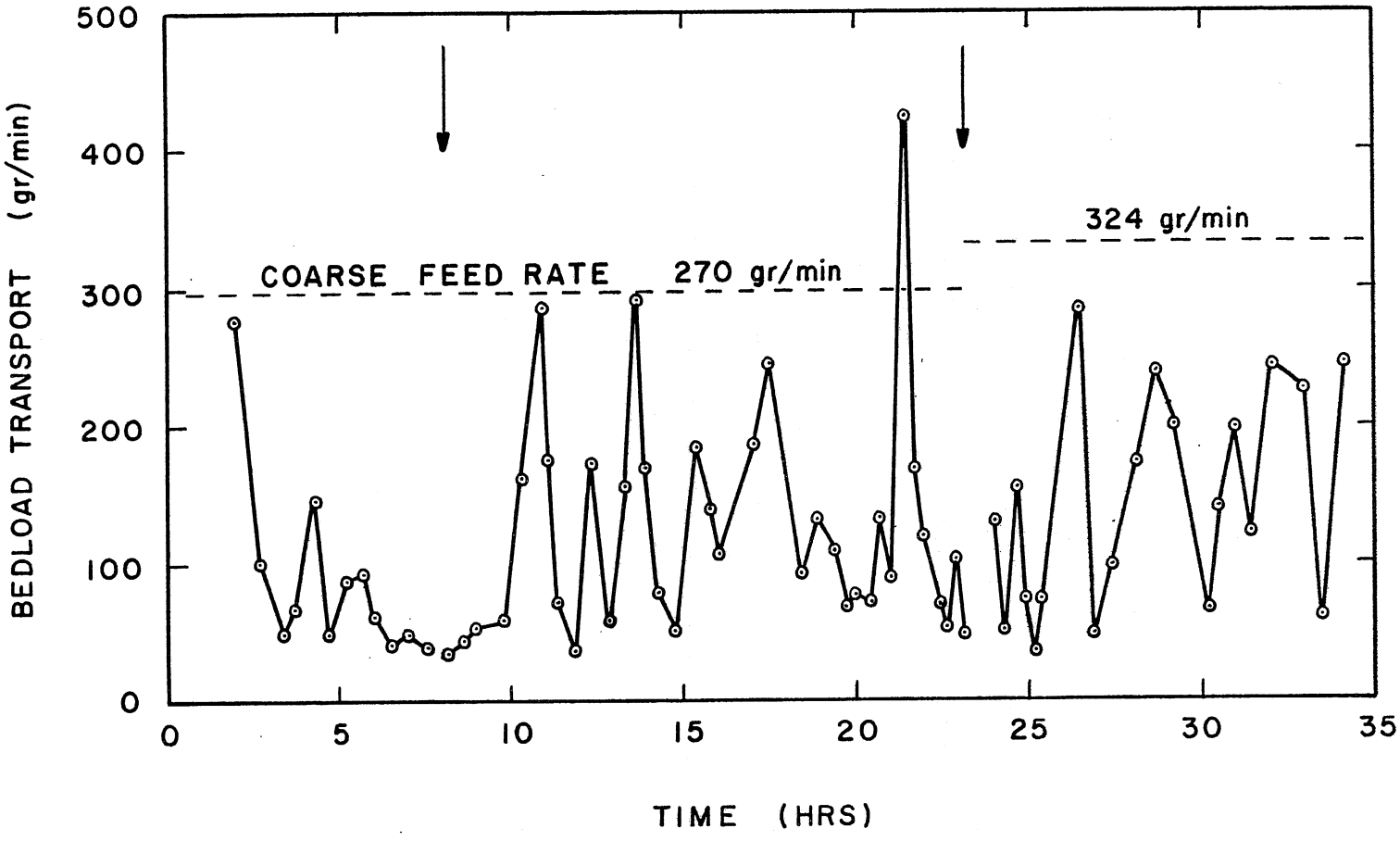

Figure 21. Bedload variation for experiment S7:E1. The arrows indicate the times at which the experiment was interrupted.

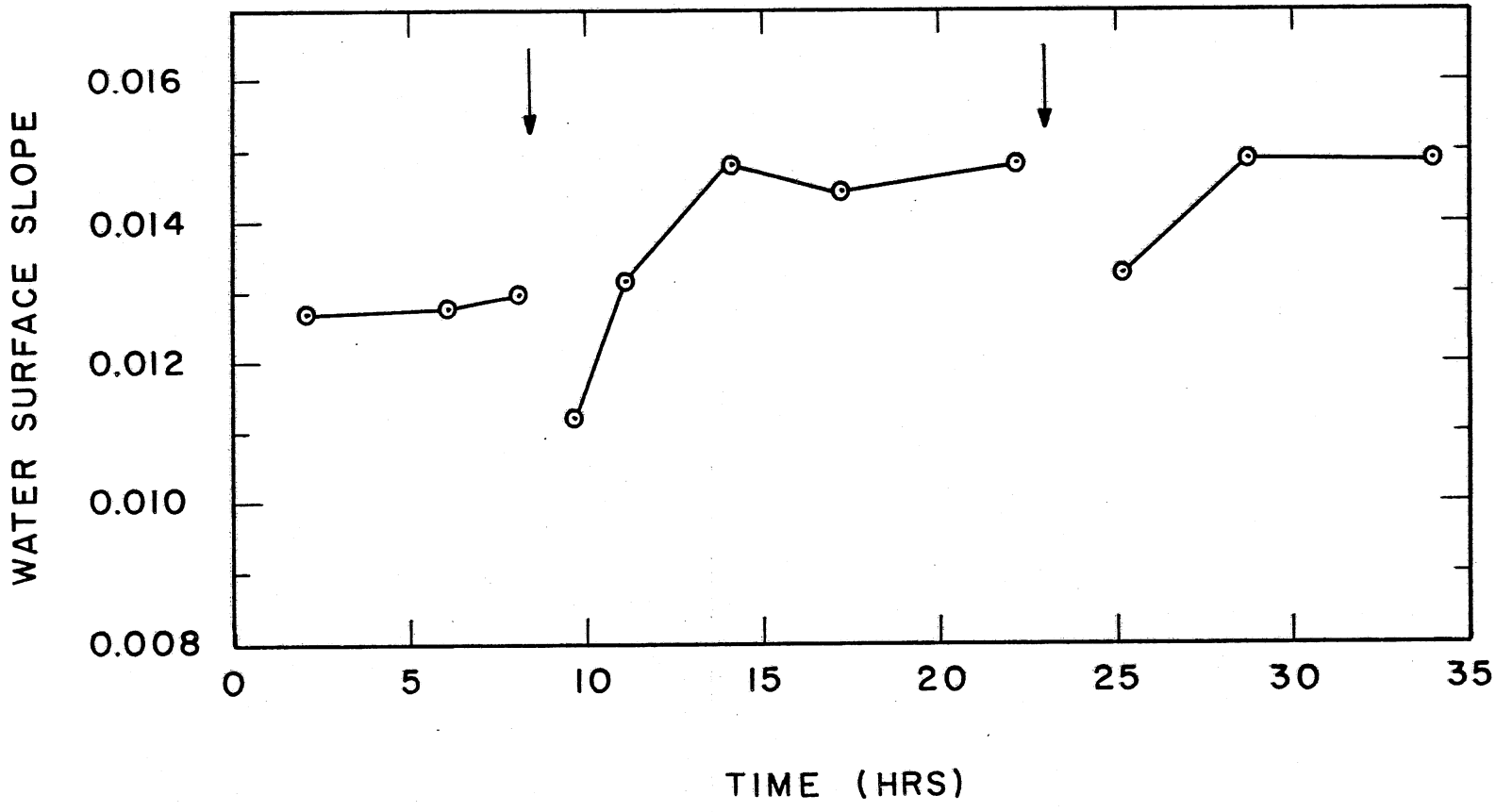

Figure 22. Water surface slope variation for experiment S7:E1. The arrows indicate the times at which the experiment was interrupted.

experiment. From Fig. 21 it seems that the experiment was stopped rather early, since the bedload at the exit was about 35% lower than the feed rate. Nevertheless, the rest of the channel characteristics, such as the water surface slope and the state of the bed, indicated that the channel was close to equilibrium.

When the channel was drained of the water, a well-developed bar pattern was revealed. Three bars, alternatively attached to the channel side walls, had formed. The first and third bars were influenced by the entrance and exit conditions, respectively. Only the second bar seemed to be fully developed. Using a point gauge, the bed elevation of the drained channel was measured in detail. This was done in cross-sections spaced in 20 cm intervals along the channel, and at intervals of 5 cm across the channel. A computer-generated plot of the lines of constant elevation based on these measurements is shown in Fig. 23. The labels on the lines indicate the vertical distance from a plane parallel to the mean channel water surface slope in centimeters.

The bed configurations obtained at the end of the first experiment are now compared with field observations. There is an abundance of field studies pertinent to bedform characteristics of gravel-bed streams. Here, a case studied by Lewin (1976), and a survey paper by Bluck (1982) are used as basis for the comparison.

Lewin observed the developments that took place in the Ystwyth River, located in mid-Wales. Part of this river was straightened in 1969, yielding a straight plane-bed gravel channel, but without bank protection works. A month later, after a period of high flow, the plane-bed was replaced by a series of regularly spaced transverse mid-channel bars. The state of the bed realized ten months later is shown in Fig. 24 (Lewin, 1976). A comparison of Figs. 23 and 24 suggests a similar bed topography. The only essential difference is due to the solid walls of the laboratory flume, which do not allow for bank erosion. A view of the second bar formed in experiment S7:E1 is also shown in Fig. 25. The lengh of this bar is about 4.3 m, its maximum width approaches the channel width, and its crest height is about 2.5 cm. Then $\lambda/B = 18$, where λ = alternate bar wave length and B = channel width; this value is close to the upper limit of the observed values of this ratio, as is noted by Ikeda (1984).

For most of the experiments in the tilting flume three to five sets of bed samples were extracted. Usually, three of them were taken along the middle bar, and one or two in the pool area.

Close-up views of the material composing the upstream, middle, and downstream parts of the second bar are shown in Figs 26, 27, and 28, respectively. A schematic of the bar sequence and the material composing the second bar is shown in Fig. 29. The above figures demonstrate clearly a variation in the size and shape of the grains along the bar. The grains of the surface at the upstream part of the bar, called the bar head, have a median size $D_{p50} = 7.2$ mm; at the middle of the bar the D_{p50} is 6.8 mm and at the downstream end, called the bar tail, the D_{p50} is 4.7 mm. The bar tail also has a significant amount of grains in the sand and silt range, which are absent in the rest of the bar (see Fig. 28 and Table A1:7). The number of disc-shaped particles decreases significantly from the head to the tail of the bar, while the number of the well-rounded grains increases.

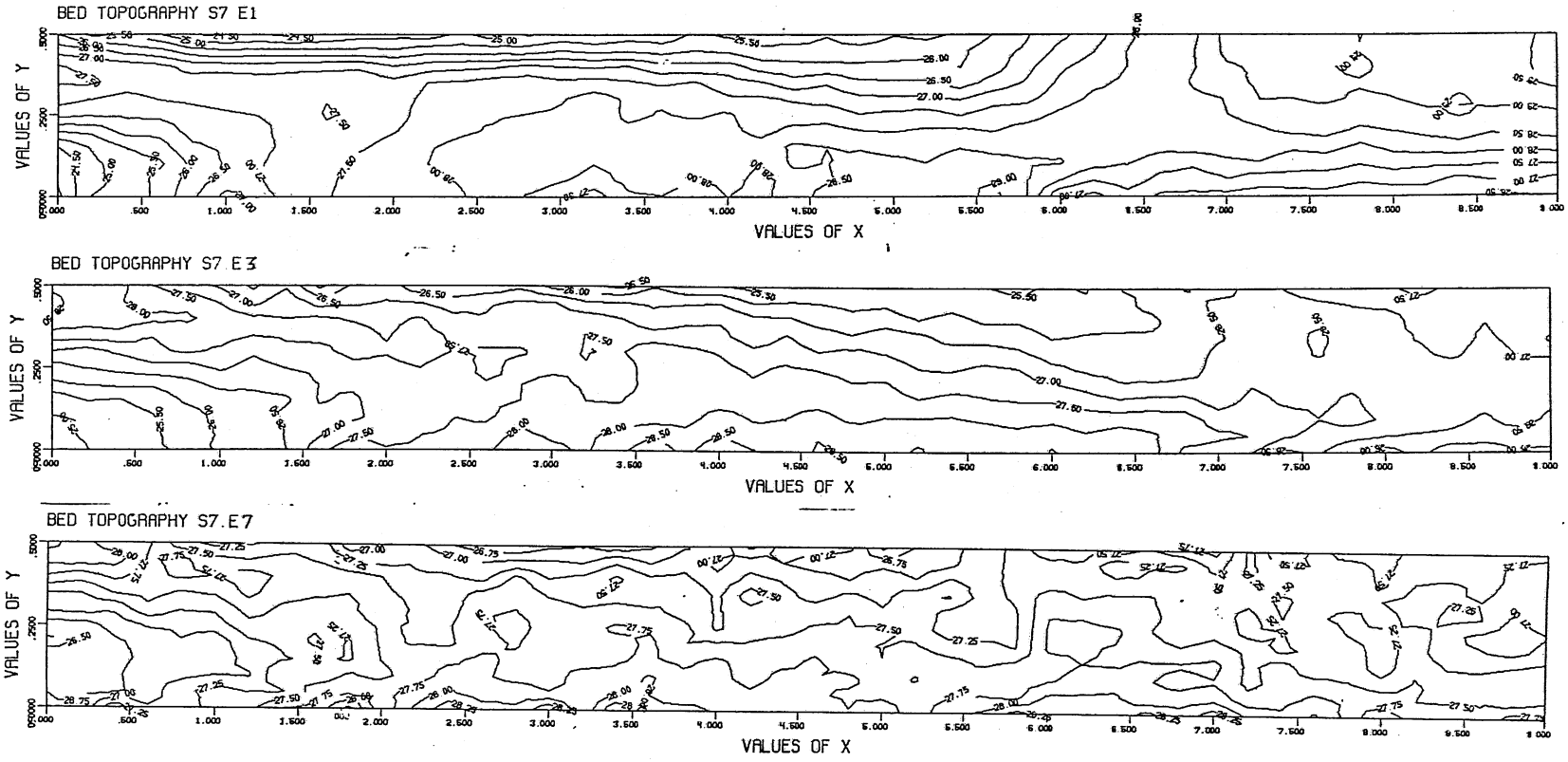

Figure 23. Plots of channel bed level lines at the end of the experiments (a) S7:E1, (b) S7:E3, and (c) S7:E7. The values of the level lines represent distance from a plane parallel to the mean water surface plane, in a direction normal to that plane. The flow direction is from left to right.

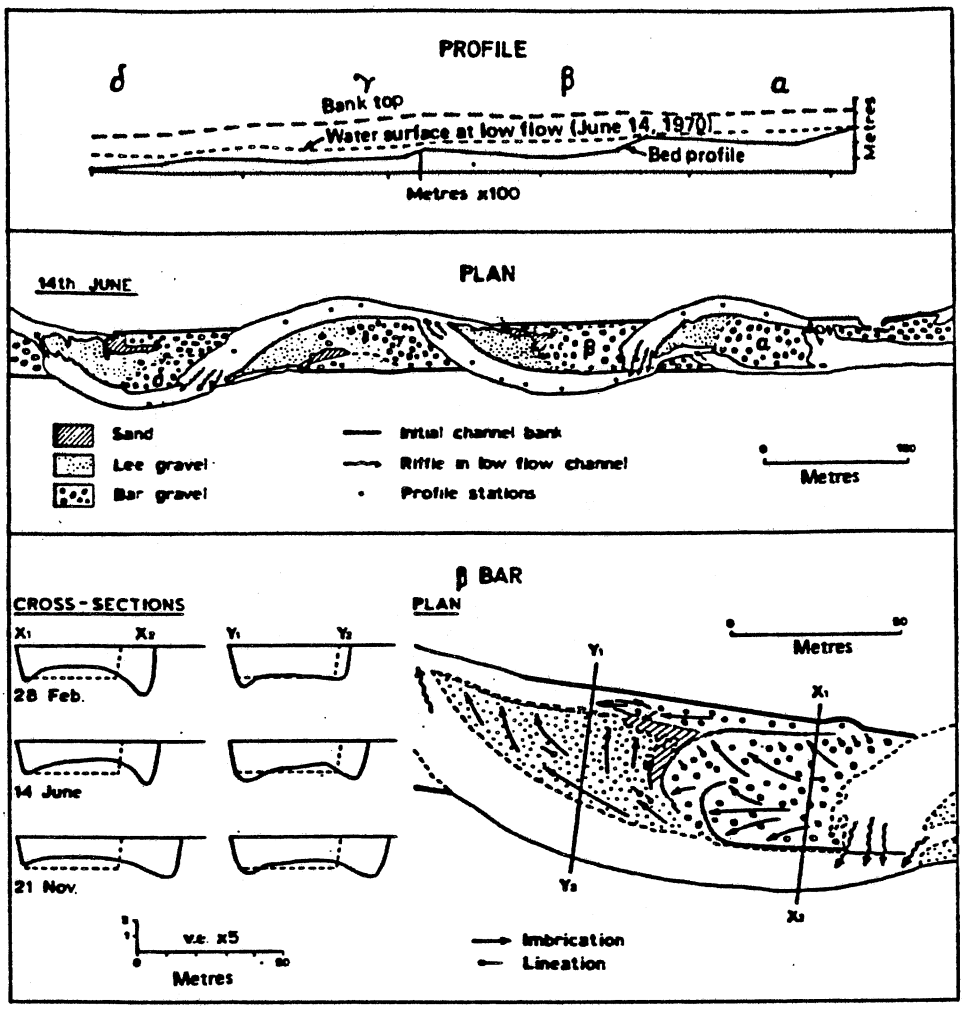

Figure 24. State of the bed ten months after straightening in a reach of Ystwyth River. After Lewin, 1976.

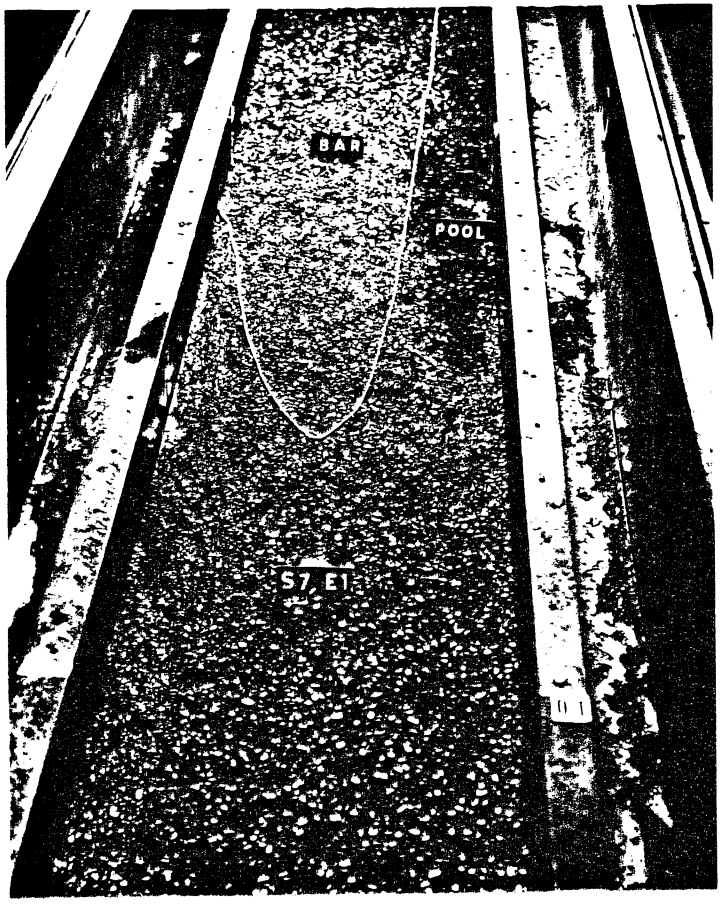

Figure 25. View of the second bar downstream of the channel entrance formed during experiment S7:E1.

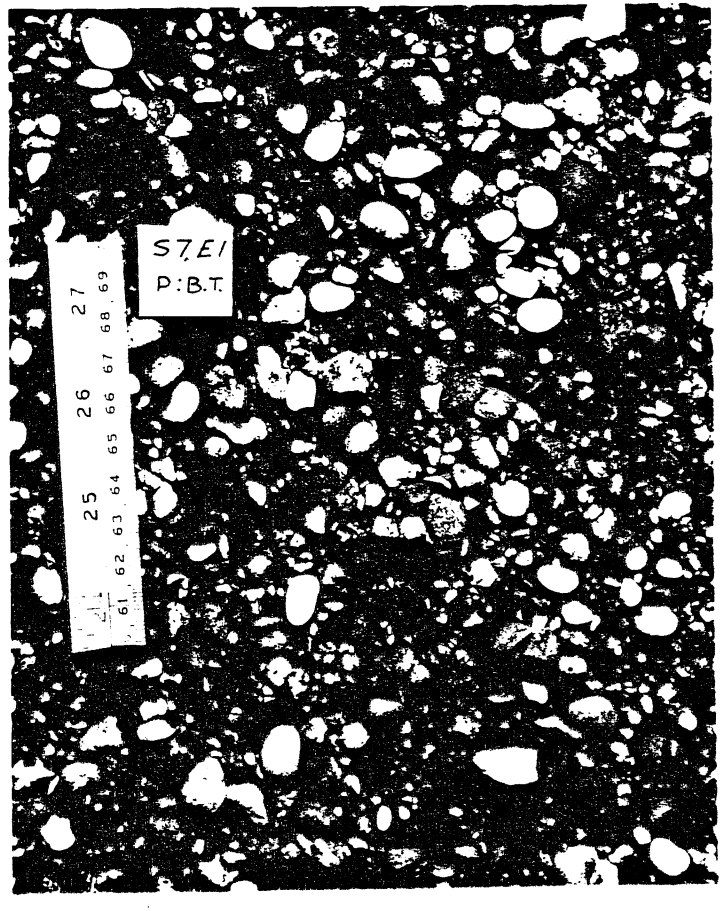

Figure 26. Close-up view of the material at the upstream part, i.e. head, of the second bar formed downstream of the entrance of the tilting flume in experiment S7:E1.

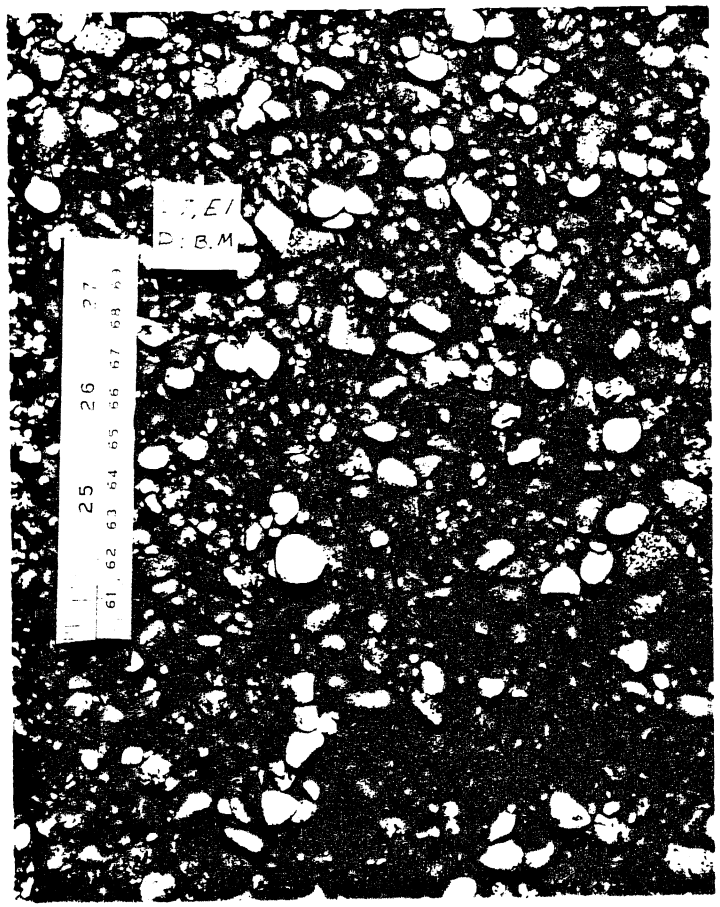

Figure 27. Close-up view of the material at the middle part of the second bar downstream of the channel entrance formed during experiment S7:E1.

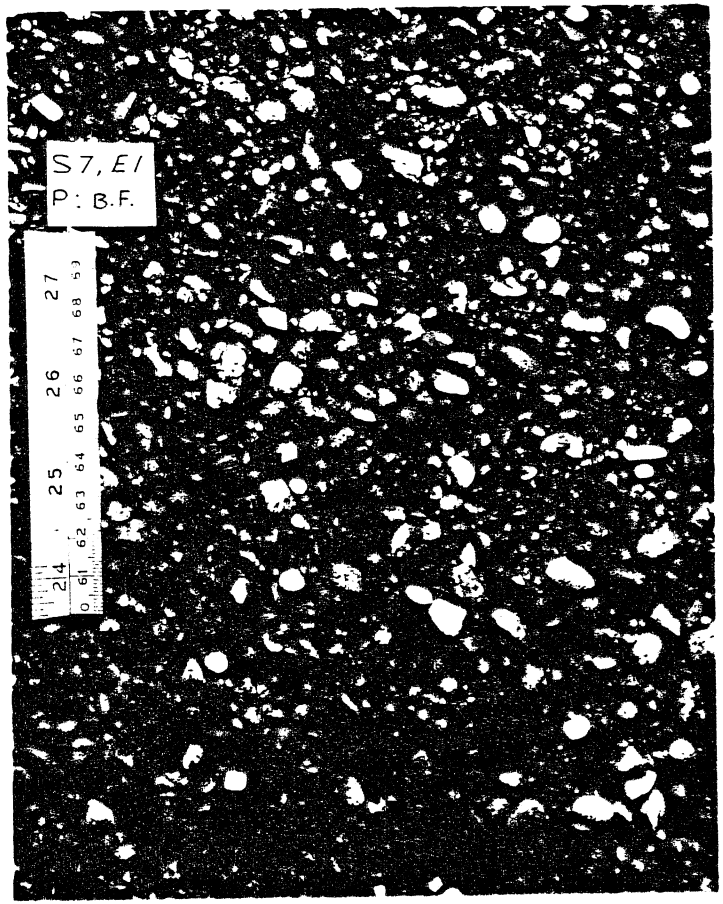

Figure 28. Close-up view of the material at the downstream part i.e. tail, of the second bar formed downstream of the entrance of the tilting flume in experiment S7:E1.

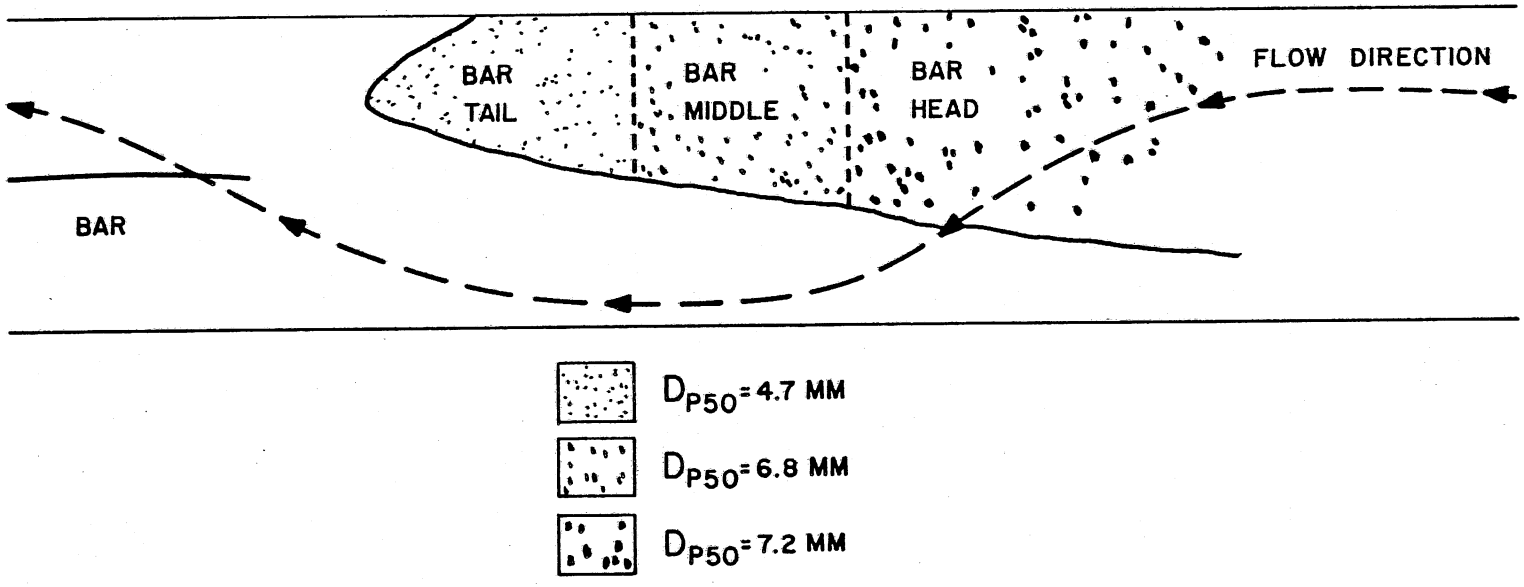

Figure 29. Schematic of the bar sequence and the surface bed material on the second bar downstream of the entrance of the channel in experiment S7:E1.

The higher percentage of disc-shaped particles at the head and middle of the bar enhances the imbricated structure, which in turn increases the stability of the grains in these areas. The bar head is also the highest point of the bar, although the height variation along the top of the bar is small (Fig. 23). The observations reported here agree in every aspect with the descriptions given by Lewin (1976) and Bluck (1982). Bluck attributes the size and shape segregation of the grains along the bar to the role of turbulence at the sediment-water interface. He explains that the larger particles at the head of the bar increase the intensity of the turbulence, resulting in downstream movement of the smaller and more rounded grains which cannot tolerate the increased turbulence intensity. These grains then settle in the bar tail, where the absence of the large particles reduces the turbulence intensity. Bluck's explanation seems to overstate the role of turbulence in the segregation process of the grains along the channel bar. The amount of water flowing over the bar might be instead the cause of this size segregation of the material at the surface of the bar. A larger part of the total flow rate passes over the bar head than over the bar tail, while most of the channel discharge goes through the channel thalweg. Consequently, the size of the grains that the flow can mobilize at the bar decreases in the downstream direction, but even at the bar head the coarsest particles cannot be mobilized. Thus selective motion of particles results in a finer bar tail and coarser bar head.

The grain characteristics mentioned in the previous paragraph refer only to the surface layer material. Samples of this layer were obtained by using clay as an adhesive to remove the particles exposed to the flow, as has been described earlier. The values for the median sizes of the surface layer quoted above indicate that this layer is significantly coarser than the original mixture used as bed material. The ersatz pavement created during the screeding process, before the beginning of the first experiment, was coarser for the tilting flume case; to wit $D_{p50} = 2.27\ D_{50}$ for the tilting flume versus $D_{p50} = 1.7\ D_{50}$ for the long flume. From the subpavement samples at the end of S7:E1, one can conclude that shape and size segregation is present only at the pavement. No significant differences among the grains of the different subpavement samples were discerned. The only measurable difference was in the finer grains, whose percentage was relatively higher in the subpavement of the bar tail. At the end of the first experiment, the relation between the median sizes of the surface layer and the substrate material was on the average $D_{p50} = 2.4\ D_{50}$. The same relation was true for the long flume experiments in the absence of fines. The material of the bottom layer had characteristics similar to the subpavement material, with increased amounts of finer grains in the bottom layer.

The material in the pool area was similar to that at the middle of the bar both in terms of size and shape. The number of smaller grains in the pavement, however, was higher in the pool area. Figure 30 provides a view of the pavement and subpavement material in the pool area. A view of the pavement, subpavement, and bottom layer at the bar head is shown in Fig. 31.

The subpavement characteristics for both the tilting and long flume experiments were essentially identical; e.g. for the tilting flume D_{50} = 2.6 mm, and the percentages of grains with diameters smaller than 1.0 mm and 0.42 mm were 24% and 9%, respectively; the corresponding values for the

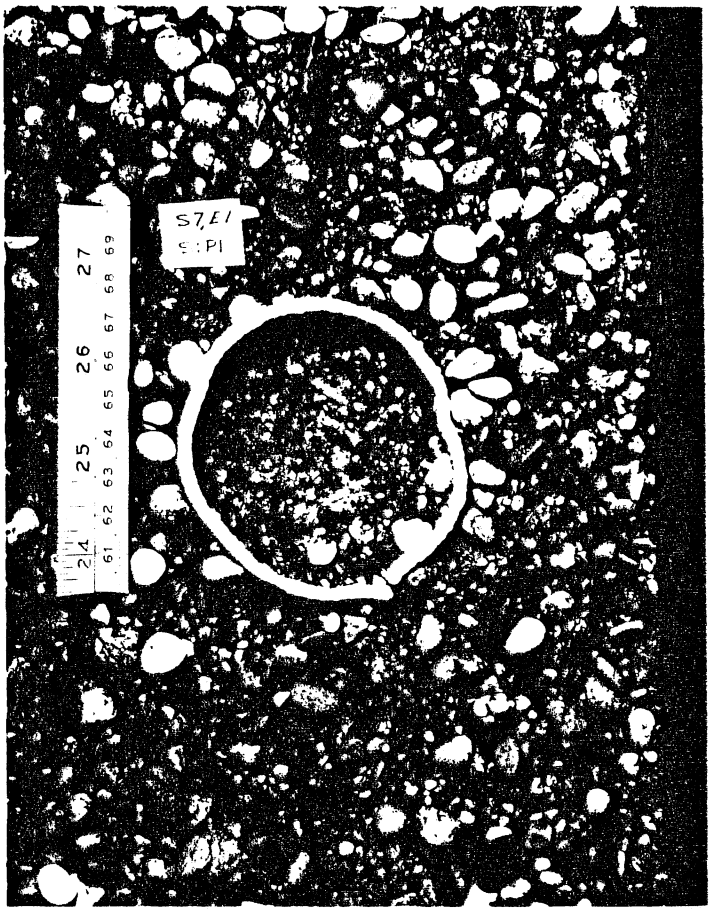

Figure 30. Bed surface (pavement layer) and subpavement at the pool area; experiment S7:E1.

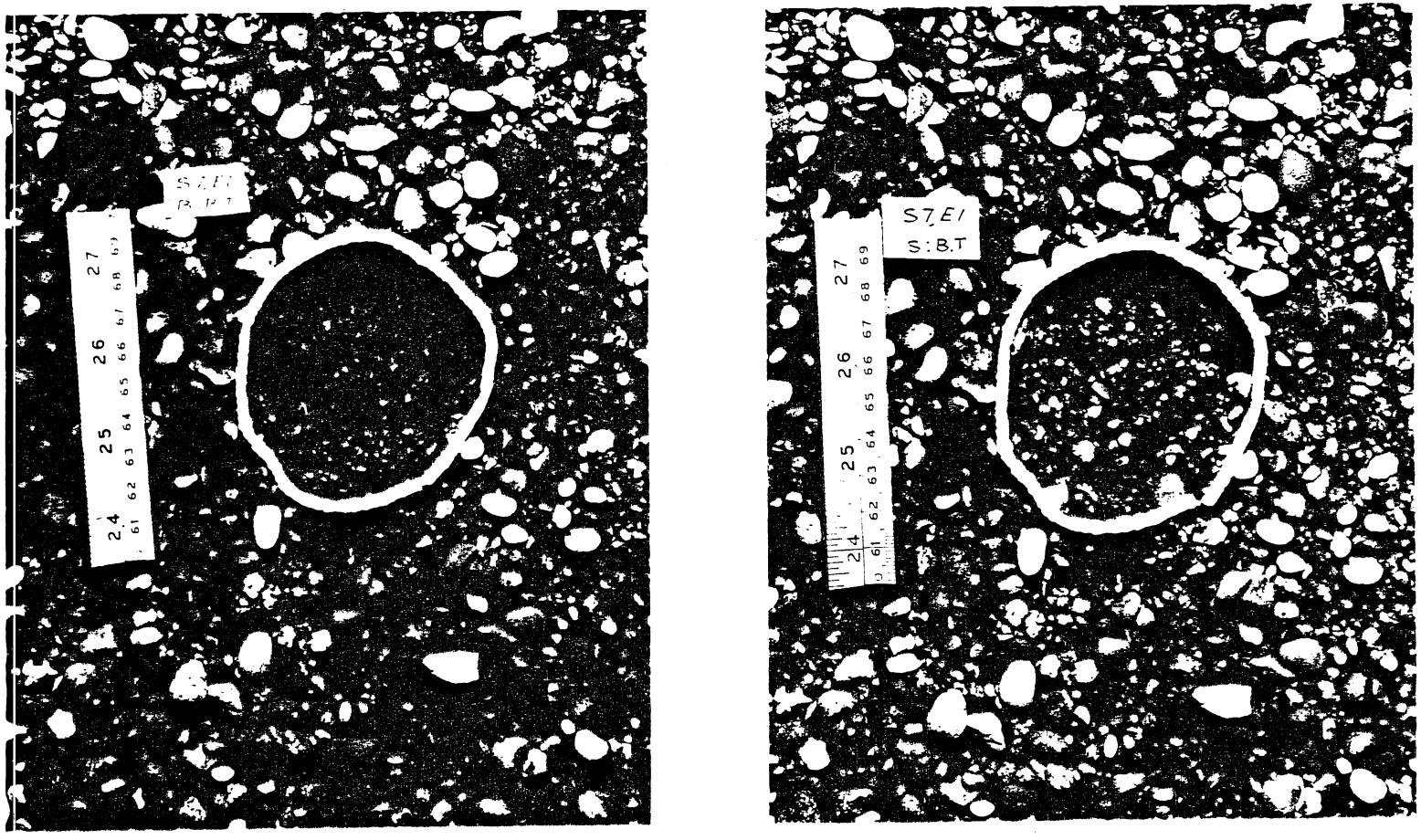

(a) (b)

Figure 31. (a) Pavement, subpavement and (b) pavement, bottom layer at the head of the second bar downstream of the channel entrance in experiment S7:E1.

long flume are D_{50} = 2.3 mm, 23% and 7.3%, respectively. The same holds true for the material of the bottom layers. The substrate material was in both cases poorly sorted (σ_g = 3.2). Thus the major differences, in terms of bed material, between the experiments without fines in the two flumes is restricted to the surface layer. The systematic variation observed in the tilting flume experiments appears to be forced by the bar structure, which is absent in the long flume experiments.

BEDLOAD TRANSPORT IN GRAVEL-BED STREAMS

Existing bedload formulae are mostly based on sand-bed stream data. These streams are characterized by uniformity of material in the vertical direction. The existence of a pavement in gravel-bed streams plays an important role in sediment transport. It is not expected that the same formulae initially derived from sand streams will necessarily apply to gravel streams (Parker et al, 1982a).

Ashida and Michiue (1972) used a similarity approach for analyzing bedload data from unpaved streams. Parker et al. (1982a, 1982b), explored the same concept for paved gravel streams, and deduced some interesting results. Parker et al. attained a first rough approximation of the problem. A more detailed approximation is sought here. The present analysis is based on the data collected by Milhous (1973) from the Oak Creek.

First, a dimensional analysis is introduced to identify the important parameters of the problem. Then a similarity approach slightly different from the one introduced by Parker et al. (1982a, 1982b) is attempted, and its implications are examined. A bedload transport formula based on this analysis is derived. The relative mobility of the particles obtained from the same analysis is compared with the field data from Oak Creek. The applicability of the similarity approach is also examined with the data obtained from the experiments conducted during this study. The ability of the new method to predict the characteristics of the particles transported as bed material is tested as well.

Dimensional Analysis

Dimensional analysis is traditionally used to arrange the variables pertinent to a certain phenomenon in a systematic way. Some insight about the phenomenon can be gained through this process.

Let the bed material size distribution be divided into N subranges. The phenomenon examined here is the bedload transport of the ith grain size subrange of the bed material in a straight reach of a gravel-bed stream. Parameters describing the fluid, the sediment, and the flow are important in this case. The fluid is described by its density ρ and viscosity μ. The task of identifying all the parameters required to describe the sediment is a tedious, if not an impossible one. Here this task is significantly simplified by considering similar types of material. This means that material of the same general shape, e.g. subrounded, and of similar size distribution is examined here. These are not overly limiting constraints since subrounded material is the type most commonly encountered in natural streams. Similarly, their size distribution is usually close to a log-normal one. Then the mean particle size D_g, the geometric standard deviation of the material σ_g, the representative diameter from the ith

size range D_i, and the density of the material ρ_s are assumed to describe the material reasonably well. The assumption of a log-normal size distribution for the bed material, although not always true, is necessary at this stage to simplify the analysis. The fluid flow is characterized by the boundary shear stress τ_o and the flow depth d. Channel width is not included here because usually bed processes are considered per unit width. Since river flow is a free surface problem, the acceleration of gravity g is also included. Parker and Peterson (1980) have suggested that bar resistance is not large during bedload transport events in gravel streams. Then the following functional relation is realized for q_{Bi}

$$q_{Bi} = f(\rho, \mu, D_g, \sigma_g, \rho_s, D_i, \tau_o, d, g, f_i) \tag{8}$$

where q_{Bi} is volumetric bedload rate per unit width of the ith grain size range, and f_i is the fraction of the subpavement material in the ith grain size range. Three fundamental dimensional units (mass, length, time) are required to describe all of the variables in (8). Thus the eleven dimensional parameters can be grouped into eight dimensionless terms. For a log-normal size distribution f_i can be dropped from Eq. (8) since it can be expressed as a function of D_g and σ_g. Then the number of the dimensionless terms in (8) is reduced to seven. There are various dimensionless terms that can be considered. The following grouping seems to be suitable for the present problem

$$\frac{R\, q_{Bi}}{f_i\sqrt{g}\,(dS)^{1.5}} = f\left(\frac{\tau_o}{\rho g R D_i}, \frac{\rho\, u_* D_g}{\mu}, \frac{D_i}{D_g}, \frac{d}{D_g}, R, \sigma_g\right) \tag{9}$$

Here f_i is used in the denominator of the dependent variable to relate the transport rate of bed material in the ith size range with the fraction contained in the source of this material. The size distribution of the subpavement material is independent of the flow conditions, while the characteristics of the pavement material do depend on the flow conditions. The use of the subpavement as a reference thus seems more appropriate. Also $R = (\rho_s/\rho - 1)$ is the submerged specific gravity, and $u_* = \sqrt{\tau_o/\rho}$ is the shear velocity. Relation (9) can be rewritten using the symbols of the dimensionless groups as follows:

$$W_i^* = f\left(\tau_i^*, R_p, \frac{D_i}{D_g}, \frac{d}{D_g}, R, \sigma_g\right) \tag{10}$$

where

$$W_i^* = \frac{R\, q_{Bi}}{f_i\sqrt{g}\,(dS)^{1.5}} = \frac{q_{Bi}^*}{\tau_i^{*1.5}} \tag{11}$$

is the dimensionless bedload parameter, $\tau_i^* = \tau_o/(\rho g R D_i)$ is the Shields stress, and $R_p = (\rho u_* D_g)/\mu$ is the particle Reynolds number. For large values of particle Reynolds number ($R_p > 1000$), and relative roughness d/D_g, these two parameters become less important when compared with the rest of the parameters in (10). The first of these assumptions is a realistic one for gravel-bed streams. Although the value of the relative roughness in gravel bed streams is usually moderately large, it is not expected to influence significantly the relation of bedload versus shear stress. Also, the term R on the right hand side of (10) can be disregarded, assuming that (10) is only applied to material of the same specific gravity (about 1.65 for quartzite). Then (10) becomes:

$$W_i^* = f\left(\tau_i^* , \frac{D_i}{D_g} , \sigma_g\right) \tag{12}$$

Similarity Approach

The concept of similarity was used by Ashida and Michiue (1972) to analyze the bedload size distribution of unpaved mixtures. Parker et al. (1982a, 1982b) applied the same concept for paved gravel-bed streams. For this purpose they used data collected by Milhous (1973) in Oak Creek. These data are considered to be among the best field data available for bedload measurements from gravel bed streams (Parker et al., 1982a). Parker et al. used only those measurements obtained during conditions when most grain sizes in the pavement would also be found in motion. The approach followed was to divide the bed material into a number of size ranges and attempt to correlate the dimensionless bedload for each range, W_i^*, with the Shields stress based on the mean particle diameter of that range, τ_i^*. They used log-log plots and least-squares log-log regression to obtain for each size range relations of the form

$$W_i^* = \alpha_i \tau_i^{*m_i} \tag{13}$$

If the exponents m_i are the same for all the size ranges, then the slope of the lines described by (13) in a log-log plot would be identical. Even if the intercept for each line, $\log \alpha_i$ is different, all the lines can then be collapsed into a single line by using a simple similarity transformation.

The plots obtained by Parker et al. (1982a) have been reproduced here (Fig. 32). They divided the bed material into ten size ranges, disregarding material finer than 0.59 mm, which could be transported either as bedload or in suspension. The values of the exponents, m_i, obtained from least-squares log-log regression analysis are shown in Table 5. These values range from 5.49 to 21.41, generally increasing with increasing size. While this analysis provided many useful conclusions concerning bedload transport in gravel streams, it also showed that "any tendency toward similarity is approximate at best," as Parker et al. (1982a) mentioned. Nevertheless, a similarity collapse was performed using a specified reference value W_r^*, for the dimensionless bedload parameter. The value

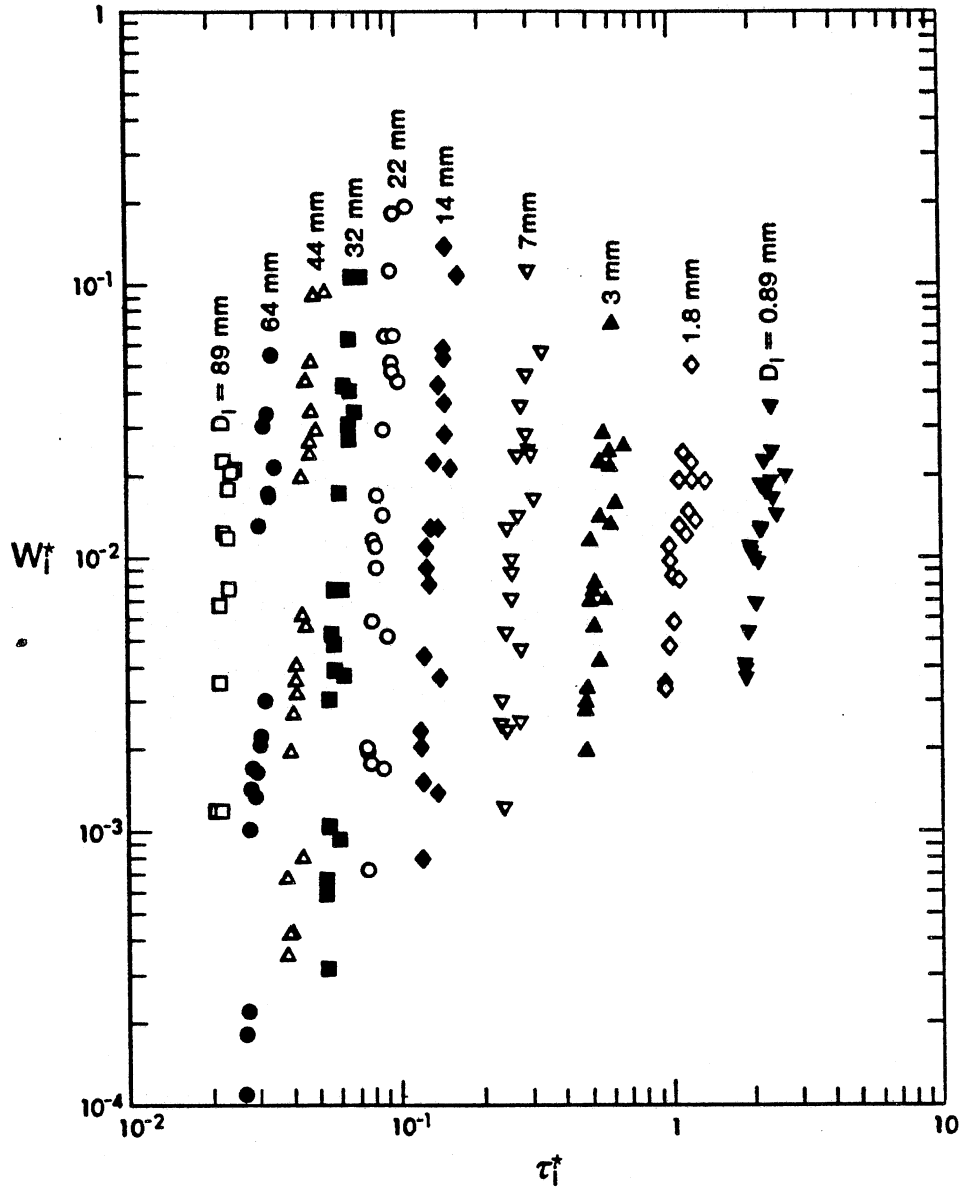

Figure 32. Plot of W_i^* versus τ_i^* for ten grain size ranges of the Oak Creek data. (After Parker et al., 1982a.)

TABLE 5

VALUES OF m_i AND m'_i DERIVED FROM THE OAK CREEK DATA

D_i (mm)	m_i	m'_i	r
88.9	15.58	9.59	0.80
63.5	21.41	14.79	0.93
44.4	16.80	13.01	0.91
31.8	15.82	13.67	0.89
22.2	14.21	13.72	0.85
14.3	12.24	13.68	0.82
7.14	9.84	13.72	0.81
3.57	7.48	13.03	0.80
1.79	5.90	12.93	0.82
0.89	5.49	14.96	0.85

chosen was $W_r^* = 0.002$, which is thought to represent conditions slightly above the threshold of motion (Parker et al., 1982a). Equation (13) can be expressed with the use of W_r^* to give

$$\frac{W_i^*}{W_r^*} = \left(\frac{\tau_i^*}{\tau_{r_i}^*} \right)^{m_i} = \phi_i^{m_i} \tag{14}$$

where τ_{ri}^* is the Shields stress capable of transporting bedload $W_i^* = W_r^*$, i.e. $\tau_{ri}^* = (W_r^*/\alpha_i)^{1/m_i}$. A log-log plot of W_i^* vs ϕ_i has also been reproduced here as Fig. 33. While the data do not collapse into a single line, they exhibit a definite trend, and they can be well represented by the mean line as shown in the same figure. The most pronounced deviation from similarity is demonstrated by the finer three grain size ranges, which fall well below the mean line at large values of ϕ_i.

The above analysis indicates a dependence of the dimensionless bedload W_i^*, on the grain size D_i. This dependence is also demonstrated in Eq. (12), the result of the dimensional analysis. This dependence is exhibited in terms of a consistent increase of the value of the exponent, m_i, with the grain size. A better similarity parameter should incorporate this dependence on D_i. It is expected that such a similarity parameter could reduce the variance of the new m_i values. A plot of m_i versus D_i/D_{50} indicates the dependence, as shown in Fig. 34. A log-log regression leads to the relation

$$m_i = 13.023 \, (D_i/D_{50})^{0.291} \tag{15}$$

with a correlation coefficient $r = 0.971$. As is shown from Table 5 and Fig. 34, the exponent m_i for the coarsest grain size, $D_i = 88.9$ mm, exhibits different behavior than the rest of the exponents. If this is excluded, then the relation based on the nine finer grain size ranges becomes

$$m_i = 13.68 \left(\frac{D_i}{D_{50}} \right)^{0.3214} \cong 13.68 \left(\frac{D_i}{D_{50}} \right)^{1/3.1} \tag{16}$$

with a correlation coefficient $r = 0.994$. If the median grain size D_{50} is replaced in the quotient D_i/D_{50}, by the mean grain size D_g then Eq. (16) changes to

$$m_i = 12.533 \left(\frac{D_i}{D_g} \right)^{0.3214} \tag{17}$$

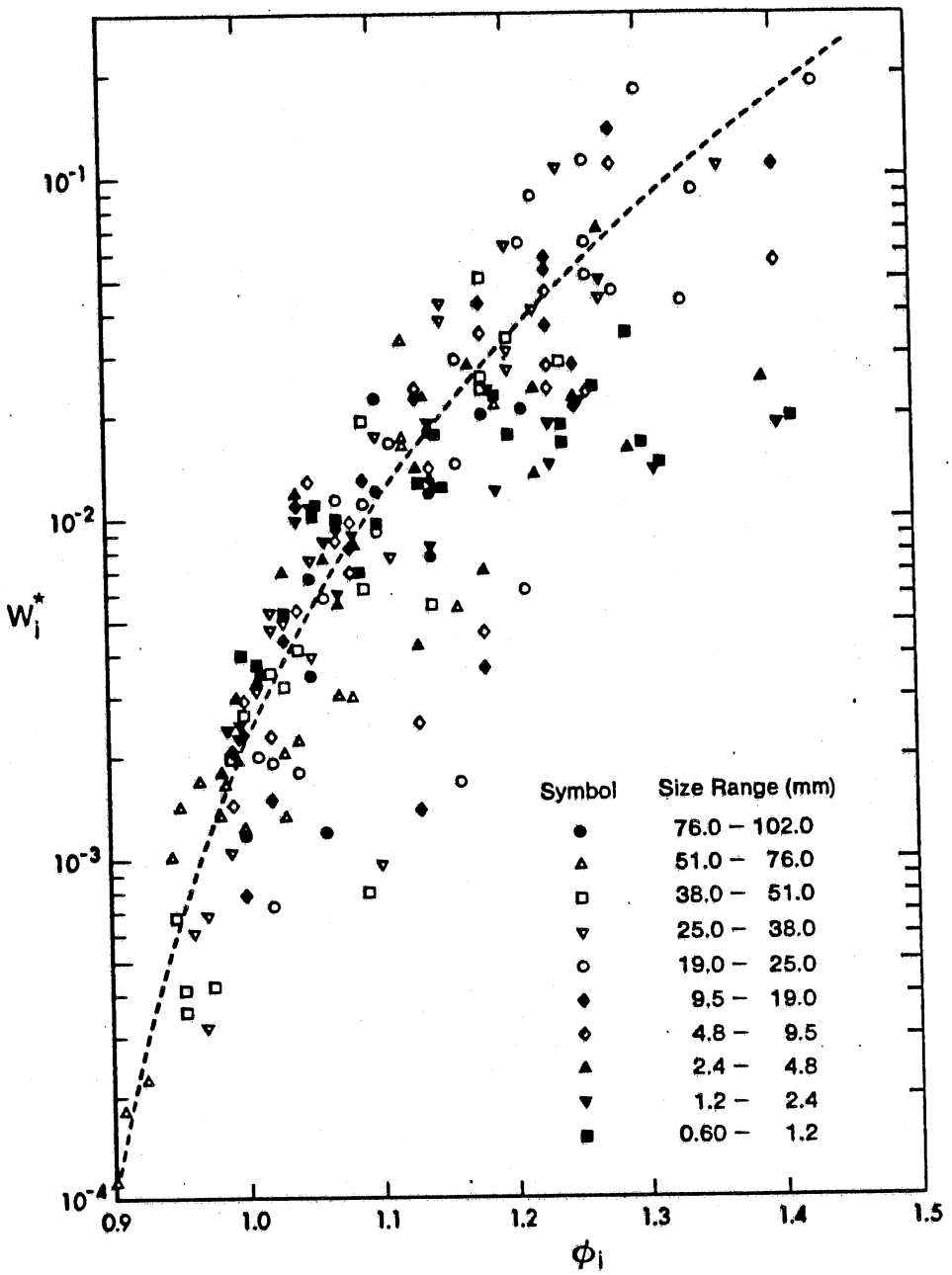

Figure 33. Similarity plot of W_i^* versus ϕ_i^* for the Oak Creek data, based on analysis of Parker et al., 1982a. (After Parker et al., 1982a.)

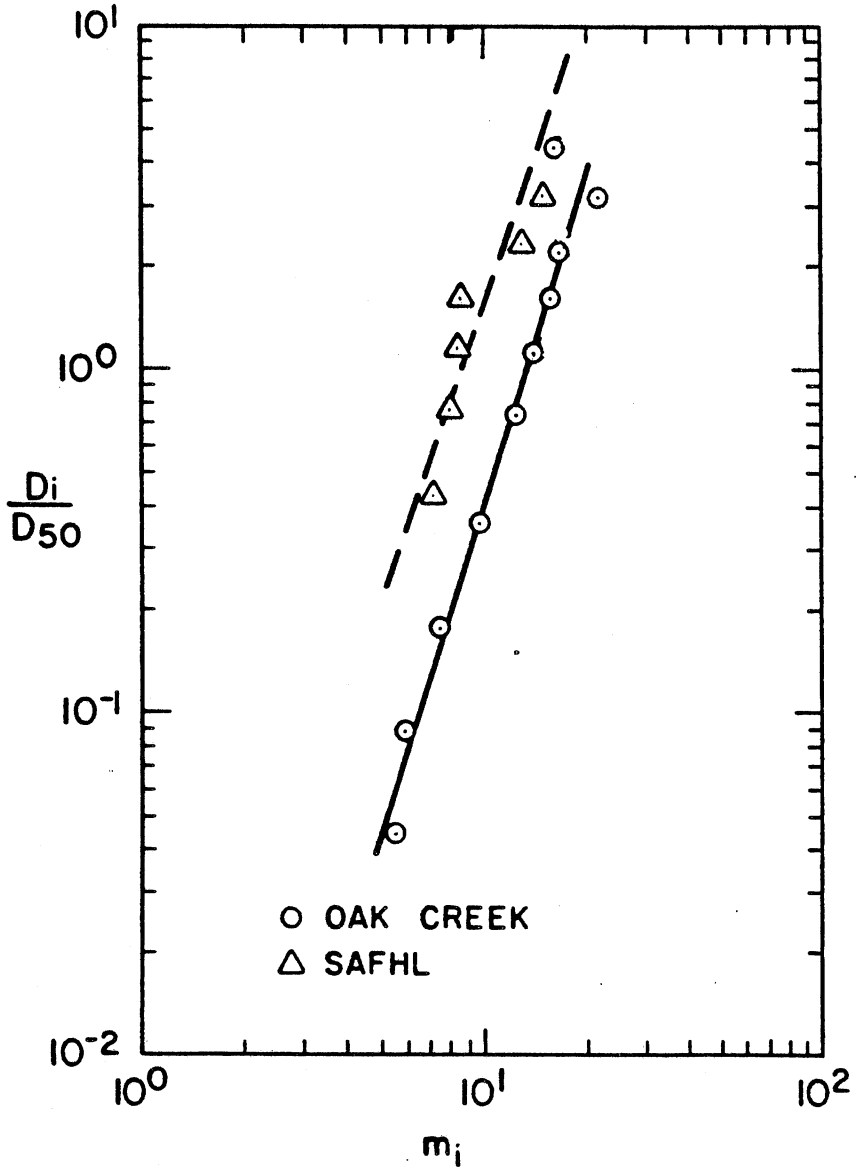

Figure 34. Plot of m_i values versus D_i/D_{50} for the Oak Creek data and the data of the present study.

In all the cases D_{50} and D_g are based on the substrate material. Equation (16) is used in this study to interpret the relation between m_i and D_i/D_{50} for the Oak Creek case.

The next logical step is to consider

$$\tau_i^* (D_i/D_{50})^{0.3214}$$

as the new similarity parameter. Plots of

$$W_i^* \quad \text{vs.} \quad \tau_i^*(D_i/D_{50})^{0.3214}$$

for each grain size range are shown in Fig. 35. The relations, obtained from least-squares log-log regression, are of the form

$$W_i^* = \beta_i \left[\tau_i^*(D_i/D_{50})^{0.3214} \right]^{m'_i} \tag{18}$$

The values of m'_i for the nine finer sizes range from 12.93 to 14.96; unlike the m_i values, they do not exhibit any trend with respect to grain size (Table 5). The value of the exponent for the coarsest size is 9.59. The exponents found by Parker et al. (1982a), m_i, vary by as much as 290 percent, while the exponents found by the present similarity approach, m'_i, vary at most by 16 percent. This is a considerable improvement. Considering the complicated phenomena surrounding the motion of grains, and the poor correlations commonly obtained, the present analysis provides a similarity parameter upon which it would be rather difficult to improve. It should, however, be kept in mind that this analysis is based only on the Oak Creek data, so any generalizations could be premature at this point.

The equation describing the similarity collapse based on the new similarity parameter is

$$\frac{W_i^*}{W_r^*} = \left[\phi_i (D_i/D_{50})^{0.3214} \right]^{m'_i} \tag{19}$$

where

$$\phi_i = \frac{\tau_i^*}{\tau_{r_i}^*} \tag{20}$$

and $W_r^* = 0.0025$. A plot of the Oak Creek data in the form of

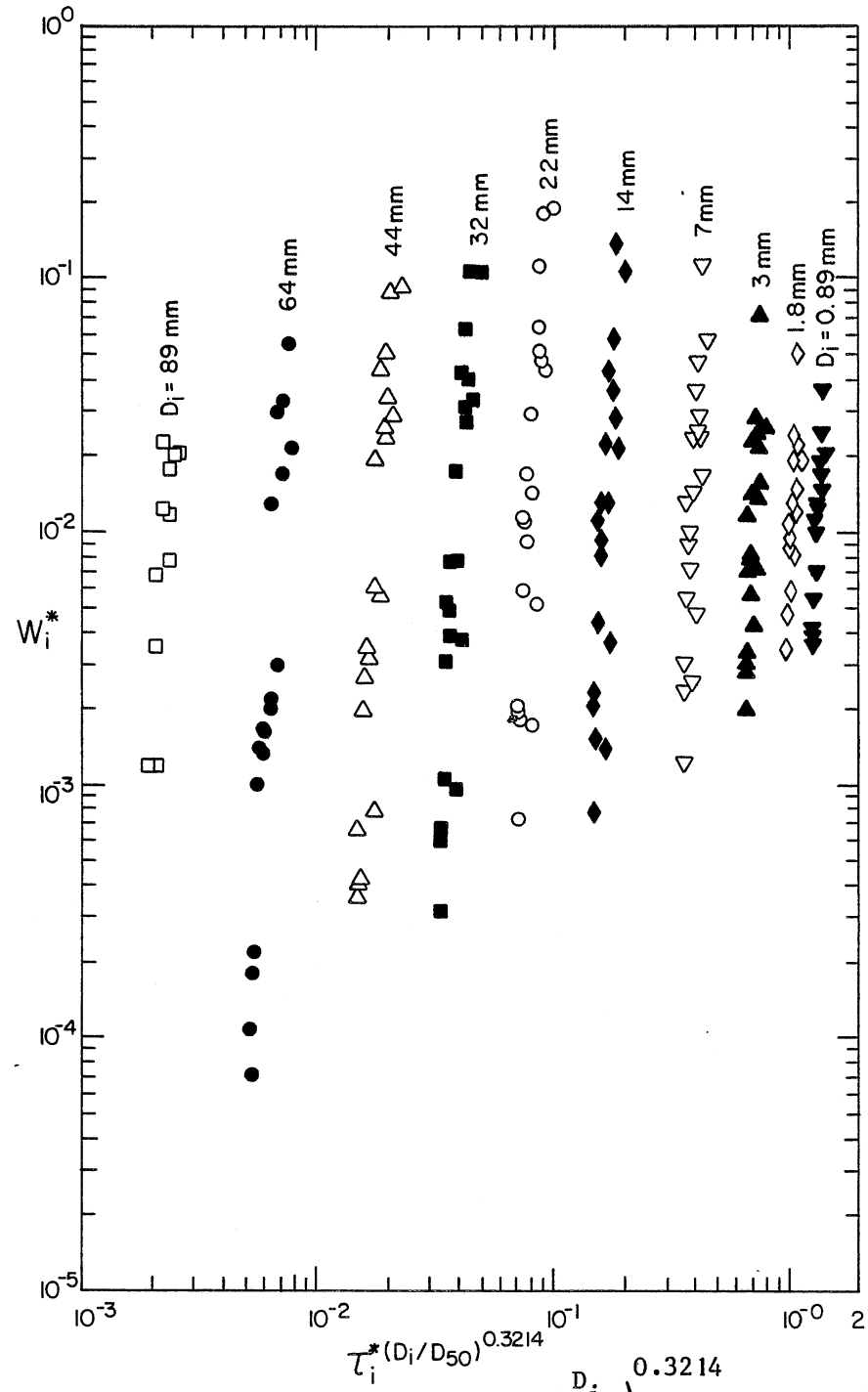

Figure 35. Plot of W_i^* versus $\tau_i^*\left(\frac{D_i}{D_{50}}\right)^{0.3214}$ for ten grain size ranges of the Oak Creek data.

$$W_i^* \quad \text{vs.} \quad \phi_i (D_i/D_{50})^{0.3214}$$

is shown in Fig. 36. Although the scatter in Fig. 36 has been reduced compared to Fig. 33, it is still significant. On the other hand the points in Fig. 36 are rather uniformly distributed, and no consistent deviations are discernible. A weighted mean value, m', is given from the expression

$$m' = \frac{1}{\sum_i f_i} \sum_i f_i \, m_i' \tag{21}$$

The value of m' computed from (21), based on the nine finer ranges, is 13.71. The line

$$\frac{W_i^*}{W_r^*} = \left[\phi_i (D_i/D_{50})^{0.3214} \right]^{13.71} \tag{22}$$

is shown in Fig. 36; it seems to represent the data points rather well.

The reference Shields stresses, τ_{ri}^*, obtained from Eq. (18) for $W_r^* = 0.0025$ are plotted against D_i/D_{50} in Fig. 37. Their correlation is expressed by the following relation

$$\frac{\tau_{ri}^*}{\tau_{r50}^*} = \left(\frac{D_i}{D_{50}} \right)^{-0.9394} \tag{23}$$

where τ^*_{r50} is the reference Shields stress that corresponds to the subpavement D_{50}, with $\tau^*_{r50} = 0.08763$. Equation (14) is derived from a log-log regression with correlation coefficient $r = -0.99996$. The corresponding relation obtained by Parker et al. has $\tau^*_{r50} = 0.0876$, and as exponent -0.982. Andrews (1983) derived a similar relation based on data from Clearwater, Snake, and East Fork river. His relation is:

$$\tau_{ri}^* = 0.0834 \left(\frac{D_i}{D_{50}} \right)^{-0.872} \tag{24}$$

An exponent of -1 implies that the dimensional bottom shear stress, τ_{ri}^*, required to provide near critical conditions, such that $W_r^* = 0.0025$, is the same for all grain sizes.

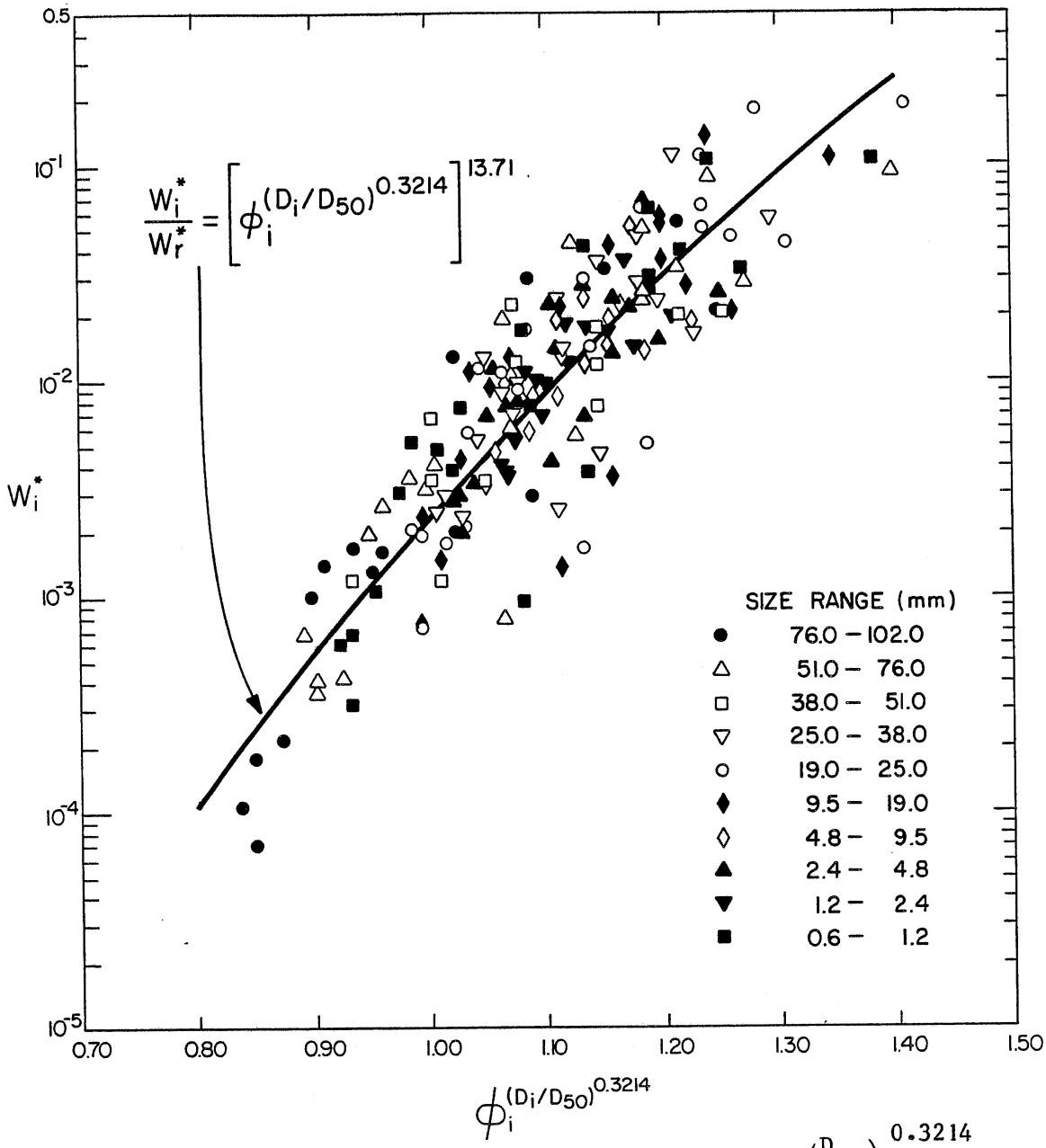

Figure 36. Similarity plot of W_i^* versus $\phi_i^{\left(\frac{D_i}{D_{50}}\right)^{0.3214}}$ for the Oak Creek data.

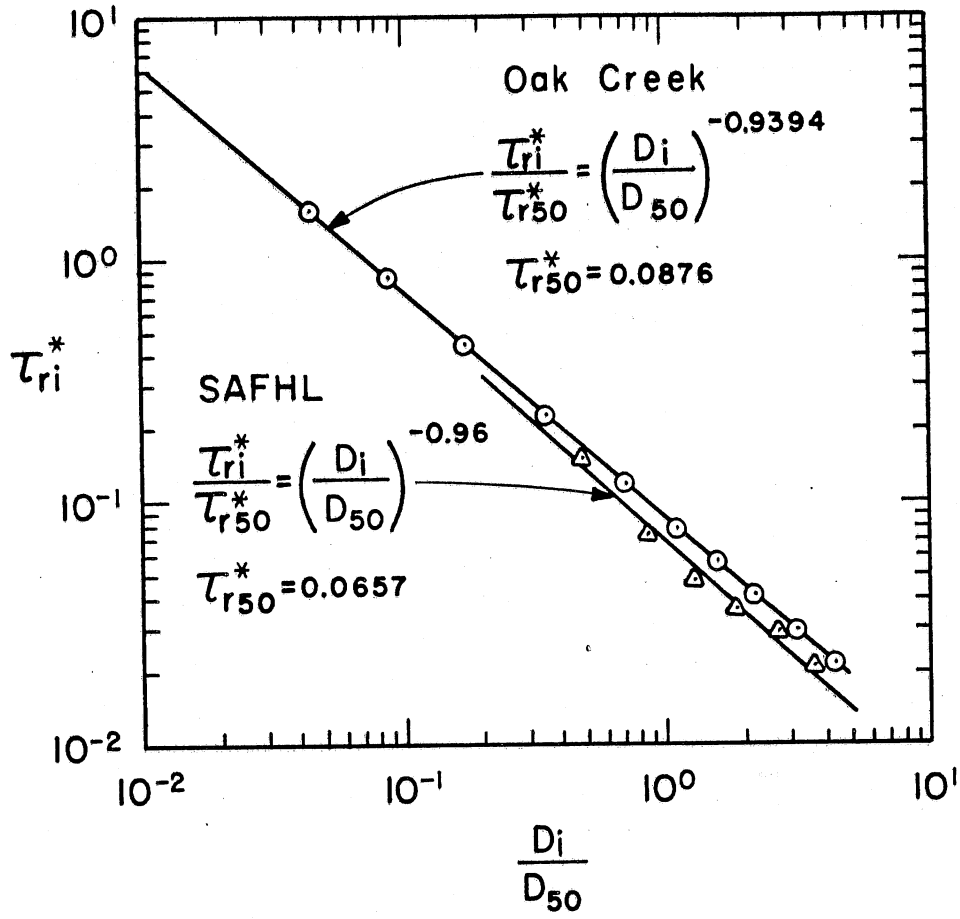

Figure 37. Plot of reference Shields stress, τ_{ri}^* versus D_i/D_{50} for the Oak Creek data, and the data of the present study.

Bedload Transport

Most of the existing bedload formulas are based on data obtained from sand-bed streams. The bed material is often fairly uniform, and there is no pavement present in such streams. The same formulas are commonly used for bedload calculations in gravel-bed streams. A representative grain size is usually recommended in this case. There is some confusion as to whether the pavement or subpavement material should be considered as the basis for this grain size. Parker et al. (1982a), in Fig. 8 of their paper, compared some of the formulas most commonly used to calculate bedload transport for gravel-bed streams with the Oak Creek data. The predictions obtained by these formulas ranged from poor to unacceptable. In the same paper they showed that a formula for bedload transport that required only the knowledge of the subpavement D_{50} would be appropriate for gravel-bed streams. This conclusion was derived under the assumptions of perfect similarity, and a value of -1 for the exponent of Eq. (14). By plotting the Oak Creek data (W^*; versus ϕ_{50}) they empirically developed such a bedload formula. They further refined this method by accounting for the deviations from similarity. In doing so they divided the bed material in three size ranges and empirically developed a bedload formula for each size range.

The present analysis is used here to develop a bedload formula that would account for sediment grading effects. From (11) and (22) the following is obtained:

$$q_{Bi} = f_i \left[\phi_i^{(D_i/D_{50})^{0.3214}} \right]^{13.71} \frac{W_r^* \sqrt{g}\,(dS)^{1.5}}{R} \tag{25}$$

Then the total bedload is given from:

$$q_B = \frac{W_r^* \sqrt{g}\,(dS)^{1.5}}{R} \sum_i f_i \left[\phi_i^{(D_i/D_{50})^{0.3214}} \right]^{13.71} \tag{26}$$

From (20) and (23), the following result can be obtained;

$$\phi_i = \phi_{50} \left(\frac{D_i}{D_{50}} \right)^{-0.0606} \tag{27}$$

Substituting (27) in (26), the total bedload formula becomes:

$$q_B = \frac{W_r^* \sqrt{g}(dS)^{1.5}}{R} \sum_i f_i \left\{ \left[\phi_{50} \left(\frac{D_i}{D_{50}} \right)^{-0.0606} \right]^{(D_i/D_{50})^{0.3214}} \right\}^{13.71} \quad (28)$$

In Fig. 38 relation (28) is tested against the data from which it was derived. As expected, the agreement seems to be reasonably good.

Relative Particle Mobility

The mobility of a particle is influenced by many factors. The weight of the particle and its protrusion into the flow are probably the most important ones. A formal definition for relative mobility of grains in mixtures is given by Parker and Klingeman (1982b). They define the relative mobility with respect to subpavement material, $(r_{ij})_s$, of grain size D_i in comparison with grain size D_j as:

$$(r_{ij})_s = \frac{q_{Bi}}{f_i} \left(\frac{q_{Bj}}{f_j} \right)^{-1} \quad (29)$$

where q_{Bi} is the volumetric bedload transport per unit width for material in the size range D_i, and f_i the percentage of the subpavement material that belongs to the same range. The grain size D_i is considered to be more mobile than D_j if $(r_{ij})_s > 1$. An analytic expression for $(r_{ij})_s$ is derived here based on the similarity analysis presented earlier. From the definition of W_i^* the following is true:

$$(r_{ij})_s = \frac{W_i^*}{W_j^*} \quad (30)$$

To simplify matters D_{50} is used instead of D_j. From Eqs. (22), (23) and (30), after some algebra, the following expression is obtained:

$$(r_{i50})_s = \left\{ \phi_{50}^{\left[(D_i/D_{50})^{0.3214} - 1\right]} \left(\frac{D_i}{D_{50}} \right)^{-0.0606(D_i/D_{50})^{0.3214}} \right\}^{13.71} \quad (31)$$

A plot of relation (31) for different values of ϕ_{50} is shown in Fig. 39. In the same figure, some data points from Oak Creek have also been included. The data exhibit significant deviation among themselves. As can be seen from the legend in the figure, for the same value, $\phi_{50} = 1.2$, three noticeably different bedload transport rates were measured at Oak Creek. Thus relation (31) is expected to follow the general trends at best. From Fig. 39 it seems that it does so reasonably well. Based on their analysis,

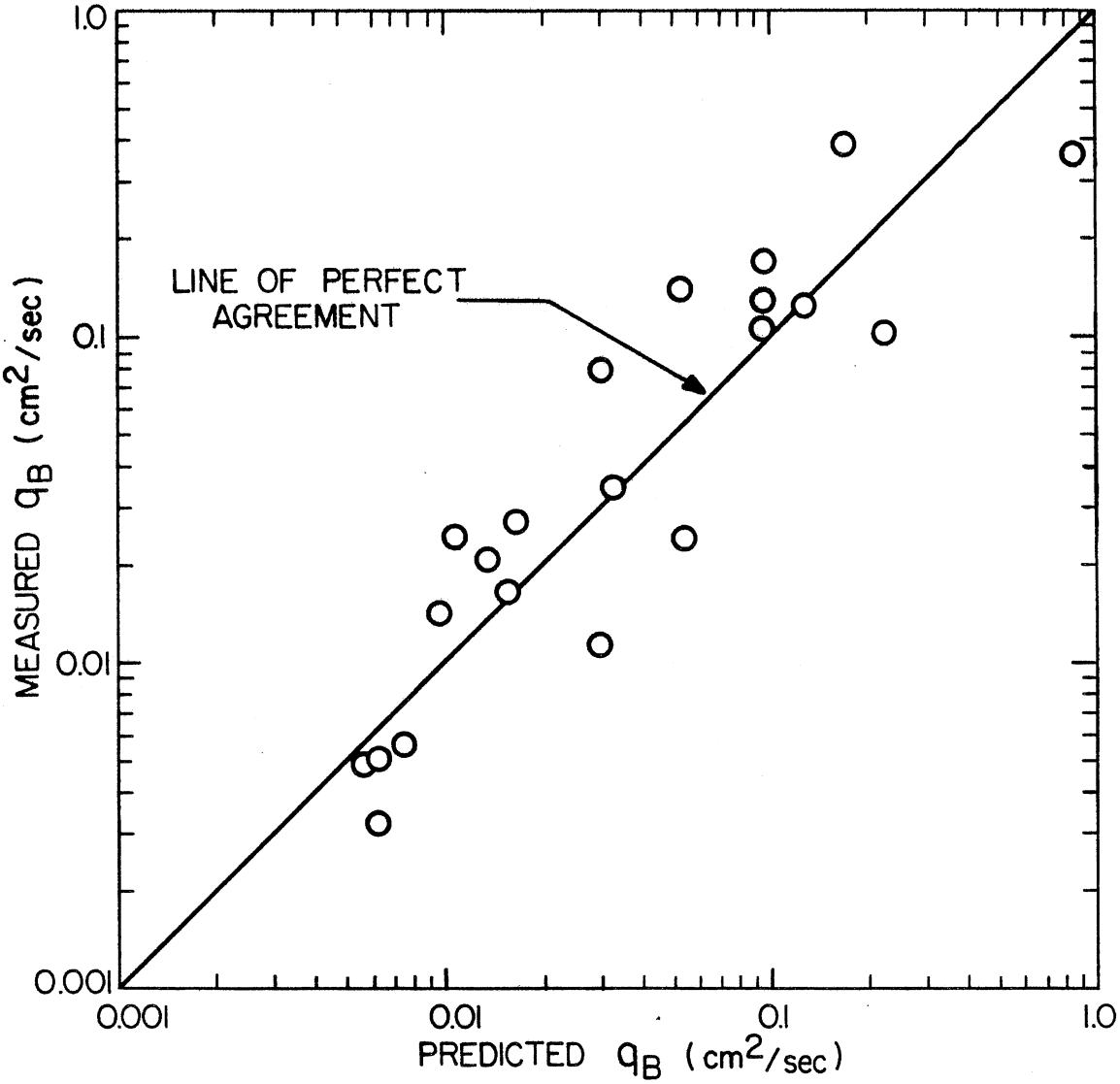

Figure 38. Total bedload relation (28) tested against the measured Oak Creek bedload values.

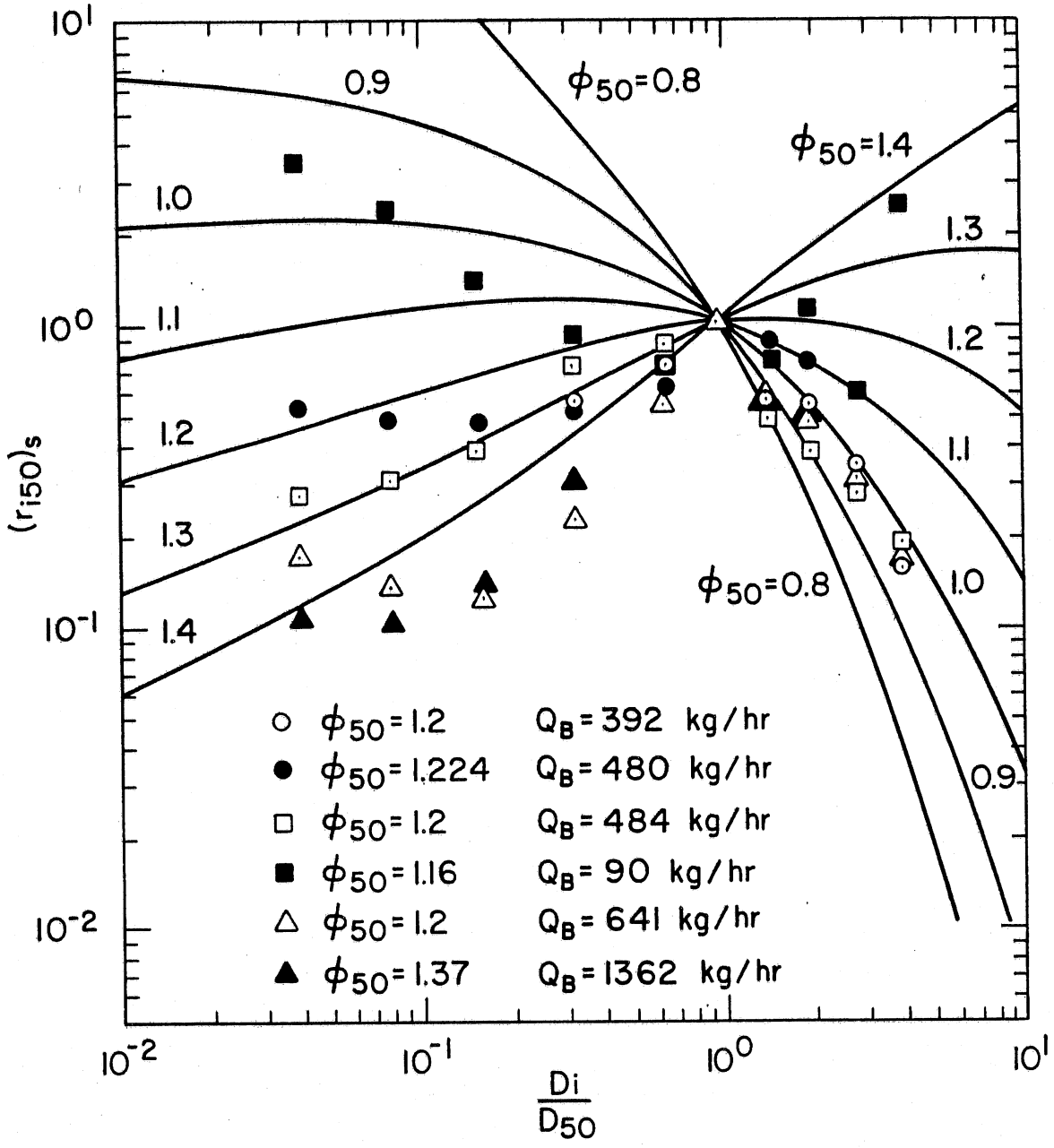

Figure 39. Relative particle mobility with respect to subpavement obtained from the present analysis, i.e. from eq. (31), compared with Oak Creek data.

Parker and Klingeman found that assuming perfect similarity, $m_1' = m_2' = \ldots = m'$, and that the exponent of Eq. (23) is -1 then $(r_{ij})_s = 1$. Then they concluded that under these conditions the bedload is identical to the subpavement material. Here it is seen from (31) that the assumptions of perfect similarity, $m_1 = m_2 = \ldots = m = 13.71$, and a value of -1 for the exponent of Eq. (23) lead to the following expression:

$$(r_{i50}) = \{\phi_{50}^{[(D_i/D_{50})^{0.3214} - 1]}\}^{13.71} \tag{32}$$

Thus conditions of equal mobility even under these assumptions are not realized in the present case.

Bedload Characteristics

In addition to prediction of bedload transport rates, information about the characteristics of the material that is in motion is often important. Relation (25) can predict the size distribution of the bedload. Bedload characteristics such as geometric and standard deviation can then be computed. This was done here for the Oak Creek data. The following formulas were used to estimate the geometric mean, $D_{\ell g}$, and standard deviation, $\sigma_{\ell g}$, of the bedload

$$D_{\ell g} = \prod_i D_{\ell i}^{f_{\ell i}} \tag{33}$$

$$\sigma_{\ell g} = \exp\left\{\sum_i \left(\ell n \frac{D_{\ell i}}{D_{\ell g}}\right)^2 f_{\ell i}\right\}^{1/2} \tag{34}$$

where $D_{\ell i}$ is the bedload grain size and $f_{\ell i}$ its percentage in the bedload. Using Eqs. (25), (33) and (34), lines indicating the variation of $D_{\ell g}$ and $\sigma_{\ell g}$ with respect to ϕ_{50} are shown in Figs 40 and 41. Values of $D_{\ell g}$ from the Oak Creek data seem to follow these two lines closely.

It is clearly seen from Fig. 40 that as ϕ_{50} increases the mean size of the bedload material increases as well. This trend has been well documented from field data for gravel-bed streams with $\phi_{50} < 2.2$.

A similar prediction method for the characteristics of the pavement material could also be developed. The same similarity approach examined here, but carried out with respect to the pavement material, can be employed to achieve this. Parker (1980) and Dhamotharan et al. (1980) found that the characteristics of the grains found in armor layers are very close to those of pavement layers created under the same flow conditions. The characteristics of the material in an armor layer might thus also be found from this method. This idea is examined in Diplas and Hills (1985).

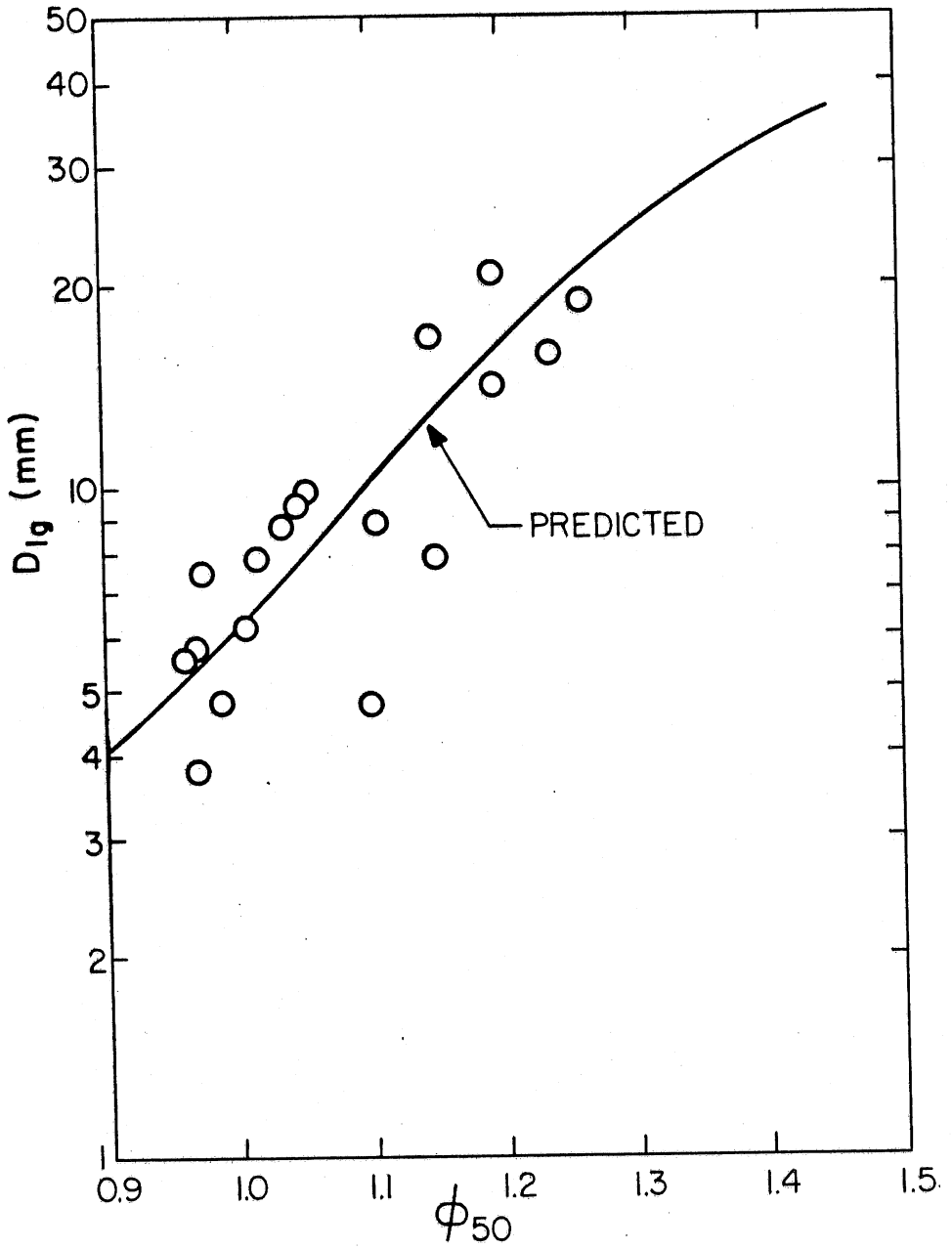

Figure 40. Bedload mean values, $D_{\ell g}$, as a function of ϕ_{50} in Oak Creek. The present method is used to obtain the curve; the open circles denote observed values.

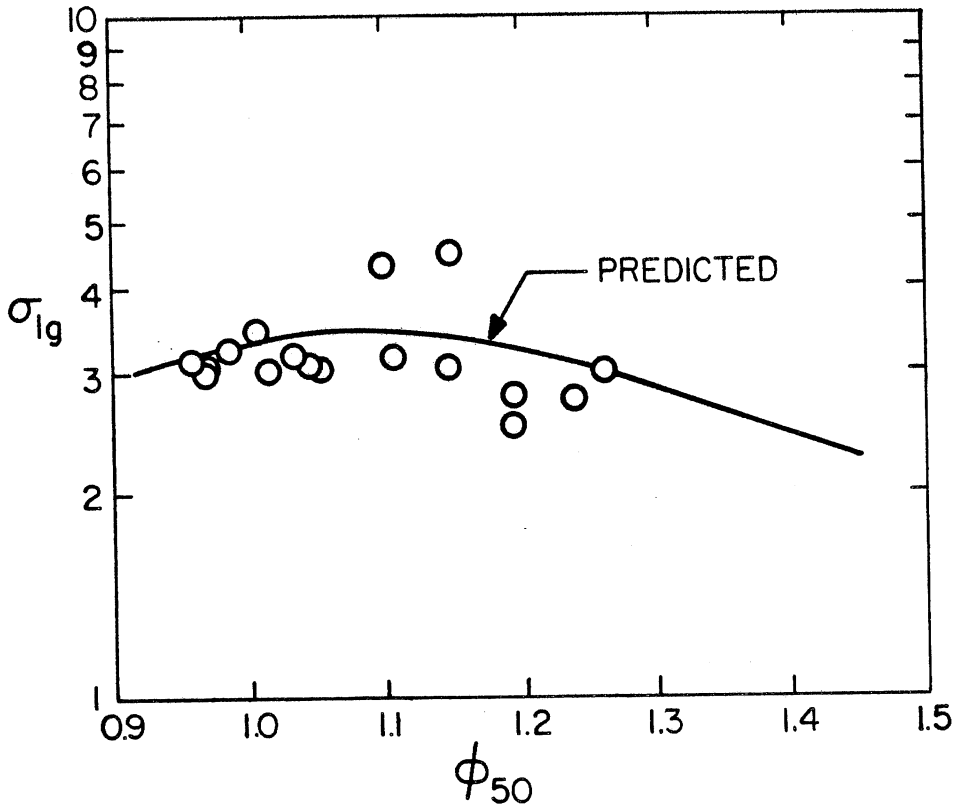

Figure 41. Bedload standard deviation, $\sigma_{\ell g}$, as a function of ϕ_{50} in Oak Creek. The present method is used to obtain the curve; the open circles denote observed values.

Further Applicability of Similarity Approach

The similarity approach developed here is examined in light of the data collected from the laboratory experiments conducted as part of this study. Plots of W_i^* vs. τ_i^* for six size ranges are shown in Fig. 42. Material finer than 0.71 mm has been excluded from the analysis. This material usually comprised only 1% or less of the bedload samples, amounts that were not considered to be sufficient for the present analysis. The SAFHL data exhibit higher deviations compared to the Oak Creek data. The present study did not initially include a detailed examination of the bedload transport. As a result, the number of bedload samples obtained was not as large as needed. Similarly, the method used to remove the bedload samples could have been more accurate. These two reasons are considered to be the main causes for the deviations.

Relations similar to Eq. (5) for each grain size are determined from lines fitted to the data by eye. The exponents, m_i, are listed in Table 6. The m_i values of the present data follow a trend similar to that of the m_i values obtained from the Oak Creek data; i.e. they increase with increasing grain size. A plot of D_i/D_{50} vs. m_i is shown in Fig. 32. Log-log regression gives the relation

$$m_i = 8.732 \left(\frac{D_i}{D_{50}} \right)^{0.348} \tag{35}$$

with a correlation coefficient r = 0.91.

From Fig. 34 and relations (16) and (35) it is seen that the slopes of these two lines are almost the same, while the intercept for each case is different.

A new plot of W_i^* versus $\tau_i^*(D_i/D_{50})^{0.348}$ for the SAFHL data is shown in Fig. 43. Lines are fitted to the data by eye. Relations analogous to Eq. (18), are developed and the exponents are listed in Table 6. These equations are of the form

$$W_i^* = \gamma_i \left[\tau_i^* \left(D_i/D_{50} \right)^{0.348} \right]^{m'_i} \tag{36}$$

The values of m_i range from 7.19 to 15.14, while the values of m_i' range from 7.24 to 10.1. Thus the values of m_i vary by as much as 111%, whereas the values of m_i' by no more than 39%. The similarity collapse for the SAFHL data is shown in Fig. 44. Here the scatter is significantly higher compared with the Oak Creek data. The deviation observed in Fig. 42 is responsible for the increased scatter. From relation (36) the following equation is obtained for the similarity collapse:

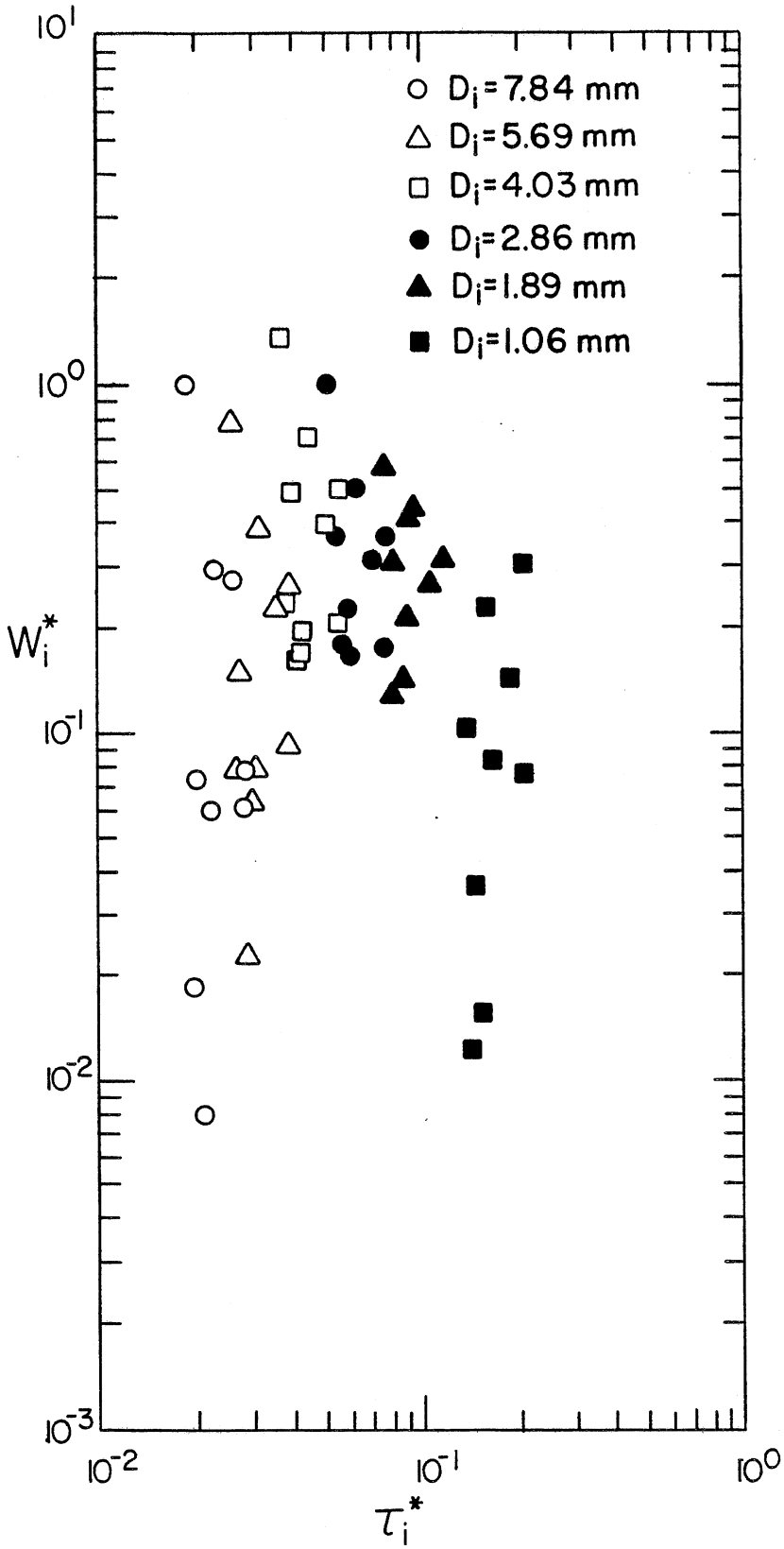

Figure 42. Plot of W_i^* versus τ_i^* for six grain size ranges of the data of the present study.

TABLE 6

VALUES OF m_i AND m'_i BASED ON THE EXPERIMENT OF THE PRESENT STUDY

D_i	m_i	m'_i
7.84	15.14	10.09
5.69	12.0	8.94
4.03	8.62	7.24
2.86	8.53	8.071
1.89	8.013	8.76
1.06	7.19	9.61

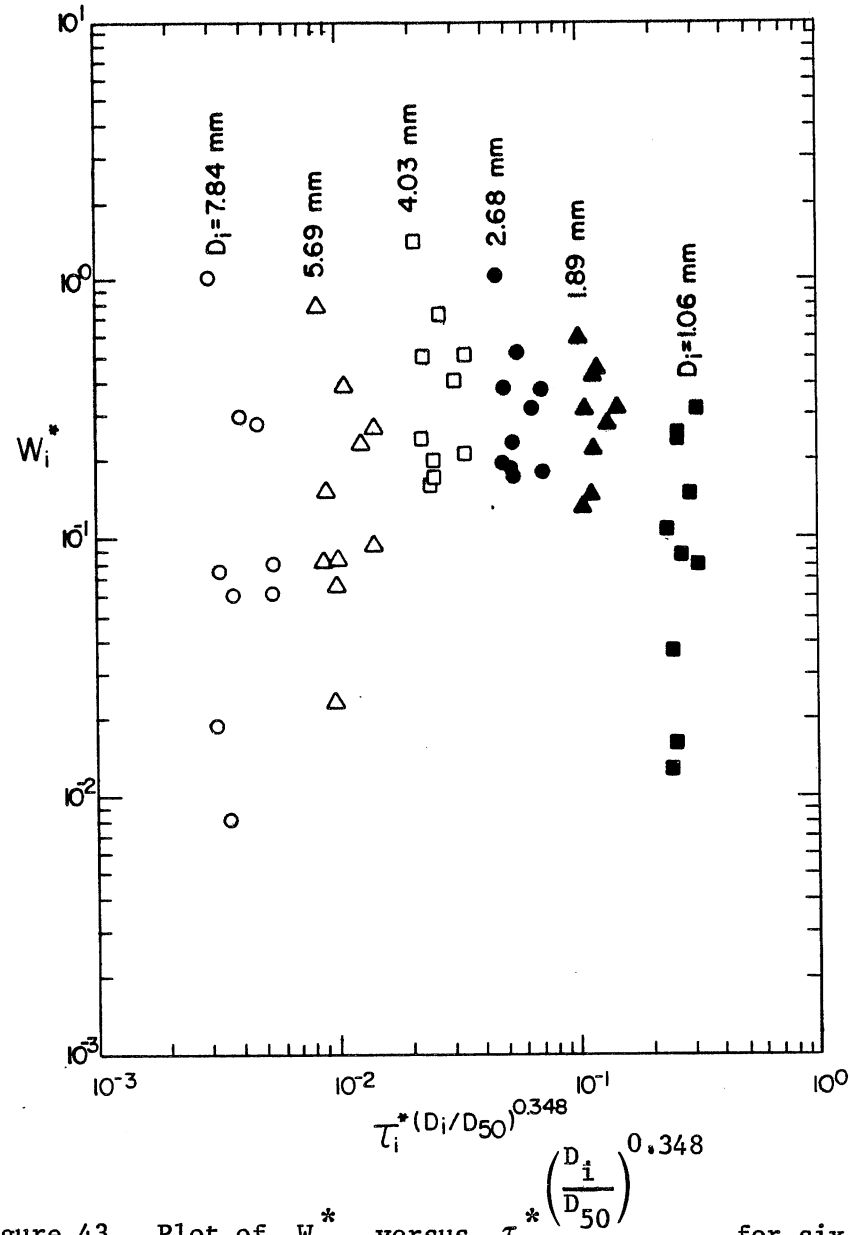

Figure 43. Plot of W_i^* versus τ_i^* for six grain size ranges of the data of the present study.

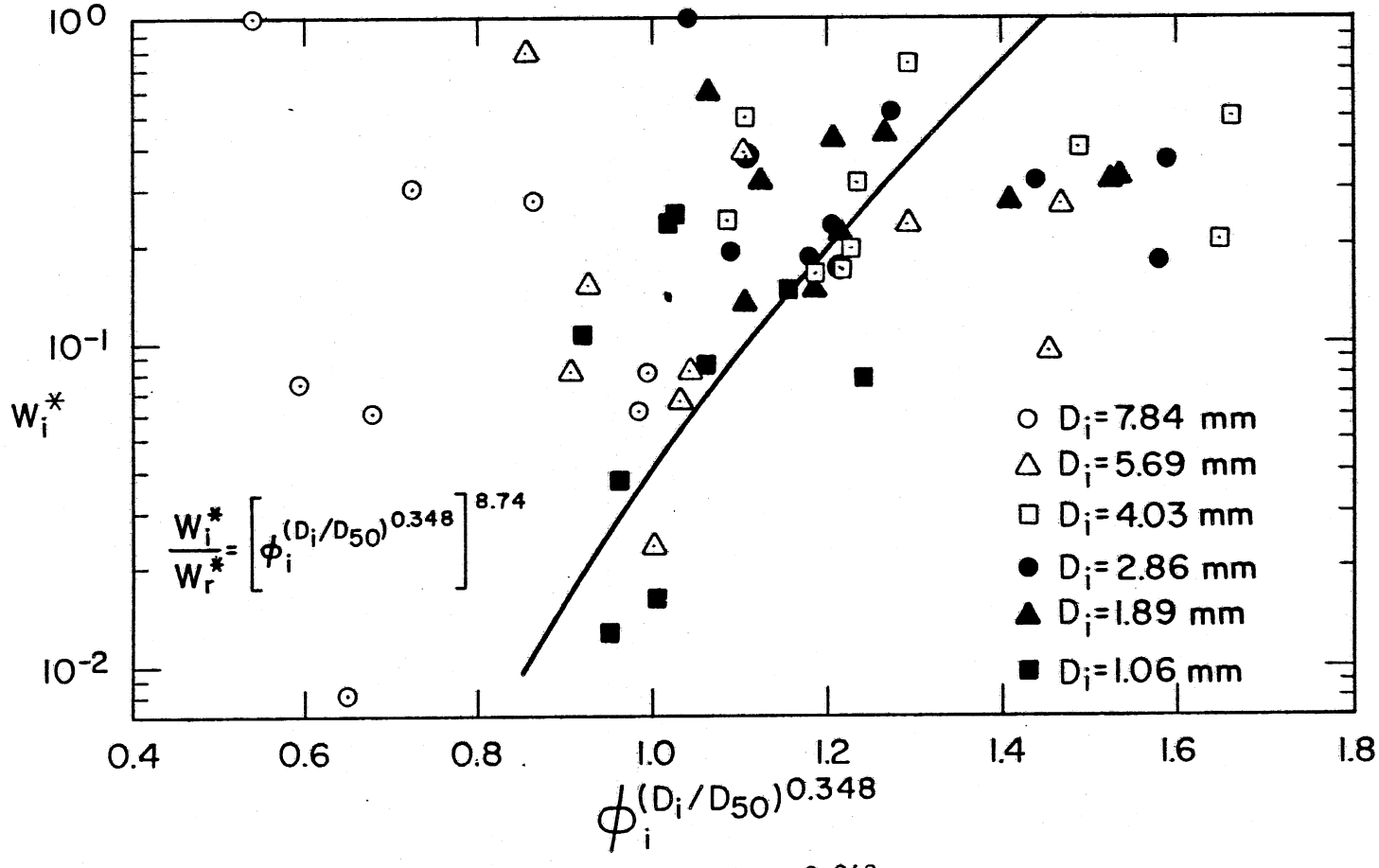

Figure 44. Similarity plot of W_i^* versus $\phi_i^{\left(\frac{D_i}{D_{50}}\right)^{0.348}}$ for the data of the present study.

$$W_i^* = W_r^* \left[\phi_i^{(D_i/D_{50})^{0.348}} \right]^{8.74} \tag{37}$$

The exponent 8.74 is the weighted mean value of the m'_i values (Eq. 20). For the SAFHL case the reference value considered for the dimensionless bedload transport was $W_r^* = 0.04$. This is sixteen times as high as the Oak Creek reference value. The absence of data points at very low bedload transport rates during the SAFHL experiments made the choice of such a high reference value necessary. The reference Shields stresses, τ_{ri}^*, obtained from (36) for $W_r^* = 0.04$ have been plotted in Fig. 37. A log-log regression gives the relation

$$\tau_{ri}^* = 0.0657 \left(\frac{D_i}{D_{50}} \right)^{-0.96} \tag{38}$$

with correlation coefficient r = -0.992.

The previous dimensional analysis indicated that the standard deviation of the bed material should also be included in the formulation of a bedload relation. Two data sets with different ranges of ϕ_{50} values cannot provide information of the dependence of W_i^* on the standard deviation of the bed material. Additional experiments with material of different standard deviation are necessary to evaluate this dependence.

8. RESULTS FROM THE EXPERIMENTS WITH FINES

LONG FLUME

The Approach to Equilibrium

Starting from the second experiment of each series, fine material was introduced into the flume. At the beginning of the second experiment, however, the major objective was to re-establish the equilibrium flow conditions reached at the end of the first experiment of the same series. The run time required by the flume to duplicate the equilibrium flow conditions ranged from three to ten hours. A duration of five hours was usually sufficient. The first experiment in each series was then used to define a baseline in the absence of fines (other than those already in the original bed-mixture). When the flume was diagnosed as being in equilibrium, a designated amount and type of fine material was introduced. The location of the fines introduction into the flume was at the downstream end, and the duration was equal to the time required by a fluid particle to travel through the channel and the piping system at the mean flow velocity. As soon as the fines were introduced into the flume, they entered the return pipelines, where they became well-mixed with the water before appearing at the channel head. The rate at which the fines were released into the flume was fairly constant, so that they were evenly distributed throughout the channel flow. In the succeeding experiments of the series, set amounts of fines were introduced into the recirculating system, so as to increase the total amount of fines therein. During the beginning of each one of these experiments the same process as that described for the second experiment of each series, was followed.

In order to facilitate the description of the experiments, three different types of concentrations are used for the fines. The first one is called system concentration and is defined as the ratio of the mass of fines and the total volume of water in the system (flume and pipes). The term system concentration is used in the long flume experiments. The second is the feed rate concentration and is used in the tilting flume experiments. This is defined as the ratio of the mass of fines feed rate and the water volume discharge. The third type is called suspension concentration and is used in both flumes. This coincides with the traditional use of the term concentration and is defined as the ratio of the mass of the fines in suspension and the volume of water.

The following program of incremental increase of fines supply was used for the experiments of Series 2, 3, 4, and 5. The amount of fines introduced into the flume during the second experiment accounted for a system concentration of 2,000 mgL^{-1}. This amount ranged from 1.3 to 1.8 kg depending on the discharge of the corresponding series. The fines added during the third experiment corresponded to a system concentration of 3,000 mgL^{-1}. The amount of these fines ranged from 2.0 to 2.7 kgr depending on the flow rate of the corresponding series of experiments. The fines released into

the long flume during the fourth, fifth and sixth experiments corresponded to system concentrations of 5,000 mgL^{-1}, 10,000 mgL^{-1}, and 10,000 mgL^{-1}, respectively. The total amount of fines introduced into the long flume during a single series of experiments ranged from 19.5 to 27 kgr. Somewhat different increments were used for series 1 and 6, as shown in Table 1. During series 6, the effects of fines accumulation into the channel bed on the bedload transport rate and water surface slope were monitored carefully. During series 4 and 5, fines with a median diameter D_{50} of 0.11 mm were used. For the other series (1, 2, 3, and 6), fines with a median diameter D_{50} = 0.080 mm were used.

Most of the fines deposited in the gravel bed soon after they were introduced into the flume. At the end of the second, third, and fourth experiments of each series the suspended sediment concentration was very low or almost zero. Only during the last two experiments of each series were the amounts of fines retained in suspension after equilibrium was reached significant.

The characteristics of the pavement and substrate material during the experiments with fines remained essentially similar to the experiments without fines. The only difference was in the percentage of fines found in these layers, which gradually increased as more fines were added to the flume. The ratio of the pavement median size to the subpavement median size, D_{p50}/D_{50}, was found to take an overall mean value of 2.24 for the second experiments of series 1 to 6; for the third, fourth fifth, and sixth experiments, averaged over the six series, the corresponding values were 2.28, 2.27, 2.28, and 2.15. On the average the bottom layer median grain size differed little from the corresponding subpavement median size (see Appendix 1).

Infiltration of Fines into the Channel Bed

There are two ways by which fine material has been observed to infiltrate into gravel beds. The first one is described by Einstein (1968). Einstein wrote that as soon as fine grains entered the gravel bed, they "slowly settled down to the bottom of the flume and gradually build up a deposit there filling the pores from the bottom up. As it has been mentioned earlier (Section 3) the material that Einstein used into his flume experiments as fines was much smaller than the coarse matrix that he used as bed material. Beschta and Jackson (1977) in their experiments used two grades of fines with median sizes of 0.2 and 0.5 mm, with a coarse matrix material with median diameter of 15 mm. The fines with D_{50} = 0.2 mm followed the Einsteinian mode of deposition. The coarser fines were inhibited from infiltrating all the way to the bottom of the gravel bed. Instead they bridged the gaps among particles of the gravel matrix, creating a seal 5 to 10 cm from the gravel surface, that restricted any infiltration of fines below that seal. Then the fines that were deposited after the seal was formed filled the pore space from the seal to the gravel surface. Both modes of infiltration have also been encountered by other researchers in the field as well as in the laboratory (Lisle, 1980; Frostick et.al., 1984; Dhamotharan et.al., 1980; Carling, 1984).

The transparent walls of the long flume, and the white color of the fines introduced into the flume, proved to be very helpful in observing the

infiltration of the fines into the gravel framework. Based on these observations and the results obtained in previous studies (Einstein, 1968; Beschta and Jackson, 1977; Lisle, 1980; Frostick et.al., 1984; Dhamotharan et.al., 1980; Carling, 1984), a model that describes the process of fines infiltration into a gravel bed can be constructed.

For a grain at the surface of the channel bed to infiltrate below the pavement, it must find a void in the surface layer at least a little larger than its size. The depth of maximum infiltration of this grain inside the flume bed depends on its size compared with the size of the framework grains, and its ability to move parallel to the layers of the framework gravel. Although the intergravel flow velocity is much lower than the mean channel velocity (Garvin, 1974), it might be instrumental in increasing the fines infiltration depth within the coarse matrix layers close to the bed surface. This was demonstrated in Carling's experiments. Carling (1984) buried in the flume bed two types of pots to measure the amount of fines that infiltrated into the bed. The first one was an impermeable can. The second one had many small holes around and at the bottom of the can, minimizing in this way the effect on the groundwater flow inside the can. It was found that on the average the impermeable pots captured 62 percent and the permeable pots 93 percent of the corresponding mean amount of fines that infiltrated into the channel bed. It is expected that the groundwater flow velocity decreases as the distance below the gravel surface increases. Then, even if the gravel framework is uniform in the vertical direction in terms of particle size, the probability of an infiltrating grain penetrating the nth matrix layer is smaller than the probability of penetrating the (n-1)th layer. Below a certain coarse matrix layer k there is no groundwater flow. Then assuming uniformity in depth of the gravel matrix, the probability that a grain infiltrates the kth layer is the same as its probability to infiltrate the (k+n)th layer.

If the substrate material is coarser than the pavement, then the pavement acts as a filter that keeps out the larger grains that are more likely to cause clogging problems. Thus, in this case higher amounts of fines may ultimately be expected to accumulate within the bed when compared with the case of substrate material similar to the pavement material. Even smaller amounts of fines infiltrate the bed when the substrate material is finer than the pavement. The latter case promotes clogging close to the subpavement layer. A large standard deviation of the subpavement material enhances further the possibility of the formation of a seal near the bed surface. The effect of the variation of the framework grain size with depth was examined by Frostick et al. (1984). If the infiltrating fines are very small compared with the pore sizes of the gravel matrix, and if the thickness of the bed is not very large, the fines are expected to reach the bottom of the bed. Additional fines introduced into the flume will continue to fill the gravel pores from the bottom up.

The probability that a grain passes through each individual coarse matrix layer is an independent event. Thus, the probability that a grain penetrates n matrix layers is equal to the product of the probabilities for each individual layer. Finally a particle that is trapped in the nth layer decreases the probability of another particle passing through this layer, while the probability for infiltration through each one of the top (n-1) layers remains the same. Thus, if the infiltrating grains cannot go

all the way to the bottom of the bed uninhibited, then it is expected that the first ones that infiltrate into the bed should outline the surface within the gravel framework that acts as a barrier for further downward infiltration. The distance of this barrier from the surface of the gravel bed should depend on the size of the infiltrating grains, among other factors.

Frostick et al. (1984) found from their field study that only 14 percent of the bed surface area of the Turkey Brook tributary was occupied by pore space. A suspended grain brought to the gravel surface either by gravity or a turbulent pulse has only a slight chance of depositing at a surface opening from where it will infiltrate inside the bed. A small grain moving as part of the bedload, although larger than the suspended grains, has much higher probability of encountering a void in the pavement large enough to allow the grain to penetrate the pavement layer. On the other hand bedload motion is a regular but rather infrequent phenomenon in natural gravel-bed streams, usually occurring only during floods, while sediment may be transported in suspension at a much wider range of flows. Thus, one would expect that in the absence of bedload transport, fine grains drawn from suspension would infiltrate deep inside the gravel bed. As soon as the bed is set in motion, small grains moving as part of the bedload would dominate the infiltration of fines into the bed. The latter grains are large enough to create a seal within the bed that would restrict any deeper infiltration of fines. Lisle (1980) observed this process in a field study. During a flood with high bedload transport and very low concentration of fines, one can expect that the bed of the stream can be purged of suspendible material to some extent, but it is rather unlikely that the material composing the seal, which might often be derived from the finer part of the bedload grains would also be removed.

During the present study, at the end of the first experiment of each series, the pavement was deficient in finer grains when compared with the original bed mixture, while the subpavement and bottom layers had a surplus of finer grains. More specifically the weight of grains with diameter smaller than 1.0 mm on the average represented 9.9 percent of the pavement material, 23.7 percent of the subpavement material, 23.5 percent of the bottom layer and 21 percent of the original bed mixture. Also, as mentioned earlier, the material of the surface layer of the bed is significantly coarser and better graded than the substrate material.

The initial slope of the channel bed was always steeper than the final equilibrium slope (Table 1). The equilibrium slope is approached by gradual aggradation of the downstream part of the channel, with simultaneous degradation of the upstream part during the first experiment of each series. In this way the substrate material of the upstream part is exposed to the flow by degradation, while the coarse layer of the downstream part tends to thicken. Thus, there is a gradual increase in the thickness of the coarse surface layer in the downstream direction. As a result, the depth of the fines infiltration into the coarse bed matrix also increased in the downstream direction. This result is demonstrated in Fig. 45, which shows the infiltration depth of the fines as it was measured from the sidewall along the flume at the end of run S4:E6. The channel slope at the end of both series 4 and 5 was about 0.0025. The initial slope for series 4 was 0.005 and for series 5 was 0.003. The average bed shear stress for

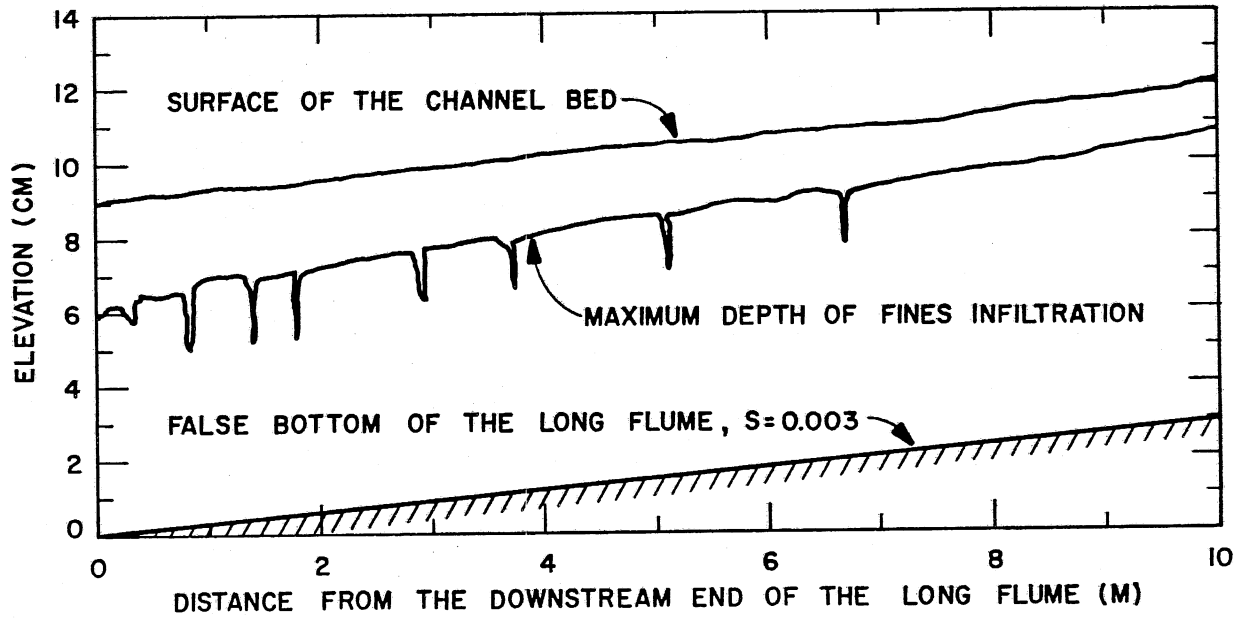

Figure 45. The depth of the fines infiltrated into the channel bed seen from the sidewall of the long flume at the end of the fourth series of experiments.

each series was roughly the same as well; i.e. 25 gr/cm sec^2 for the fifth series and 27 gr/cm sec^2 for the fourth series. The same type of fine material was used in both series. The average infiltration depth in series 4 was about 2.7 cm; a value of 2.35 cm was obtained for series 5. The more drastic change between the initial and final slopes in series 4 is considered to be the reason for the larger infiltration depth obtained for this series.

The fines introduced into the flume during the second experiment of each series, which are white in color, created a clearly visible interface within the bed framework. This interface separated the bed material into two regions. No fines infiltrate in the region below the interface. Instead it appears that the fine grains deposit in all levels above the interface, with the bulk of the filling progressing from the interface upwards to the gravel surface.

The initial slope for both series 5 and 6 was 0.003. Similarly, the corresponding final slopes were equal to 0.0025. The average bed shear stress was about 25 gr/cm sec^2 for both cases. The average infiltration depth for series 5 was 2.35 cm, a value of 2.65 cm was obtained for series 6. In comparing series 5 and 6, it seems that the finer grade used as fines during series 6 is responsible for the increased average infiltration depth observed in this series.

All the phenomena relevant to fines infiltration into the coarse bed material observed during the present study, as well as in previous studies, seem to be explained reasonably well by the model presented here.

In order to visually demonstrate the infiltration of fines into the channel bed, three to four matrix layers were cleaned of their finer material in part of the bed during the first series. This was achieved by imposing a local constriction to the flow, which increased significantly both the local channel flow velocity and the local groundwater flow. Figure 46 shows a view of the channel bed from the side wall at the end of the sixth and seventh experiments. The total amount of fines that had been introduced into the flume by the end of the sixth experiment accounted for a system concentration of 10,000 mgL^{-1}, with 10,000 mgL^{-1} more being introduced during the seventh experiment. Figure 47 shows a view of the fines infiltrated into the channel bed seen from the sidewall at the end of S1:E8. The bed was not disturbed in this case.

The model described here is a qualitative one. Some practical guidelines have been established from experience with earthen dams, where the gravel framework is used to filter sands. According to these guidelines the coarse matrix material is an effective filter if the gravel D_{15} is less than five times the infiltrating fines D_{85}, and larger than five times the D_{15} of the fines. These criteria are valid when the coarse material size distribution curve is roughly parallel to the size distribution curve of the fines. As Beschta and Jackson (1977) point out, in this case the coarse matrix layer restricts the coarser part of the fines from infiltrating into it, which in turn restricts the finer part of the fines. Eventually a seal is built up that acts as a barrier against any infiltration of fines beyond it.

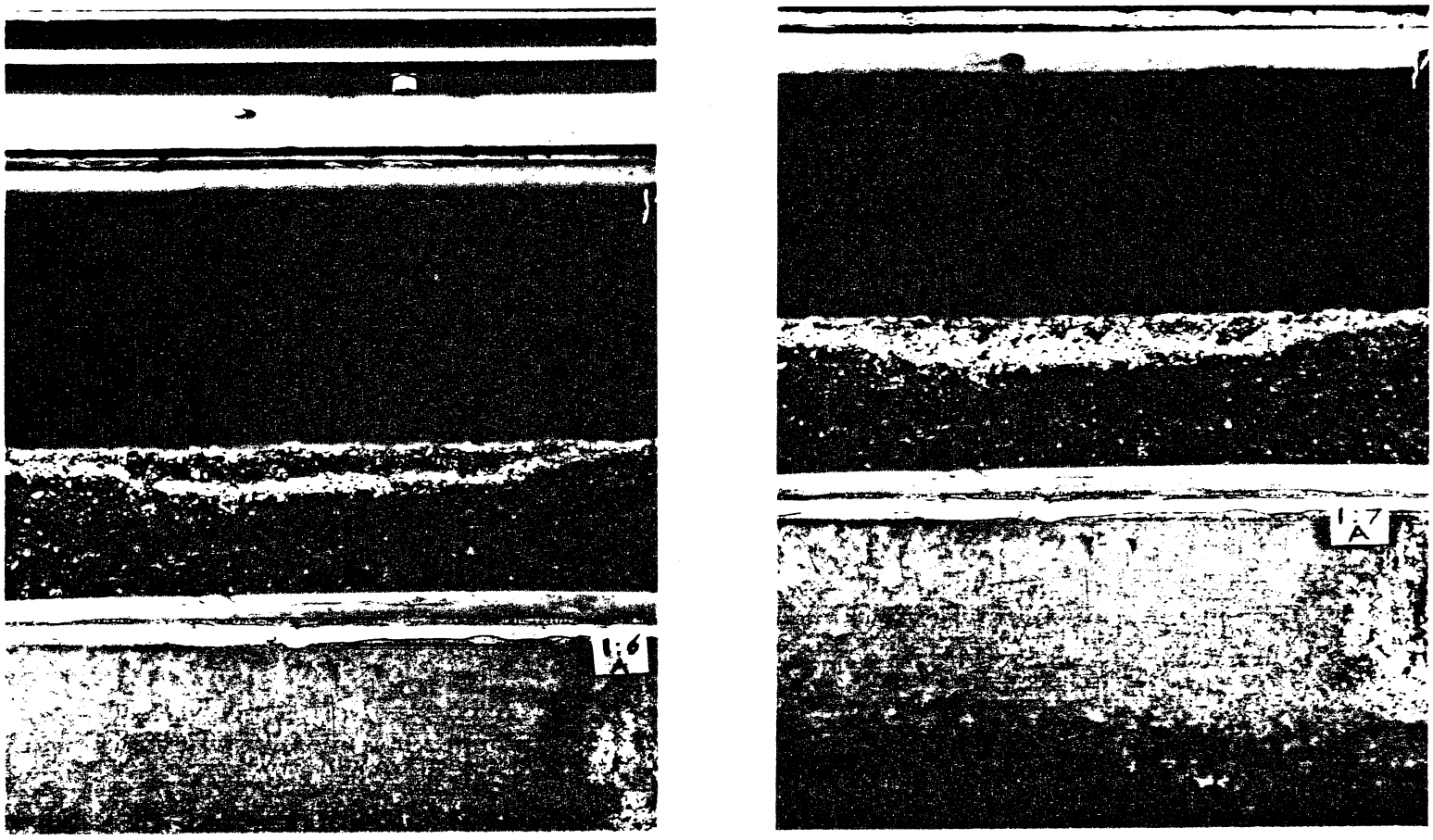

(a) (b)

Figure 46. The bed of the long flume has been locally cleaned of its finer grains for a few coarse layers, adjacent to the bed surface. (a) A view of the fines infiltration from the channel sidewall at the end of the run S1:E6. (b) A view of the fines infiltration from the sidewall at the end of run S1:E7.

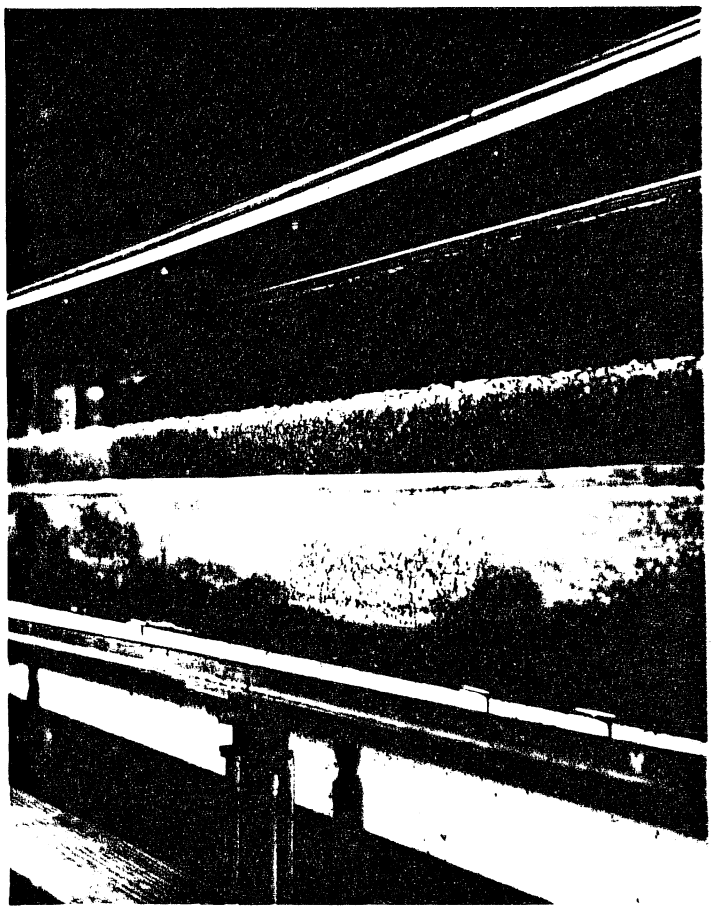

Figure 47. A view of the fines infiltrated into the channel bed seen from the channel sidewall at the end of S1:E8. The bed was not disturbed here. Flow direction is from right to left.

Finally, considering the fact that in gravel-bed streams the surface layer of the bed is coarser than the substrate, if clogging is to occur when fines infiltrate into the bed, it should not be far below the surface layer. That is, it should be close to the subpavement layer or the bottom layer as bottom layer is defined the layer below the subpavement. The depth of the seal that was created within the bed matrix by the fines introduced into the flume ranged from 5 to 10 cm in the experiments conducted by Beschta and Jackson (1977). This depth of the seal expressed in terms of bed material characteristics ranged from 2.5 to 5 D_{90}. During the present experiments the fines introduced into the channel never infiltrated deeper than the bottom layer of the channel bed in any appreciable amounts; i.e. when fines were found in any measurable amounts in the matrix layer below the bottom layer, they never exceeded 1 percent by weight of the material of this layer. Most of the times the top of the bottom layer corresponded to the maximum infiltration depth of the fines. This depth was about 2.1 cm from the surface of the bed or in terms of matrix material 2.4 D_{p90} or 3 D_{90}. For a more conservative estimate it is considered that the bottom of the bottom layer indicates the maximum infiltration depth. In the latter case this depth takes an average value of 3.5 cm, or 4.1 D_{p90}, or 5.0 D_{90}. In the present experiments the fines introduced into the channel never infiltrated deeper than the bottom layer in any appreciable amounts. A view of the pavement, subpavement and bottom layers is shown in Fig. 48 for the experiment S5:E6. In this case the fines have not infiltrated in any appreciable amounts below the subpavement. In some experiments considerable amounts of fines were found in the bottom layer.

Effects of Fines Accumulation on the Bedload Transport

Part of the present study deals with the effect of the fines introduced into the flume on the channel flow characteristics. The effects of the fines on the water surface slope of the channel, the velocity profile, and the bedload transport rate were observed during the experiments conducted in the long flume. The sixth series was specifically designed to study these effects as its main objective. This series consists of three consecutive experiments. During the first experiment the channel approached equilibrium in the absence of fines. During the second experiment quantities of fine material were introduced into the flume three times. The first amount represented a system concentration of 10,000 mgL^{-1}, and the second and third represented a system concentration of 5,000 mgL^{-1} each. This first amount of fines that was released into the flume yields rather high initial concentration in comparison to the second experiments of the previous series. This was done for a reason; during the preceding series it was observed that even after an amount of fines corresponding to system concentration of 10,000 mgL^{-1} had been introduced into the flume, at the equilibrium state of the flume all of it had infiltrated into the channel bed without affecting the flow characteristics above in any measurable way. During the third experiment, three more amounts of fine material were introduced into the flume. They represented system concentrations of 5,000 mgL^{-1}, 5,000 mgL^{-1}, and 10,000 mgL^{-1}, respectively, in the order that they were released into the flume. Before an amount of fines was introduced into the channel, it was first verified that the channel was really in equilibrium.

The variation of the water surface slope with time for the sixth series is shown in Fig. 49. This slope fluctuates slightly with time but

exhibits no specific trend. Similarly the velocity profile did not change during the course of this series. These results were shown to be true also for the other series of experiments. During the present experiments, the mean flow concentration of suspended sediment actually contained in the flow at the equilibrium state never exceeded 3,000 mgL^{-1}. Lumley (1978) suggested that the minimum concentration that could affect flow characteristics is around 8,000 mgL^{-1}.

The variation of the bedload transport rate during the sixth series is shown in Fig. 50. This figure displays a considerable variation in the bedload transport rate with time. Since there were no noticeable changes in the water surface slope or the velocity profile in time during the sixth series, it seems that the factor likely to be responsible for the otherwise unexplained bedload variation is the accumulation of fines in the bed. As is mentioned earlier, when the first fines deposit on the bed, they infiltrate the bed until they create a seal. The fine material that subsequently infiltrates the bed fills the pores of the coarse matrix from the seal toward the surface of the bed. The seal is usually established somewhere in the subpavement or bottom layer.

The grains that participate in the bedload transport almost always originate from those grains that are exposed to the fluid forces, that is, the surface layer of the bed material. When a small amount of fines is introduced into the flow, they eventually settle deep enough in the bed, somewhere around the bottom of the subpavement, so that they do not interfere with the grains of the surface layer. At this stage, then, the bedload transport rate is not affected. The upper limit for this amount of fines for the sixth series represented a system concentration around 10,000 mgL^{-1} (Fig. 50). As more fines accumulate in the bed, the layer containing fines fills upward, they are approaching the bottom of the surface grains. As the fines start impregnating the pores of the surface, they increase the stability of surface grains, resulting in a gradual reduction of the bedload transport rate. This is shown schematically in Fig. 51. The bedload transport rate in the absence of fines takes a value of 115 gr/min at the end of the first run of the sixth series. The lowest bedload transport rate was realized during the second run of the sixth series. This lowest bedload transport rate was measured to be equal to 50 gr/min, which represents a 57 percent reduction in the value of the bedload transport rate in the absence of fines. Dhamotharan et al. (1980) encountered the same phenomenon. They observed a 30 percent reduction in the bedload transport rate when fines were fed into the flume, compared with the bedload rate in the absence of fines.

As even more fines are introduced into the channel, the subpavement gradually becomes saturated with them, and the interstices between the grains of the pavement start to fill. During this process the mobility of the pavement particles is further reduced, while the top of the pavement becomes smoother, and the mobility of the grains moving on the surface of the pavement is increased. When the fines that have accumulated in the bed reach an appropriate value, the bedload rate stops declining. A further increase in the amount of fines in the bed results in an increase of the bedload transport rate. It is presumed that at the point where the bedload stops decreasing, the fines have rendered the pavement grains virtually immobile, and the bedload is composed only of particles that move on the

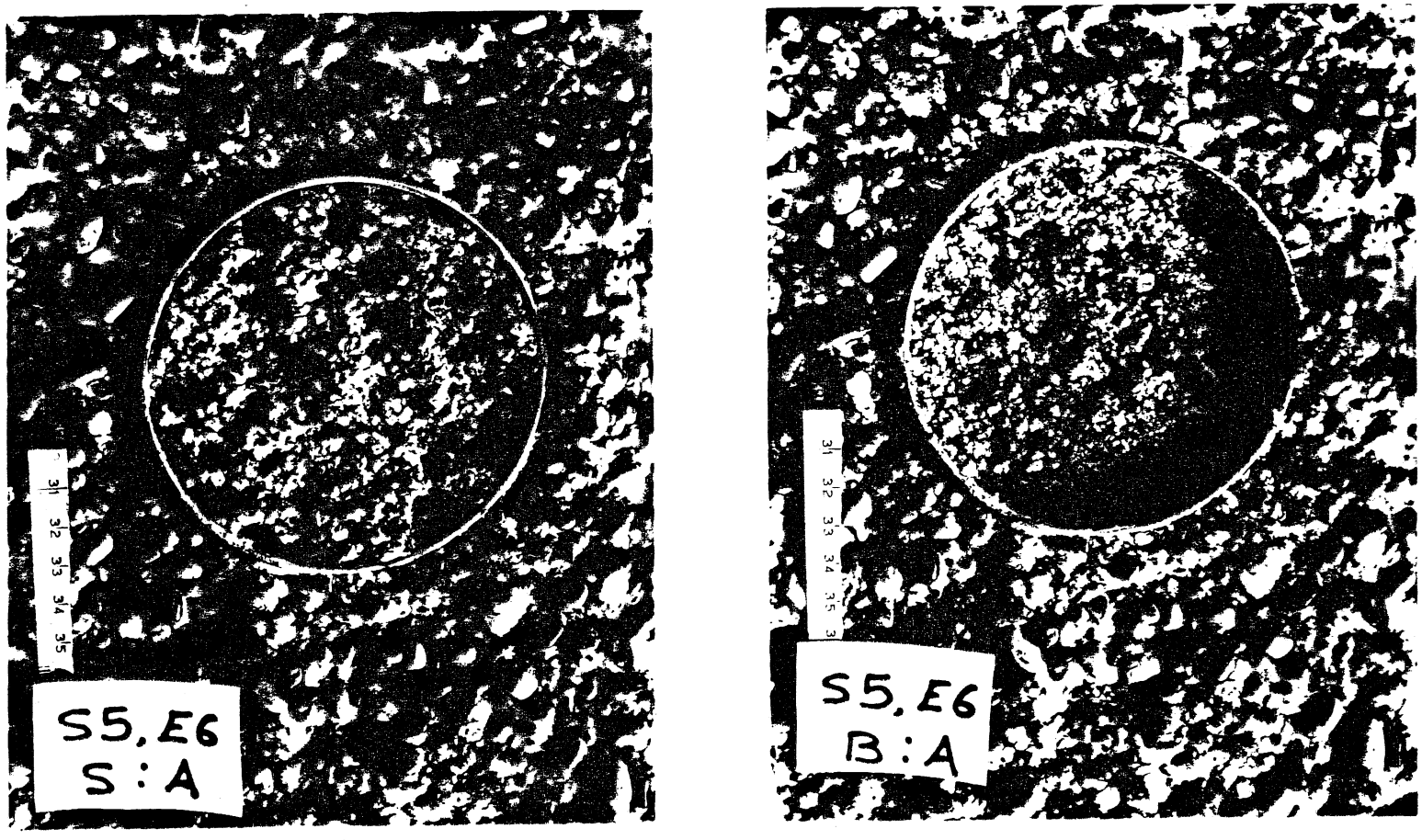

(a) (b)

Figure 48. (a) A view of the pavement and subpavement layers. (b) A view of the pavement and bottom layers. The fines have not infiltrated in the bottom layer in any appreciable amounts. The photographs are from S5:E6.

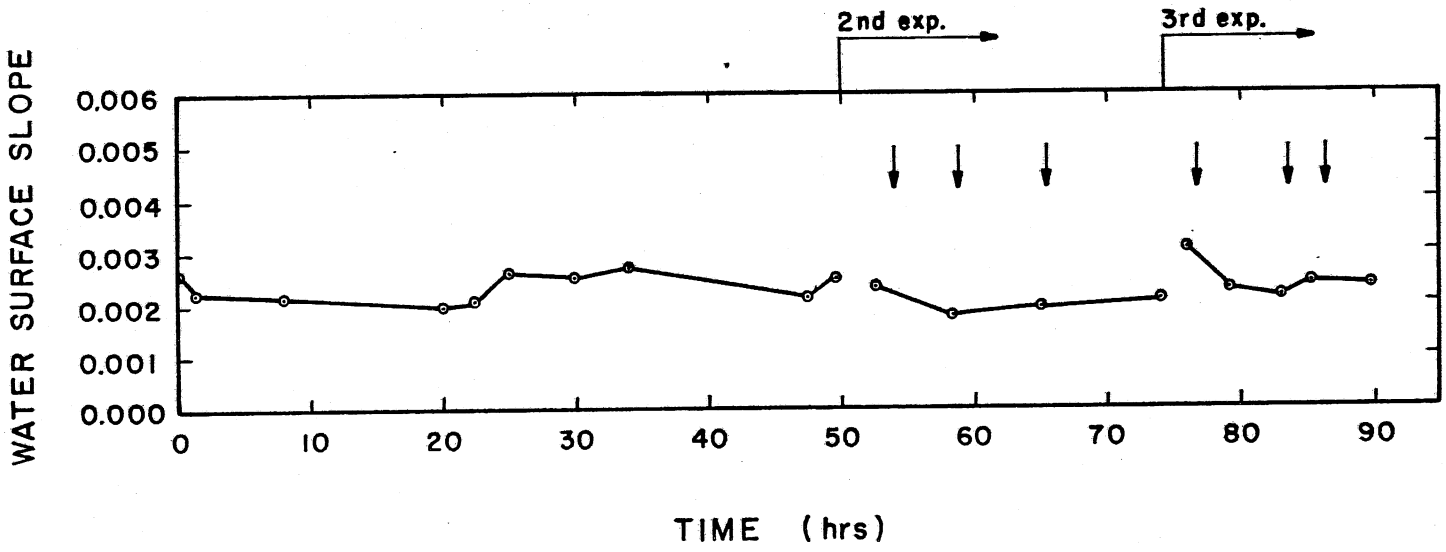

Figure 49. Variation of water surface slope with time during the sixth series of experiments. The vertical arrows indicate the times at which fines were introduced into the flume. For the quantity of fines released each time into the flume see Table 1.

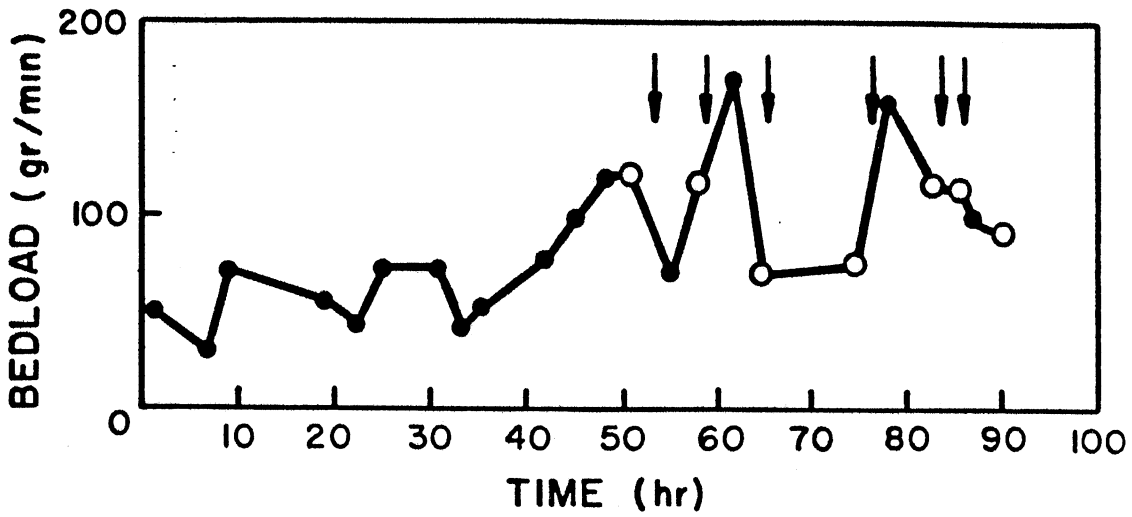

Figure 50. Bedload variation with fines addition during the sixth series of experiments. The open circles represent equilibrium bedload values. The vertical arrows indicate the time at which additional fines were introduced into the long flume. For the amounts introduced each time see Table 1.

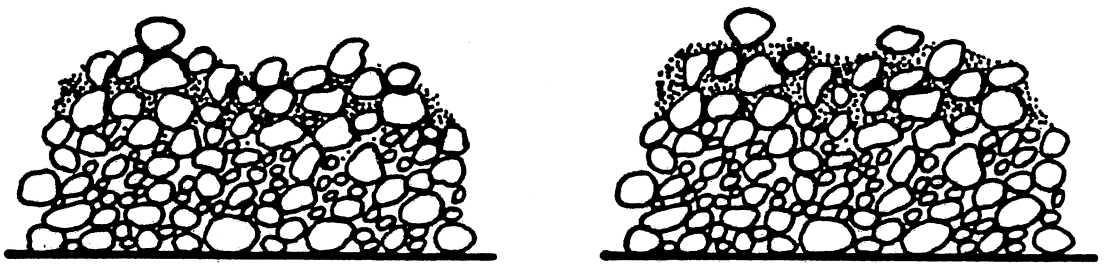

Figure 51. Illustration of fines deposition in the bed. (a) Fines saturated the subpavement and have also been deposited within the bed surface layer. (b) Fines have saturated the bed surface layer.

top of the pavement. A further increase in the fines of the bed, while not affecting the stability of the now-saturated with fines grains in the pavement layer, enhances the mobility of the grains moving on top of it by reducing the roughness of the pavement surface (Fig. 51). The bedload transport rate under these conditions approaches the original transport rate, when no fines had been introduced into the flume yet. In this state the number of moving grains has been significantly reduced, but the rest periods between motions are much shorter than in the case of grains moving on a pavement in the absence of fines.

By adding even more fines, the bed gradually changes from gravel to sand as the gravel is buried; it ultimately becomes completely covered with fines. At this state ripples, bedforms characteristic of sandy beds, appear on the bed of the channel (Fig. 52). At the same time the suspended sediment concentration of the flow increases, and the availability of grains from the original bed mixture declines and eventually vanishes, with bedload rate following the same pattern (Fig. 50). It should be mentioned that the term bedload used here includes only those bedload grains that come from the original bed mixture. It was not possible to account for the fines that moved as bedload.

From the present experiments it was roughly estimated that when the amount of the introduced fines comprised about five percent of the subpavement material by weight, the bedload transport rate started to decline. When these fines comprised roughly five percent of the pavement material the bedload rate started to increase. On the average the thickness of the subpavement layer was 1.5 cm, while average values for the D_{50} and D_{90} grain sizes of the subpavement material were 2.24 mm and 7.0 mm, respectively. The surface layer thickness was about equal to the D_{p90} of the pavement material. For the long flume experiments D_{p90} = 8.5 mm. It should be emphasized that the numbers given here with regard to the percentage of fines in the pavement and subpavement are only tentative estimates.

The size distribution of the bedload in these experiments remained roughly constant during each series, with the median size still very close to the subpavement D_{50}.

Intergravel flow may also be considered to promote the instability of the bed surface grains. The reduction of this flow in the presence of fines can be a contributing factor to the increased stability of these grains. If such an effect is present, it should be rather small because the onset of the bedload decline coincided with the presence of fines in the top of the subpavement, where direct contact with the pavement grains was visible.

TILTING FLUME

Seven experiments were conducted in the tilting flume. During the first experiment the flow rate was 12.8 lt/sec, the coarse material feed rate was adjusted to 5.4 gr/sec, and no fines were fed into the flume. During the second experiment, fines were fed into the flume. The fines used in the tilting flume experiments had a median size of 0.11 mm. The fines feed rate was 2.0 gr/sec, which corresponds to a feed rate concentration of 156 mgL^{-1}, with water discharge and coarse feed rate being

the same as in the case of the first experiment. The only thing that changed in the third experiment was the fines feed rate, which was increased to 4.3 gr/sec, or 350 mgL^{-1} mean flow concentration. The fourth experiment started under the same flow conditions as those of the previous experiment. Four hours later the flow rate was gradually reduced to the point that bedload transport became negligible. At the same time the coarse material feed was cut off and the fines feed rate was decreased to 2.7 gr/sec. The flow rate that was found to provide bed conditions at or close to the threshold of motion was 6.3 lt/sec. The feed rate concentration for the fourth experiment was 430 mgL^{-1}. No fines were fed into the flume during the fifth experiment, but everything else was kept the same as for the fourth experiment. The sixth experiment was identical to the first one. In the seventh experiment the flow rate was increased to 15.4 lt/sec and the coarse feed rate became 12.5 gr/sec, with no fines being fed into the flume. The duration of the experiments in their order of execution was 34, 25, 14.5, 9, 19, 11 and 10 hours.

The feed rate concentrations quoted above for the experiments with the tilting flume are considerably lower than the initial system concentrations typically quoted for the experiments in the long flume. It is important, however, to realize the difference in configuration. In the feed configuration of the tilting flume, fines must eventually exit the system at the same rate they enter in. In the process, the gravel is subjected to a continuous rain of fines. Even at these low feed rate concentrations, then, the fines entered in the bed are generally built up to significant values. On the other hand, the dumping of as much as 5,000 $mg\ell^{-1}$ of system concentration of fines into the long flume results in a one time depositional event, after which the water may clarify completely.

The purpose of the first experiment was to establish a bedform pattern that would resemble those commonly encountered in natural gravel-bed streams. During the next three experiments, the degree and nature of the pollution of the channel bed was examined when fine material was fed into the flume under various flow conditions. The ability and extent to which the stream could purge itself of the fines was tested during the last three experiments. Possible modifications in the bedform structure were also carefully monitored throughout this series.

The bedload variation in time during the last six experiments of the seventh series is shown in Fig. 53. The water surface slope variation in time for the same experiments is shown in Fig. 54.

Because of the different modes of operation of the two flumes used in the present study, some of the results obtained appear to be in discord. For example the pavement was significantly coarser in the tilting flume experiments. A mean value of all the median sizes found in the pavement samples was 6.11 mm for the tilting flume and 5.15 mm for the long flume. This may be correlated with a deficiency of the tilting flume pavement in grains with diameters in the range from 1.4 mm to 3.36 mm. This material is near the subpavement median size, which, as was shown in Fig. 39, has the highest mobility of all grain sizes in the pavement for the ϕ_{50} values around one. Values of ϕ_{50} in this range are typical in the present experiments. Two constraints of the tilting flume experiments were the rate and the size distribution of the coarse material fed into the flume, both being

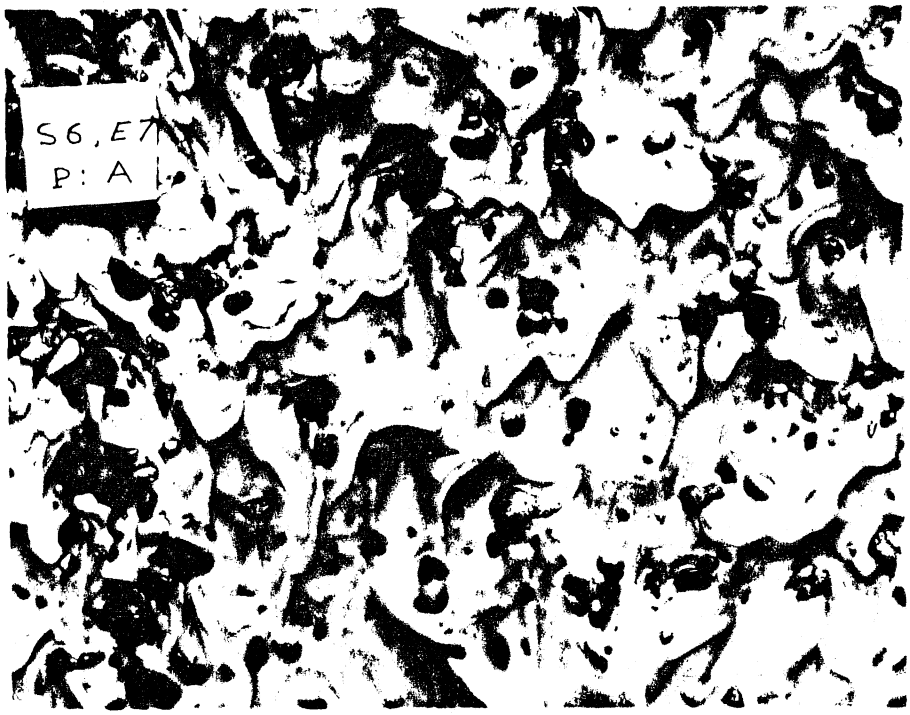

Figure 52. View of the channel bed at the end of run S6:E7. A rather well developed ripple configuration is present on the channel bed. The flow direction is from the top to the bottom of the photograph.

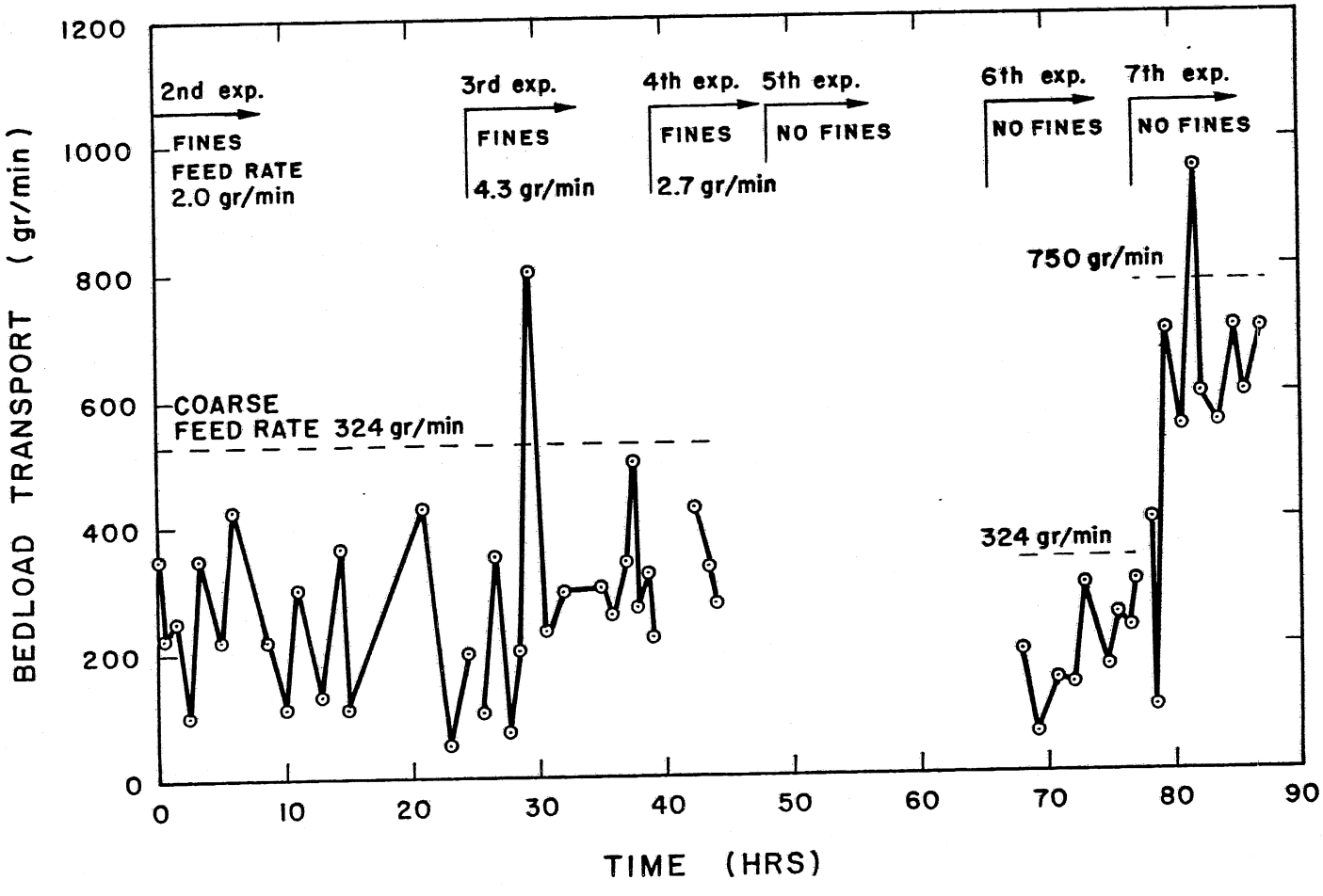

Figure 53. Variation of bedload transport rate, measured at the downstream end of the tilting flume, with time during the last six experiments of the seventh series.

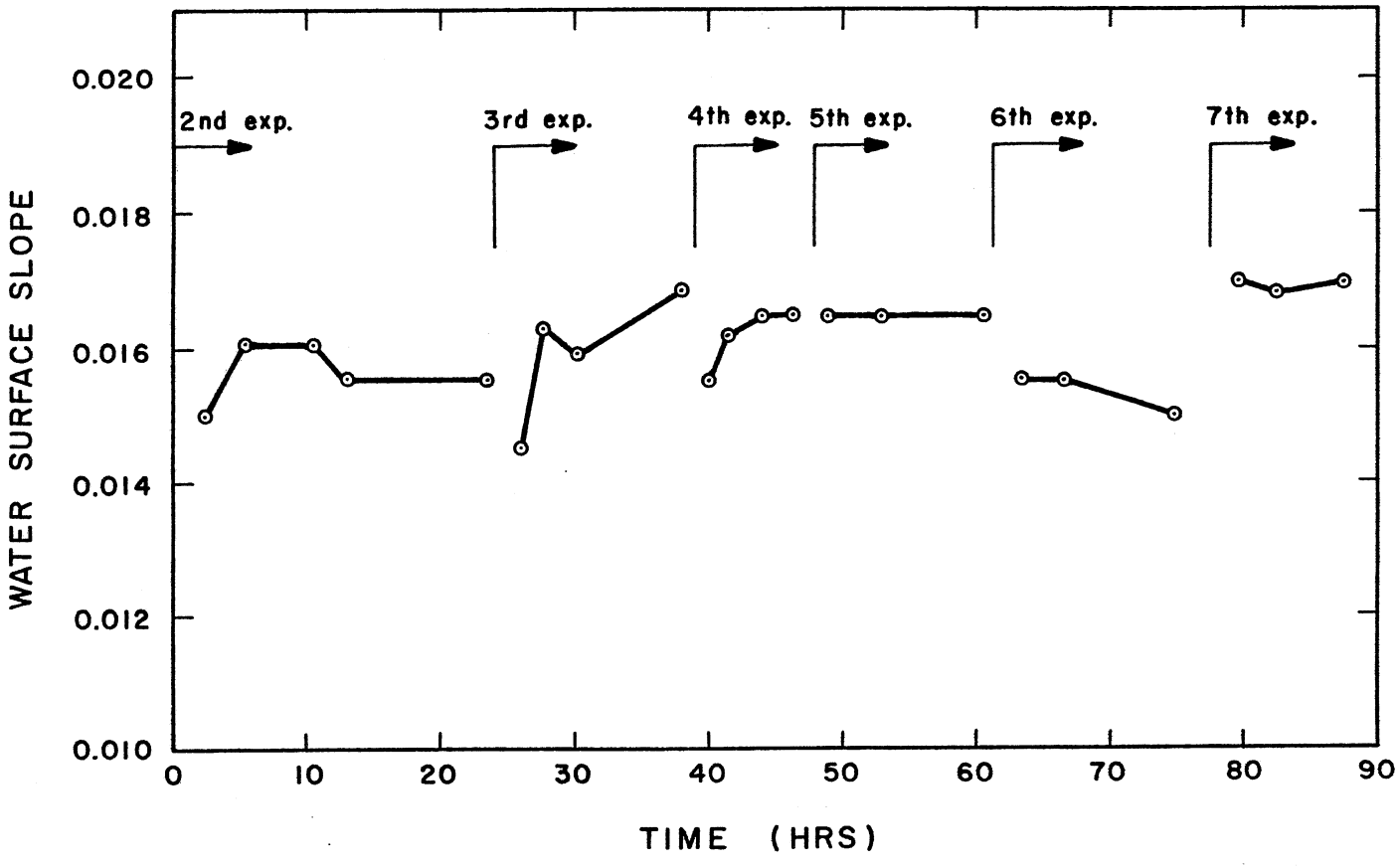

Figure 54. Variation of water surface slope with time during the last six experiments of the seventh series.

predetermined. For the channel to be in equilibrium, the bedload transport rate and size distribution at the channel exit should thus match the corresponding values for the feed. As a result, the finer half of the material fed into the flume should go through the flume at the same rate as the coarser half. To accomplish this, the tilting flume increases the number of coarser particles in the pavement and simultaneously decreases the number of the finer, intrinsically more mobile grains. The material in the size range from 1.4 to 3.36 mm comprised about 34 percent of the original bed mixture and about 55 percent of the bedload in the long flume experiments. Because of the recirculating nature of these experiments, however, this material cannot be washed away, nor can it effectively infiltrate below the pavement, because of its size. Thus, it will always remain on the surface, resulting in a smaller median size for the pavement in the long flume experiments. In the tilting flume, typical values for the percentage of the pavement material that belongs to the range 1.4 to 3.36 mm is 15 percent; 38 percent of the material is coarser than 6.68 mm. For the long flume experiments the corresponding values are 26 and 24 percent, respectively.

As will be recalled from section 6.2, a pattern of alternate bars was formed during the first experiment. During the second experiment the morphological change of the bed was insignificant except for an average aggradation in the channel as a whole of about 0.5 cm, and a half-meter downstream migration of the middle bar. The variation of the grain size of the pavement along the middle bar was less pronounced compared with the first experiment. The median size of the pavement at the tail of the bar was 5.47 mm, and at the bar head was 6.23 mm. Most of the fine material that deposited on the channel bed was found in the subpavement of the middle and the tail of the bar, as well as in the subpavement of the pool. Only minimal amounts of fines were found anywhere in the pavement, nor were fines found in the subpavement at the bar head. The flow over the bar downstream of the head is fairly tranquil, and so promotes the deposition of the suspended grains. A smaller amount of fines was also deposited uniformly in the bottom layer, without exhibiting any significant disparities along or across the flume.

During the third experiment, the fines feed rate was increased. As a result, fines were deposited in the subpavement of the bar head, as well as in the pavement of the bar tail and the pool area. The amount of fines in the subpavement of the pool was further increased during this experiment (see Appendix 1). The bed topography at the end of the third experiment was measured with a point-gauge; a computer generated plot of the lines of constant elevation is shown in Fig. 23.

The fourth experiment was used to examine the sedimentation of the channel in the absence of bedload motion. As is shown in Fig. 55, fines have been deposited throughout the channel pavement, although in higher amounts in the bar tail and lee areas. A close-up view of the pavement and subpavement material at the bar tail can be seen in Fig. 56. The surface and bottom layers at the bar head are shown in Fig. 57. Finally the surface layer at the pool at the end of the fourth experiment is shown in Fig. 58.

The ability and extent to which the channel was able to clean its bed of fines in the absence of bedload motion was examined in the fifth

experiment. The fines that were deposited in the subpavement and the bottom layers remained intact. The pavement was partially cleaned. In areas of swift flow, such as the bar head, the pavement was cleaned almost completely. The cleaning process was less efficient in areas of slower flow, such as in the pool, particularly at the bar tail. A view of the surface layer of the bar tail is shown in Fig. 59. Figure 60 demonstrates the cleaning process during the fifth experiment at the head of the bar. As is seen from this figure the pavement has been completely purged of the fines, while fines are still present in the subpavement layer. The same process for the pool area is evident in Fig. 61. Other researchers (Milhous, 1973; Frostick et al., 1984) have also emphasized the necessity of the pavement mobilization if the cleaning is to be effective.

During the sixth experiment the flow rate was increased so as to be capable of mobilizing even the coarsest grains of the pavement. The cleaning process under broken pavement conditions was examined in this experiment. Both the pavement and subpavement layers of the channel bed were effectively purged from the fines during this experiment. On the other hand, an increase in the amount of fines in the bottom layer was observed. During the course of the present experiment the channel bed aggraded roughly by 0.4 cm as a whole and the middle bar propagated downstream by 0.7 m. As a result, part of the material that belonged to the subpavement layer at the end of the fifth experiment became part of the bottom layer at the end of the sixth experiment. This is probably one of the causes of the increased amounts of the fines found in the bottom layer. The results of this experiment indicate that flow conditions of broken pavement can effectively remove the fine material from the channel bed as deep as the subpavement. The fines in the bottom layer are not affected. A view of the channel bed at the end of the sixth experiment is shown in Fig. 62. The pavement and subpavement material at the bar tail are shown in Fig. 63.

Experiments 2 to 6 engendered only small changes in the channel morphology created in experiment 1. The bar structure remained more or less the same, and the bar tail remained finer than the bar head.

The seventh and last experiment was designed to simulate a rather infrequent flood, and examine the effectiveness of such a flood in the process of cleaning the bed of fine material. The bedload transport rate in this experiment was about two and one half times the bedload transport of the sixth experiment. The bed topography at the end of this experiment is shown in Fig. 23. As is seen from this figure, the channel bed is almost completely flat. No fines were found in the extracted samples of pavement, subpavement and bottom layer. The absence of fines in the bottom layer is probably partially due to a slight aggradation of the channel bed during the experiment. Fines were found in small amounts a little deeper than the bottom layer. A vertical cut of the whole bed material revealed a thin layer that included small amounts of fines, about one millimeter thick spanning throughout the channel width. This layer was deeper inside the bed under the pool. This is in agreement with the increased aggradation required in the pool to provide a flat bed. Compared with the sixth experiment it seems that fewer fine grains are left in the channel bed at the end of the seventh experiment. This is probably the result of partial cleaning of the channel bed from fines during the last experiment. A view

Figure 55. A view of the fines deposition on the channel bed of the tilting flume at the end of the fourth experiment. Flow is from top to bottom.

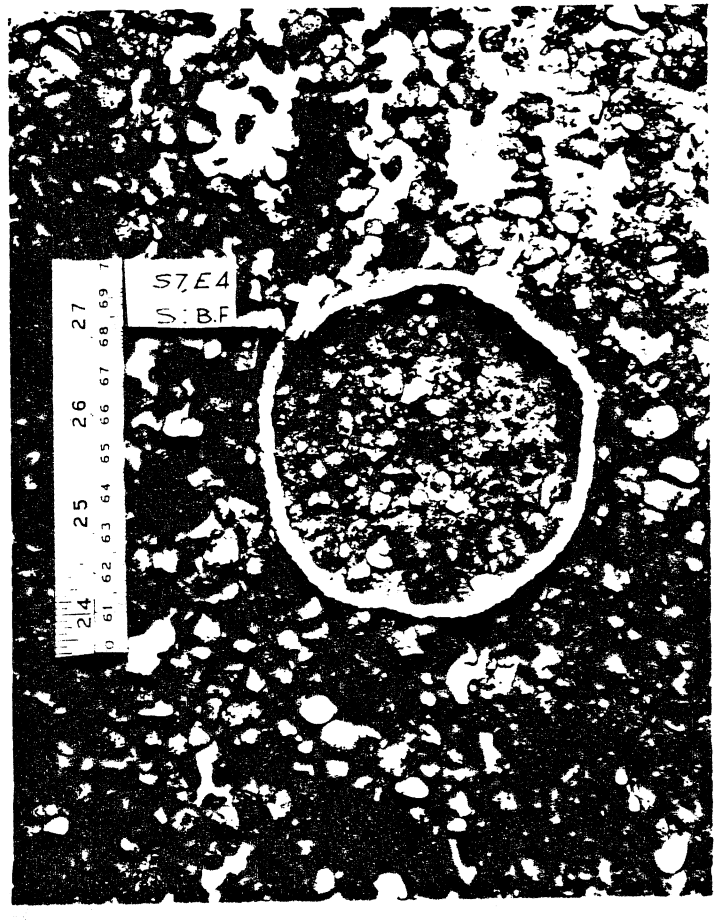

Figure 56. A view of the deposition of fines on the pavement and subpavement of the bar tail after run S7:E4. Flow is top to bottom.

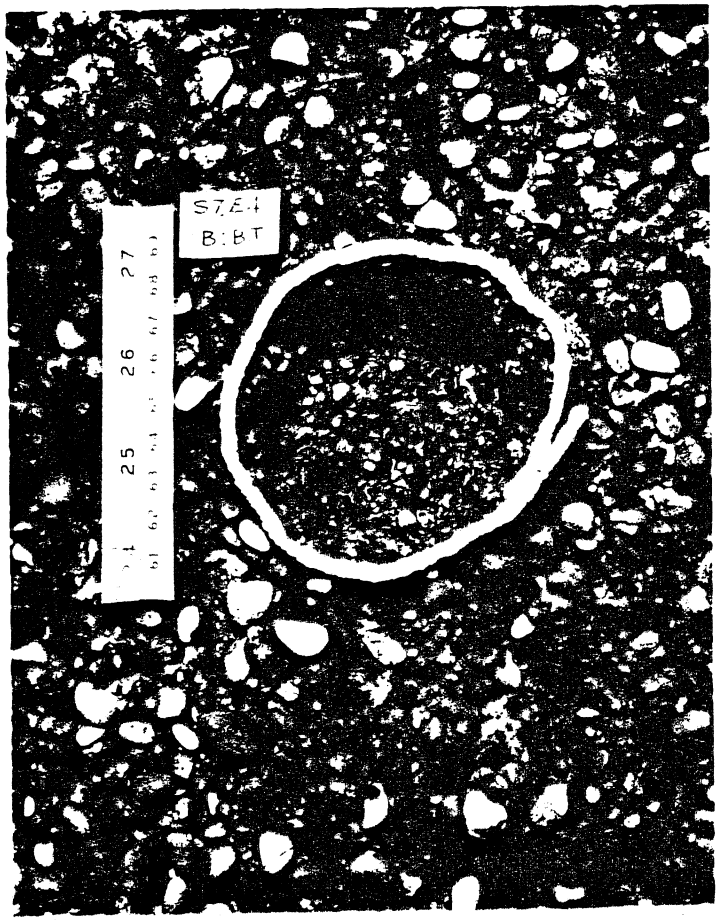

Figure 57. The surface and bottom layers at the bar head at the end of run S7:E4. Flow direction is from top to bottom.

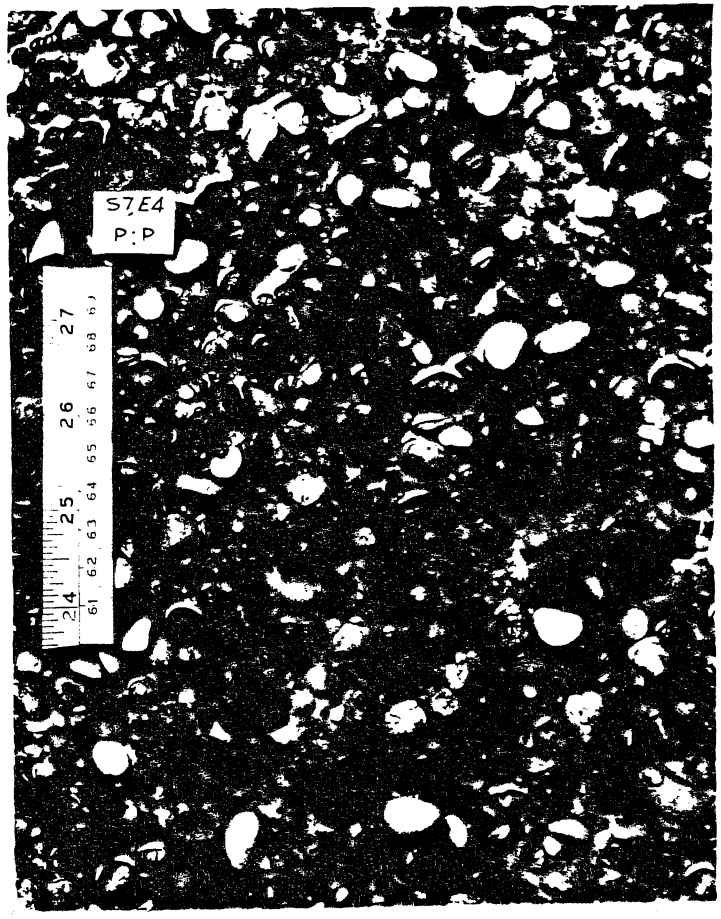

Figure 58. The surface layer in the pool after run S7:E4. Flow is from top to bottom.

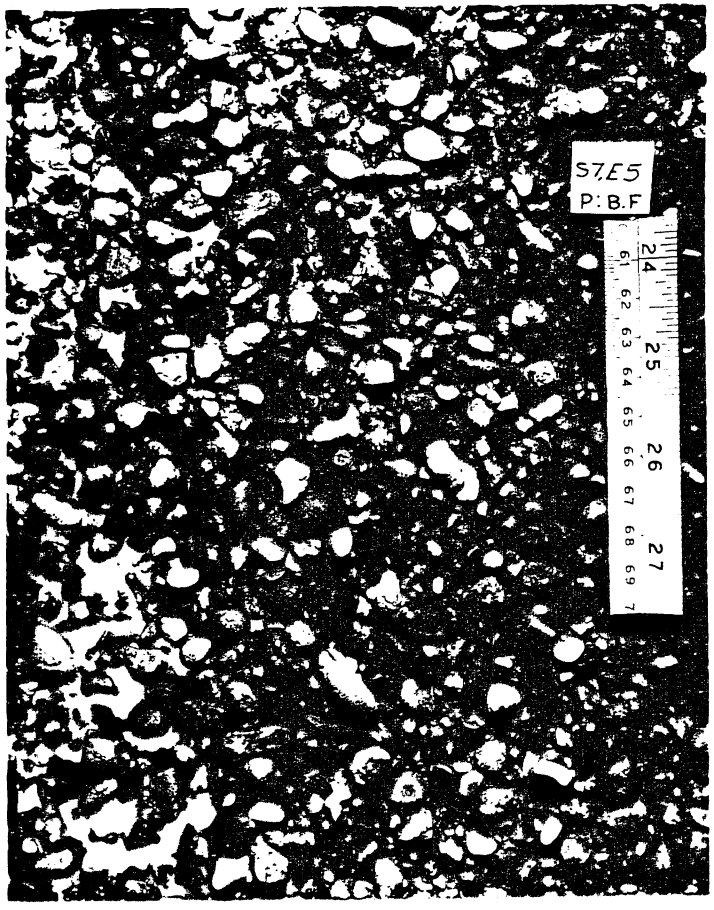

Figure 59. A view of the bed surface at the bar tail after run S7:E5. Flow direction is from top to bottom.

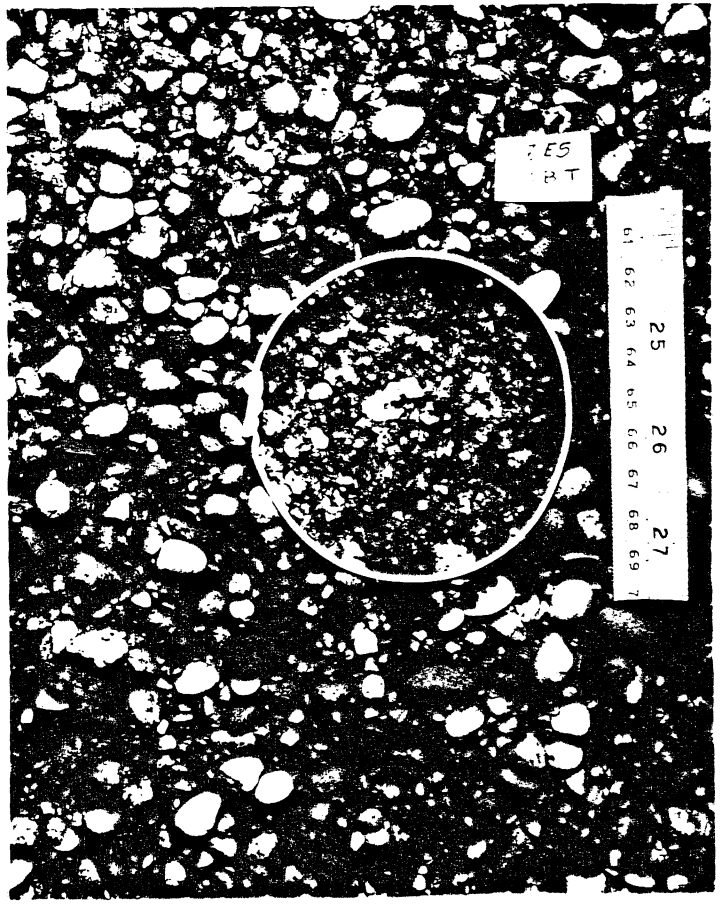

Figure 60. The surface and subsurface layers at the bar head after run S7:E5. Flow is from top to bottom.

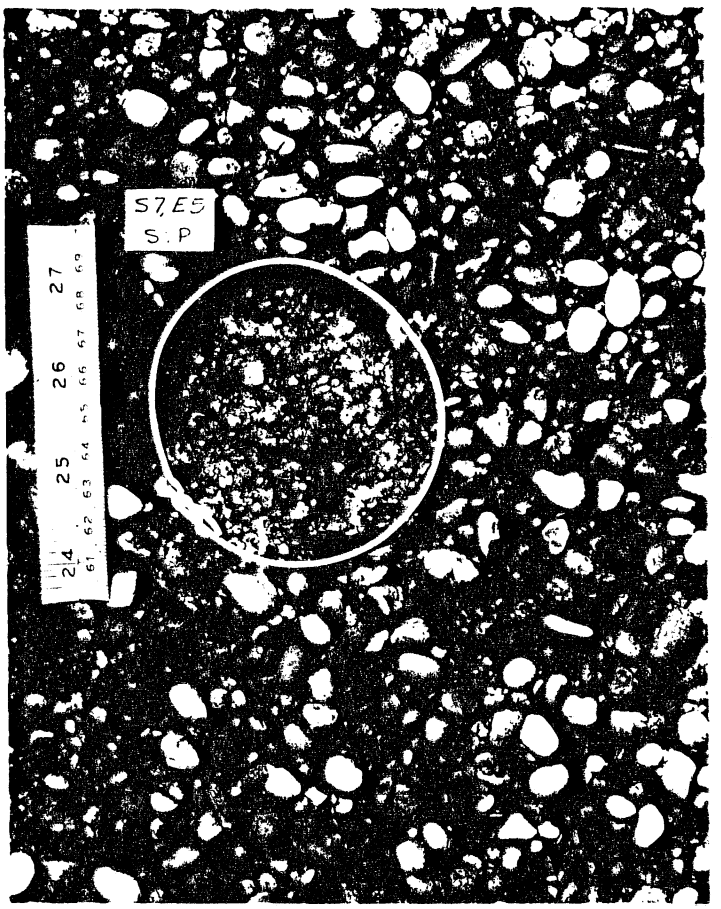

Figure 61. The pavement and subpavement layers in the pool after run S7:E5. Flow is from top to bottom.

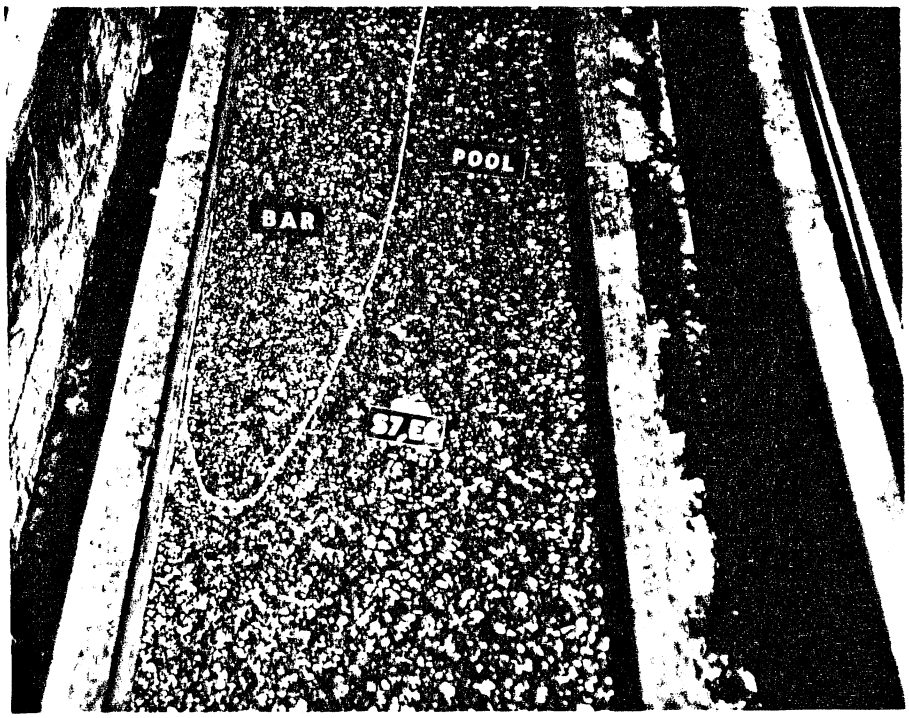

Figure 62. A view of the bed surface of the tilting flume after run S7:E6. The flow direction is from top to bottom.

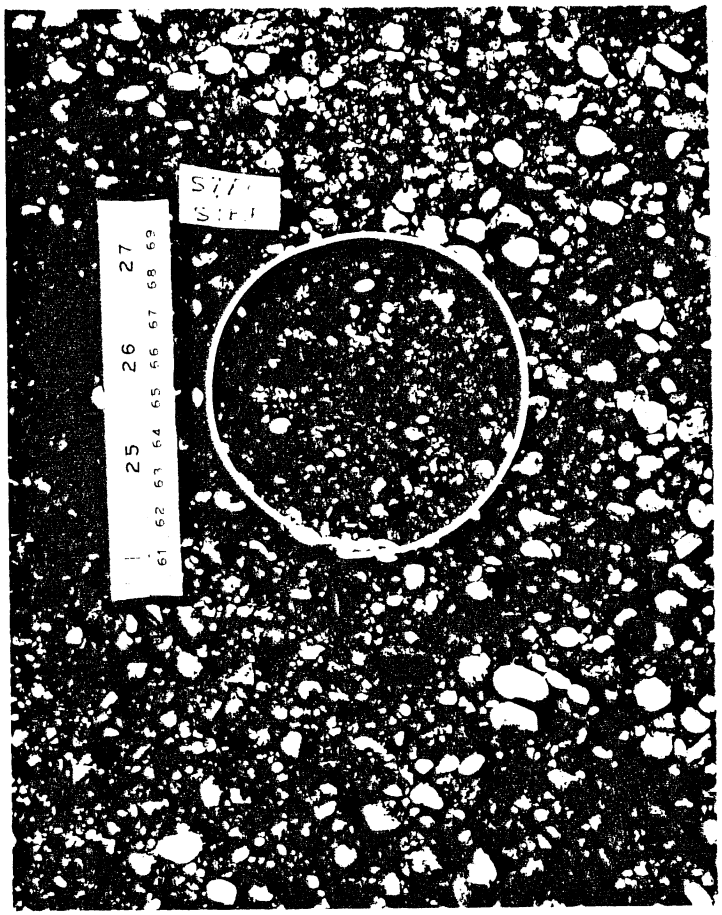

Figure 63. Pavement and subpavement layers at the bar tail after run S7:E6. The flow direction is from top to bottom.

of the layer deep within the bed where fines remain at the end of the seventh experiment is shown in Fig. 64.

It seems reasonable to assume that the forces that can entrain a small grain from the subpavement can also push the grain deeper into the bed. This is probably partially responsible for the increased amounts of fines at the bottom layer at the end of the sixth experiment, as well as for the deeper infiltration of fines, in the vicinity of the bar, during the seventh experiment. Beschta and Jackson (1977) mentioned that an increased jiggling motion of grains at the bed surface forced the seal created by the fines introduced into the flume deeper into the bed. They considered turbulent pulses to be responsible for this phenomenon. Similarly, Lisle (1980) observed that the seal was established deeper into the bed in areas of higher flow energy. Complete elimination of the fines from the bed is thus rather unlikely unless an episodic event takes place. On the other hand, it seems that the channel bed can be purged of most of its fines by an appropriately high flood with an appropriately low load of fines.

The grains with diameter larger than 0.177 mm and smaller than 0.42 mm belong to the original bed mixture or to the coarse material fed into the flume, and comprise the finer part of this material. The grains with diameter smaller than 0.177 mm are derived from the fines fed into the flume. As can be seen from Appendix 1, the amount of material in the range 0.177 to 0.42 mm in the subpavement and bottom layers after the first of the tilting flume experiments reached values that did not change during the remaining six experiments. For the substrate the grains in this range comprised about 8 percent of its material; for the bottom layer, the corresponding value is 8.3 percent. The constancy of these values throughout the experiments suggests that no material from that range was entrained by the flow from the subpavement and bottom layers. The grains with diameter smaller than 0.177 mm behaved differently. Their amounts in the pavement and subpavement increased during the first four experiments and decreased during the last three experiments. The particles in the latter range can be transported in suspension by the channel flow while the others are too heavy to be suspended in significant quantities. One can then conclude that the grains that are likely to be entrained by the flow from the subpavement or bottom layer are only those that can be suspended by the flow.

It should be also mentioned that when the fines had infiltrated either the subpavement or bottom layer throughout the channel bed and had saturated these layers, the amount of fines in each of these layers was roughly the same everywhere, about 6 percent by weight. In the experiments in the tilting flume no part of the channel bed was ever exposed to air. Also in most of these experiments the bedload transport rate, although considerably lower than the pool area through which most of the bedload was moving, did not vanish even at the tail of the bar.

Correlation Between Mean Flow Concentration and Amount of Fines in the Flume Bed

For a two-dimensional flow the equation of the mean suspended sediment mass balance can be written as

$$\frac{\partial c}{\partial t} + \frac{\partial uc}{\partial x} = - \frac{\partial}{\partial z} \left(\overline{w'c'} - v_s c \right) \tag{39}$$

where u is the local flow velocity in the x-direction and c the local concentration, both averaged over turbulence; x denotes the downstream direction along the channel, and z denotes the direction upward normal to channel bed; w' is the fluctuating velocity component in the z-direction, and c' the fluctuating local concentration. When Eq. (39) is integrated along the channel depth from a point very close to the channel bed, z = b, up to the water surface, z = d, a bulk balance for the suspended sediment contained within a layer of flow defined by the limits of the integral is obtained

$$\frac{\partial}{\partial t} \int_b^d c\,dz + \frac{\partial}{\partial x} \int_b^d uc\,dz = \left[\overline{w'c'} - v_s c \right]_{z=b} \tag{40}$$

where v_s denotes the fall velocity of the suspended material. The right hand side of Eq. (40) denotes the mean vertical volumetric flux of suspended sediment across a plane parallel to the channel bed and at a distance b from it. This term is composed of two parts; the first one, $\overline{w'c'}\,|_{z=b}$, gives the rate at which sediment is entrained by turbulence from the layer below the plane z = b, while the second part, $-v_s c|_{z=b}$, provides the rate at which suspended sediment deposits below that plane from the flow above it. At the equilibrium state entrainment is equal to the deposition rate.

Akiyama and Fukushima (1985) wrote the entrainment term as follows

$$E(b) = \overline{w'c'}\,|_{z=b} = v_s E_s \tag{41}$$

where E_s represented a dimensionless entrainment rate. When the entrainment term is compared with the deposition term at an equilibrium state, E_s coincides with the equilibrium concentration at z = b. Akiyama and Fukushima (1985) stated that while the deposition rate is a property of the watersediment flow, the entrainment rate depends on the fluid forces acting on the bed and the bed characteristics as well. By using dimensional analysis reasoning and data available from the literature, Akiyama and Fukushima (1985) obtained an empirical relation for E_s when both the bed material and the suspended sediment are composed of the same type of particles. In functional form, for uniform material, this relation takes the form

$$E_s = f\left(\frac{u_*}{v_s}, R_p \right) \tag{42}$$

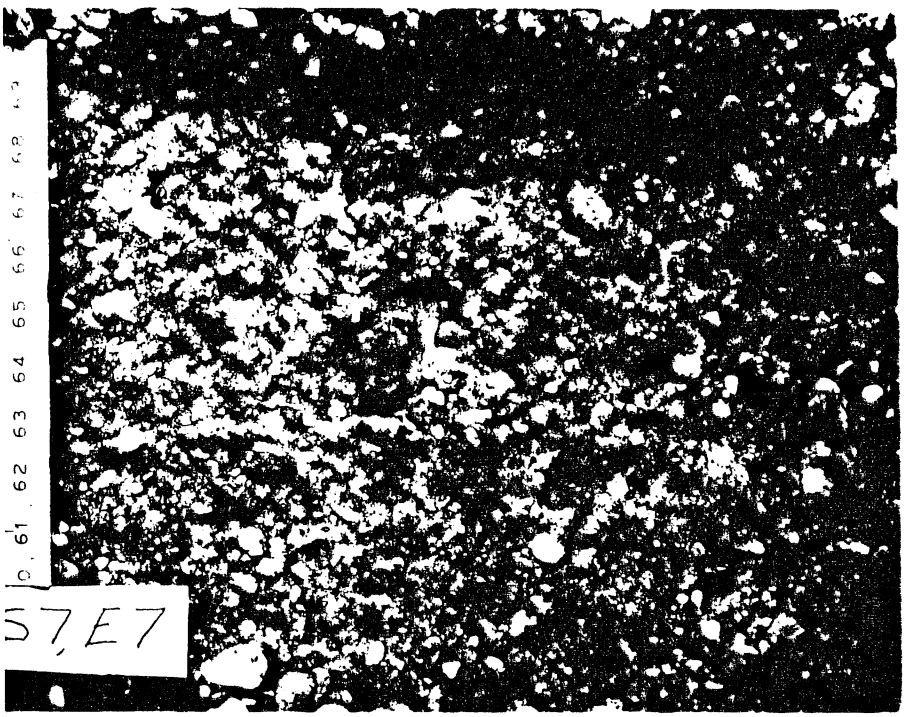

Figure 64. The layer of fines inside the channel bed after run S7:E7.

A similar relation was obtained for nonuniform material. Parker (1982) used the Rousean distribution of suspended sediment to obtain a relation between the equilibrium concentration at z = b and the vertically averaged volumetric concentration of the flow, C. Equation (42) can accordingly be modified to

$$C = f_1\left(\frac{u_*}{v_s}, R_p\right) \tag{43}$$

A formulation such as Eq. (43) would be very desirable for the phenomenon examined in this study; i.e. the problem of obtaining a functional expression for the mean flow concentration as a function of the flow parameters and the amount of fines accumulated in the bed. The presence of both coarse and fine material on the channel bed makes the present problem much more difficult to solve.

As is mentioned earlier, the deposition rate is independent of the flume bed conditions. On the other hand the entrainment rate depends on not only the influence of the boundary forces, but also on the presence of suspendible material in the bed. Suspendible material must be present in the bed, if the flow is to entrain any grains. So the question that arises here is at what point the fines in the bed can be entrained by the flow. The bedload transport rate is expected to influence this process. Nevertheless, in the present experiment it was observed that unless the suspendible material appeared in the surface bed layer, the entrainment rate was very small. This observation does not contradict with the cleaning process that took place in the last three experiments in the tilting flume. During these experiments the incoming water was completely free of fines, and the cleaning of a rather small amount of fines hidden inside the bed is possible even with very small entrainment rates, given the fairly lengthy duration of the experiments. So, regardless of the bedload motion most of the fines removed from the flow deposit within the channel bed as long as no fines are present in the pavement layer. This implies that the fines do not interact significantly with the flow until they have almost saturated the subpavement layer.

Then for the present case Eq. (43) may be modified to

$$C = g\left(\frac{u_*}{v_s}, \tau^*_{50}, R, \frac{d}{D_{p50}}, C_f\right) \tag{44}$$

where C_f is a measure of the amount of fines in the pavement and τ^*_{50} indicates the mobility of the coarse grains of the bed. The term d/D_{p50}, is very large for sand-bed streams, and was showed by Akiyama and Fukushima (1985) to be of lesser importance compared with the other parameters in Eq. (42). In gravel-bed streams, however, d/D_{p50} may reach moderately large values, and cannot be disregarded as parameter beforehand. The limited number of data obtained during the present study do not permit a complete delineation of Eq. (44). For those experiments in the long flume for which

fines were present only in the subpavement, the measured mean flow concentrations were very small, i.e. around 50 mgL^{-1}, and they did not exhibit any consistent correlation with the amount of fines in this layer. It should be mentioned, that due to the very low concentrations during these experiments, the possibility of considerable error is large, which in turn makes these measurements rather unreliable.

Two types of fine material were used during the present study; they differ only in terms of grain size. One of them had a median diameter of 0.11 mm, and the other a median diameter of 0.08 mm. For the experiments for which reliable measurements of mean flow concentration were made, the bed shear stress did not vary significantly. It seems that only the measurements of the mean flow concentration and percentage of fines in the pavement provided a fairly wide range of values. Therefore the only variables of Eq. (44) that can possibly be correlated based on the data of the present study are: the percentage of fines by weight in the pavement layer, and the mean flow concentration. The rest of the parameters in Eq. (44) do not provide a sufficient range.

The mean flow concentrations obtained for flows for which fines were present in the pavement layer have been plotted in Fig. 65 as a function of the percentage of fines by weight found in this layer. Only six reliable data points were obtained from the present experiments, four from the long flume and two from the tilting flume experiments. A fairly consistent semilogarithmic relation appears to hold in this case. A semilogarithmic linear regression results in the following relation

$$C_f = 10.1 \log[8.6 \times 10^{-3} C] \qquad (45)$$

with a correlation coefficient of r = 0.89. The parameter used to describe the amount of fines in the pavement, i.e. C_f , is easy to measure, but may not be the most representative one. A parameter indicating the percentage of the bed surface area occupied by the fines is more difficult to measure, but it might be more descriptive of the conditions at the channel bed. On the other hand, in the field the fines that deposit on the channel bed are often of a similar color to the coarse matrix particles, so they cannot be as easily distinguished as in the present experiments where the color of the fines used was white. In such a case the parameter used here to describe the quantity of the fines in the pavement, i.e. percentage of fines by weight, might be more suitable for real life applications. As is shown in Fig. 65, the minimum mean flow concentration required for the appearance of fines in the pavement is about 200 mgL^{-1}. This agrees with the absence of fines in the pavement layer during the second experiment in the tilting flume, where the fines feed rate was 156 mgL^{-1}. Using the areal sampling technique to remove the surface layer of the bed, it was found that when the surface layer was almost completely covered with fines, their percentage in the areal sample was only about 25 percent. The corresponding mean flow concentration for given flow conditions and fines grain size should be close to the capacity of the flow to carry this material in suspension. Coleman (1981) conducted some experiments to examine the effect of sediment concentration in an open channel flow on the value of Von Karman's constant κ. Coleman used three types of material as

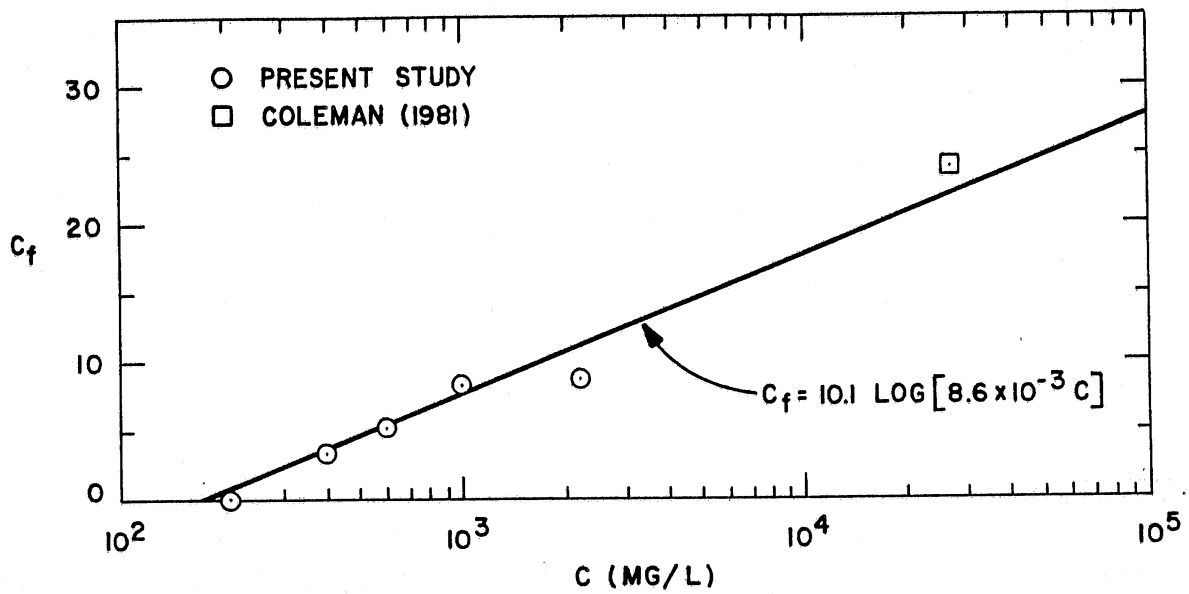

Figure 65. Mean flow concentration of fines, C , versus percent of fines in the pavement by weight, C_f .

fines with geometric mean diameters of 0.105 mm, 0.210 mm, and 0.420 mm, respectively. In one of his experiments the flow was saturated with the 0.105 mm fines under flow conditions similar with the ones of the present experiments. This point from Coleman's experiments is plotted in Fig. 59. As is seen from this figure, Coleman's point follows the trend indicated by the data points obtained from the present experiments. Coleman's point was included in the regression used to derive Eq. (45).

SOME OBSERVATIONS

The effects of the flow characteristics on the amounts of fines that deposit on or infiltrate inside the bed would be valuable information to know. The results obtained from the present study indicate that the amount of fines that can ultimately infiltrate the subpavement layer is independent of the boundary shear stress or other flow parameters. This amount was the same for all the experiments in the long flume, and corresponded to a capacity beyond which no more fines deposit in the subpavement. For the tilting flume experiment this amount was a little higher, but still roughly the same throughout the channel bed. On the other hand the size of the infiltrating sediment, as well as the Shields stress, seem to affect the depth of infiltration of the fines.

As indicated by Eq. (44), it is expected that the amount of fines at the surface layer should be influenced by the Shields stress, the size of the infiltrating grains, the particle Reynolds number, and the mean flow concentration. Unfortunately the present experiments do not cover a wide enough range of Shields stresses, or fines with significantly different grain size, to support or reject this dependence. For the mean flow concentration, however, there is evidence (Fig. 65) which indicates that a higher mean concentration results in increased amounts of fines in the pavement, if other flow parameters are kept constant.

A direct comparison of the tilting and long flume experiments can be made. A condition for compatibility regarding the mean flow concentration is that its equilibrium value in the long flume should be the same as the one attained with a constant fines feed rate in the tilting flume. Under such circumstances the results from both flumes compare favorably in terms of the amount of fines that have infiltrated within the bed or deposited in the pavement. Of course it should be borne in mind that the differences in the Shields stress was rather small among different experiments.

DISCUSSION

An attempt to summarize the material discussed in this chapter is made here. As soon as fines are introduced into the channel, they start depositing on the bed, infiltrating below its surface. The depth of infiltration depends on the difference in size between the infiltrating grains and the coarser bed matrix, and the boundary Shields stress. If the fines are much smaller than the coarse matrix, they infiltrate all the way to the bottom of the bed and start to fill the crevices of the bed material upwards. As long as there are fines suspended in the channel flow, they will keep depositing in the bed until they have saturated the subpavement layer, regardless of the other flow parameters. When the fines appear on the surface bed layer, an equation such as Eq. (44) has the potential to

predict the amount of fines deposited at this layer as a function of mean flow concentration and other flow parameters.

What is realistically expected to happen in nature is as follows: when there is no bedload motion over a gravel bed initially free of fines, all the material that infiltrates the channel bed is removed from the flow. This material is expected to be fine, and usually infiltrates deep inside the bed framework. When bedload transport takes place, the infiltration process is dominated by the finer grains that are part of the bedload. During this time the bed matrix filters the coarser grains that infiltrate the bed, which in turn filter the finer of the infiltrating grains until a seal is created. This seal is composed mostly of particles from the original bed material. The depth of this seal depends on the size of the infiltrating particles, the variation of the size of the grains of the bed framework with depth, the standard deviation of the material of each individual bed layer, and finally the value of the boundary Shields stress. As soon as the bed is saturated with these fines, the infiltration process is once more based on the suspended grains that settle on the channel bed. The same process is repeated here regarding the creation of a seal, which is based now on suspendible material rather than bedload. The depth of this seal is influenced by the same parameters as the coarser seal. A coarser surface layer with relatively uniform material, and substrate material with fairly large standard deviation is a rather common state of gravel-bed streams. Such conditions support the formation of a seal made from the suspendible material in the subpavement or the bottom layer.

If the channel bed is not mobilized, then a channel flow without any suspended material can at most remove the fines from the surface layer of the bed. Conditions of mobilized pavement are required if layers below the surface are to be purged of the fines. During the process of removing the fines from the subpavement or the bottom layer, part of the fines may be driven farther inside the bed. If a seal that is made of the suspendible material is within the subpavement or bottom layer, the bed can be purged from most, if not all, of the fines that have infiltrated the bed under mobile conditions. During the present experiments, the fines were flushed from the bed up to the bottom of the subpavement, which is about 2.1 cm from the surface of the bed, or 2.4 D_{p90}. Frostick et al. (1984) found from their experiments that at the thalweg the fines can be removed from the channel bed from a depth of up to 8 cm. This depth corresponds to 2.4 D_{p90}.

When an alternate bar structure exists on the bed, and the flowing water covers these bars over their total length, then the fines first dropping out of the flow are most likely to be deposited in the subpavement of the bar tail and the pool. As more fines deposit into the bed, they progressively infiltrate the subpavement throughout the channel, while fine grains start appearing in the pavement of the pool and the bar tail. As more fines are fed into the flume, the subpavement eventually becomes saturated, and fines appear in abundance on the surface layer. Equation (44) is expected to govern the amount of fines existing in the surface layer.

During the cleaning of the channel bed from the fines, the same process takes place in reverse order. That is, the fines are first removed

from the surface layer of the bar head, and subsequently removed from the pavement of the pool and bar tail.

Finally, it should be emphasized here that only the suspendible fines can be removed from the channel bed. The seal that was created from the finer part of the original bed material does not appear to be affected during the cleaning process of the channel bed.

REFERENCES

1. Adams, J. N. 1980. Variations in Gravel Bed Composition of Small Streams in the Oregon Coast Range. MS Thesis, Oregon State Univ., Corvallis, Oregon. 160 pp.

2. Adams, J. N. and R. L. Beschta. 1980. Gravel Bed Composition in Oregon Coastal Streams. Can. J. Fish. Aquat. Sci., 37:1514-1521.

3. Akiyama, J. and Y. Fukushima. 1985. Entrainment of Noncohesive Bed Sediment Into Suspension. St. Anthony Falls Hydraulic Laboratory Ext. Memo No. 195, University of Minnesota, Minneapolis, Minnesota. 14 pp.

4. Anderson, H. W. 1971. Relative Contributions of Sediment from Source Areas and Transport Processes. In: Forest Land Uses and the Stream Environment, J. T. Krygier and J. D. Hall, eds. Oregon State Univ., Corvallis, Oregon. pp. 56-63.

5. Andrews, E. D. 1983. Entrainment of Gravel from Naturally Sorted Riverbed Material. Geological Soc. of Amer. Bulletin, 94(10):1225-1231.

6. Ashida, K. and M. Michiue. 1972. Study on Hydraulic Resistance and Bedload Transport Rate in Alluvial Streams. Transactions, Japan Society of Civil Engineering, 206(10):59-69.

7. Beschta, R. L. 1982. Comment on: Stream System Evaluation on Spawning Habitat for Salmonids, by M. A. Shirazi and W. K. Seim. Water Resources Res., 18(4):1292-1295.

8. Beschta, R. L. and W. L. Jackson. 1977. The Intrusion of Fine Sediments into a Gravel Bedded Channel. Report, School of Forestry, Oregon State University, Corvallis, Oregon. 57 pp.

9. Bjorn, T. C., M. A. Brusven, M. P. Molnau, and J. H. Milligan. 1977. Transport of Granitic Sediment in Streams and its Effects on Inserts and Fish. Forest, Wildlife and Range Experiment Station, Univ. of Idaho, Moscow, Idaho. 43 pp.

10. Blackwelder, R. F. and J. H. Haritonidis. 1983. Scaling of the Bursting Frequency in Turbulent Boundary Layers. Jour. Fluid Mech., Vol. 132, pp. 87-103.

11. Bluck, B. J. 1982. Texture of Gravel Bars in Braided Streams. In: Gravel-Bed Rivers, R. D. Hey, J. C. Bathurst and C. R. Thorne, eds. Wiley-Interscience. pp. 339-355.

12. Bray, D. I. and M. Church. 1980. Armored versus Paved Gravel Beds. J. Hydraul. Div., ASCE, 106(HY11).

13. Brown, G. W. 1974. Forestry and Water Quality. Report, School of Forestry, Oregon State Univ., Corvallis, Oregon.

14. Cantwell, B. J. 1981. Organized Motion in Turbulent Flow. Annual Review Fluid Mech., 13:457-515.

15. Carling, P. A. 1981. Discussion of Armored versus Paved Gravel Beds by D. I. Bray and M. Church. J. Hydraul. Div., ASCE, 107(HY9).

16. Carling, P. A. 1984. Deposition of Fine and Coarse Sand in an Open-Work Gravel Bed. Can. J. Fish. Aquat. Sci., 41:263-270.

17. Coleman, N. L. 1981. Velocity Profiles with Suspended Sediment. J. of Hydraul. Research, 19(3):211-229.

18. Dhamotharan, S., A. Wood, G. Parker, and H. Stefan. 1980. Bedload Transport in Gravel Streams. St. Anthony Falls Hydraulic Laboratory, Proj. Report 190, University of Minnesota, Minneapolis, Minnesota. 75 pp.

19. Diplas, P. 1983. Self Formed Straight Channel Characteristics with Bedload Only. MS Thesis, University of Minnesota, Minneapolis, Minnesota. 128 pp.

20. Diplas, P. and R. Hills. 1985. A Similarity Approach for the Bedload Transport in Gravel-Bed Streams. In preparation for submission to Water Resources Research.

21. Egiazaroff, I. V. 1965. Calculation of Non-Uniform Sediment Concentrations. J. Hydraul. Div., ASCE, 91(HY4):225-247.

22. Einstein, H. A. 1968. Deposition of Suspended Particles in a Gravel-Bed. J. Hydraulic Div., ASCE, 94(HY5):1197-1205.

23. Erman, D. C. and D. Mahoney. 1983. Recovery after Logging in Streams With and Without Bufferstrips in Northern California. California Water Resources Center, University of California, Davis.

24. Ettema, R. 1980. Scour at Bridge Piers. School of Engineering, Rep. No. 216, University of Auckland, Auckland, New Zealand.

25. Fenton, J. D. and J. E. Abbot. 1977. Initial Movement of Grains on a Stream Bed: The Effect of Relative Protrusion. Proc. Royal Society, London, 353A:523-537.

26. Frostick, L. E., P. M. Lukas, and I. Reid. 1984. The Infiltration of Fine Matrices into Coarse-Grained Alluvial Sediments and its Implications for Stratigraphical Interpretation. J. Geol. Soc. London, 141: 955-965.

27. Garvin, W. F. 1974. The Intrusion of Logging Debris into Artificial Gravel Streambeds. Report No. 27, Oregon State University, Water Resources Research Institute, Corvallis. 79 pp.

28. Gibbons, D. R. and E. O. Salo. 1973. Annotated Bibliography of the Effects of Logging on Fish of the Western United States and Canada. USDA For. Serv., Gen. Tech. Rep. PNW-10. 145 pp.

29. Grass, A. J. 1971. Structural Features of Turbulent Flow over Smooth and Rough Boundaries. J. Fluid Mech., 50:223-256.

30. Harrison, C. W. 1923. Planting Eyed Salmon and Trout Eggs. Trans. Am. Fish. Soc. 53:191-200.

31. Ikeda, S. 1984. Prediction of Alternate Bar Wavelength and Height. J. Hydraul. Div., ASCE, 110(HY4):371-386.

32. Iwamoto, R. N., E. O. Salo, M. A. Madej, and R. L. McComas. 1978. Sediment and Water Quality: A Review of the Literature Including a Suggested Approach for Water Quality Criteria. Report, EPA Region X, Seattle.

33. Johnson, J. W. 1942. The Importance of Considering Sidewall Friction in Bed-Load Investigations. Civil Engineering, 12(6):329-331.

34. Kellerhals, R. and D. I. Bray. 1971. Sampling Procedures for Coarse Fluvial Sediments. J. Hydraul. Div., ASCE, 97(HY8):1165-1180.

35. Klingman, P. C., and R. T. Milhous. 1970. Evaluation of Bedload and Total Sediment Yield Processes on Small Mountain Streams. Report, Water Resources Institute, Oregon State University, Corvallis, Oregon.

36. Koski, K. V. 1966. The Survival of Coho Salmon Egg Deposition to Emergence in Three Oregon Coastal Streams. MS Thesis, Oregon State University, Corvallis, Oregon. 84 pp.

37. Leighly, J. B. 1932. Toward a Theory of the Morphological Significance of Turbulence in the Flow of Water in Streams. University of Calif., Publications in Geography, Vol. 6, pp. 1-22.

38. Lewin, J. 1976. Initiation of Bed Forms and Meanders in Coarse-Grained Sediment. Geol. Soc. of America Bulletin, 87:281-285.

39. Lisle, T. 1980. Sedimentation of Spawning Areas during Storm Flows, Jacoby Creek, North Coastal California. Presented at the fall meeting of the American Geophysical Union, San Francisco, Dec. 8. 13 pp.

40. Lotspeich, F. B. and F. H. Everest. 1981. A New Method for Reporting and Interpreting Textural Composition of Spawning Gravel. Research Note PNW-369, USDA, Forest Service, Pacific Northwest Forest and Range Experiment Station, Corvallis, Oregon. 11 pp.

41. Luchnik, T. S. and W. G. Tiederman. 1983. Bursting Rates in Channel Flows and Drag-Reducing Channel Flows. Eighth Biennial Symposium on Turbulence, September, 1983. La-Rolla University, Missouri.

42. Lumley, J. L. 1978. Two-phase and Non-Newtonian Flows. In: Topics in Applied Physics 12, P. Bradshaw edit. Springer, New York. pp. 289-324.

43. Megahan, W. R., and W. J. Kid. 1972. Effects of Logging and Logging Roads on Erosion and Sediment Deposition from Steep Terrain. J. For. 70(3):136-142.

44. Milhous, R. T. 1973. Sediment Transport in a Gravel Bottomed Stream. Ph.D. Thesis, Oregon State Univ., Corvallis, Oregon. 232 pp.

45. Milhous, R. T. 1981. Discussion of Armored versus Paved Gravel Beds, by D. I. Bray, and M. Church. J. Hydraul. Div., ASCE, 107(HY9).

46. Paintal, A. S. 1971. Concept of Critical Shear Stress in Loose Boundary Open Channels. J. Hydraul. Res., 9(1):91-113.

47. Parker, G. 1980. Experiments on the Formation of Mobile Pavement and Static Armor. Report, Dept. of Civil Engineering, Univ. of Alberta, Canada.

48. Parker, G. 1981. Discussion of Armored versus Paved Gravel Beds, by D. I. Bray and M. Church. J. Hydraul. Div., ASCE, 107(9):1120-1121.

49. Parker, G. 1982. Conditions for the Ignition to Catastrophically Erosive Turbidity Currents. Marine Geology, 46:307-327.

50. Parker, G. and A. W. Peterson. 1980. Bar Resistance of Gravel-Bed Streams. J. Hydraul. Div., ASCE, 106(HY10):1559-1575.

51. Parker, G., P. C. Klingeman, and D. L. McLean. 1982a. Bedload and Size Distribution in Paved Gravel-Bed Streams. J. Hydraul. Div., ASCE, 108(HY4):544-571.

52. Parker, G., and P. C. Klingeman. 1982b. On Why Gravel-Bed Streams Are Paved. Water Resources Res., 18(5):1409-1423.

53. Parker, G., S. Dhamotharan, and H. Stefan. 1982c. Model Experiments on Mobile Paved Gravel-Bed Streams. Water Resources Res., 18(5):1395-1408.

54. Phillips, R. W. 1965. Effect of Fine Material on Salmon and Trout Redds. Meeting on Erosion and Sedimentation in the Northwest 1964-65 Flood Season. Water Supply and Water Pollution Control Subcommittee. Columbia Basin Interagency Committee, Portland, Oregon.

55. Phillips, R. W. 1971. Effect of Sediment on the Gravel Environment and Fish Production. In: Forest Land Uses and the Stream Enviroment, J. T. Krygier and J. D. Hall, eds. Oregon State Univ., Corvallis, Oregon. pp. 64-70.

56. Phillips, R. W., and H. J. Campbell. 1961. The Embryonic Survival of Coho Salmon and Steelhead Trout as Influenced by Some Environmental Conditions in Gravel Beds. Pac. Marine Fish. Comm., 14th Annual Report. pp. 60-73.

57. Proffitt, G. T. 1980. Selective Transport and Armouring of Non-Uniform Alluvial Sediments. Ph.D. Thesis, University of Canterbury, Christchurch, New Zealand. 203 pp.

58. Shea, M., and J. S. Mathers. 1978. An Anotated Bibliography on the Effects of Roads on Aquatic Systems. Report, Ontario Ministry of Natural Resources, Canada.

59. Sheridan, W. L. 1962. Water Flow Through a Salmon Spawning Riffle in Southeast Alaska. USDA Fish and Wildlife Serv., Spec. Sci. Rep. No. 407. 20 pp.

60. Shirazi, M. A., and W. K. Seim. 1981. Stream System Evaluation with Emphasis on Spawning Habitat for Salmonids. Water Resources Res., 17(3):592-594.

61. Sowers, G. B., and G. F. Sowers. 1970. Introductory Soil Mechanics and Foundations, Macmillan, 3rd. ed., London.

62. Sutherland, A. J. 1967. Proposed Mechanisms for Sediment Entrainment by Turbulent Flows. J. Geophysical Research, 72(24):6183-6194.

63. Swanston, D. N., and F. J. Swanson. 1976. Timber Harvesting, Mass Erosion, and Steepland Geomorphology in the Pacific Northwest. In: Geomorphology and Engineering, D. R. Coates, ed. Dowden, Hutchinson and Ross Inc., Stroudsbourg, Pa. pp. 199-221.

64. Vanoni, V. A., and N. H. Brooks. 1957. Laboratory Studies of the Roughness and Suspended Load of Alluvial Streams. Sedimentation Lab., California Institute of Technology, Pasadena, Calif., Rep. No. E-68.

65. Vaux, W. G. 1968. Intragravel Flow and Interchange of Water in a Stream Bed. Bulletin, U. S. Fisheries and Wildlife Service, 66(3): 479-489.

66. Zimmer, D. W., and R. W. Bachmann. 1978. Channelization and Invertebrate Drift in Some Iowa Streams. Water Resourc. Bul., 14(4):868-883.

APPENDIX 1

Statistical Characteristics of the Bed Samples

The statistical characteristics of the bed samples extracted at the end of each experiment have been tabulated in the following seven tables. The symbol E0 refers to the channel at the beginning of each series before any experiment has been performed, just after the channel has been screeded. When the letters A, B, C, are used they indicate the number of the sets of bed samples removed at the end of the corresponding experiment. In Table A1:7 the words bar tail, bar middle, bar head, and pool are used to describe the location from where a set of bed samples was obtained. These locations are shown in a schematic of the bed of the tilting flume in Fig. 29. The size of D_{50}, D_{84} and D_{16} is expressed in milimeters. The expression % < .42 mm indicates the percentage of the material in the sample by weight whose size is smaller than 0.42 mm.

TABLE A1:1 First Series of Experiments

		E0			E1		E2	E3	E4		E5	E6	E7	E8		
		A	B	C	A	B			A	B				A	B	C
PAVEMENT	D_{50}	4.6	4.0	5.4	4.8	4.1	5.0	5.0	4.8	5.2	5.0	5.2	4.3	4.0	3.4	6.2
	D_{84}	7.8	6.4	7.6	8.0	7.8	8.4	7.8	7.8	9.2	8.2	8.2	7.4	6.0	7.4	8.4
	D_{16}	2.2	1.9	2.4	1.0	0.8	1.5	2.4	0.9	2.5	2.2	1.4	1.8	1.3	1.4	2.7
	σ_g	1.9	1.9	1.8	2.8	3.1	2.4	1.8	2.9	1.9	1.9	2.4	2.0	2.2	2.3	1.8
	% < .42 mm	1.0	1.0	1.0	7.1	3.1	1.8	3.7	3.6	1.4	1.2	1.6	1.6	6.4	1.2	2.5
	% < .125 mm	1.0	1.0	1.0	0.7	1.0	0.8	3.1	0.4	1.0	0.8	0.9	1.0	2.8	1.0	1.0
	% < 1.0 mm	1.5	2.3	1.8	16.0	18.1	9.5	6.0	17.5	2.6	3.0	11.0	4.0	13.8	7.0	7.0
SUBPAVEMENT	D_{50}	3.7	2.3	2.6	1.8	1.8	2.1	1.9	2.3	1.7	1.9	1.8	2.0	2.0	2.1	1.8
	D_{84}	6.8	6.0	6.5	4.8	5.4	5.2	5.4	5.7	4.6	4.4	5.2	5.6	5.8	6.0	5.0
	D_{16}	1.3	0.8	1.0	0.5	0.5	0.5	0.5	0.6	0.5	0.5	0.5	0.5	0.3	0.4	0.4
	σ_g	2.3	2.8	2.5	3.1	3.2	3.2	3.2	3.2	3.2	3.0	3.2	3.4	4.2	3.7	3.5
	% < .42 mm				11.4	10.4	10.5	10.0	9.5	13.8	12.3	10.0	13.1	18.1	15.4	16.3
	% < .125 mm	0.1			0.5	0.4	0.6	1.3	0.6	10.4	1.8	3.6	5.5	12.0	8.8	7.4
	% < 1.0 mm	14.0	22.0	16.0	34.5	23.5	30.0	30.0	26.2	36.0	33.0	32.0	31.0	13.0	28.0	33.0
BOTTOM LAYER	D_{50}													2.1	2.7	2.1
	D_{84}													6.2	6.4	5.7
	D_{16}													0.3	0.8	0.6
	σ_g													4.3	2.8	3.2
	% < .42 mm													18.7	7.6	9.2
	% < .125 mm													11.9	3.4	1.0
	% < 1.0 mm													31.0	18.5	26.7

Where applicable dimensions are in millimeters.

TABLE A1:2 Second Series of Experiments

		E0		E1		E2		E3	E4	
		A	B	A	B	A	B		A	B
PAVEMENT	D_{50}	4.6	4.0	6.0	5.8	5.6	5.4		4.7	4.7
	D_{84}	8.0	7.5	9.2	8.2	8.5	7.8		7.5	8.5
	D_{16}	1.6	1.7	1.7	1.5	1.5	2.2		1.5	0.9
	σ_g	2.3	2.1	2.3	2.3	2.4	1.9		2.2	3.0
	% < .42 mm	2.3	2.1	2.6	4.6	2.2	2.0		4.8	5.9
	% < .125 mm	1.5	1.2	1.8	0.7	1.2	0.8		4.0	3.8
	% < 1.0 mm	8.0	6.3	8.2	12.0	11.8	5.6		9.0	17.0
SUBPAVEMENT	D_{50}	2.9	2.6	2.2	2.3	2.4	2.8		1.9	2.2
	D_{84}	6.7	6.9	6.6	5.4	6.2	6.4		5.5	6.1
	D_{16}	1.1	0.9	0.6	0.5	0.5	0.6		0.5	0.5
	σ_g	2.5	2.8	3.4	3.2	3.4	3.3		3.4	3.7
	% < .42 mm	3.0	4.6	8.9	10.2	9.3	8.9		13.5	14.7
	% < .125 mm	0.2	0.3	0.1	0.2	1.8	1.1		4.1	5.7
	% < 1.0 mm	14.0	18.3	28.2	28.5	28.0	23.7		31.5	32.0
BOTTOM LAYER	D_{50}	2.9	2.3	3.1	2.8	2.1	3.3		2.0	2.1
	D_{84}	6.6	5.4	6.8	6.8	4.6	7.1		4.9	5.6
	D_{16}	1.2	0.7	1.0	1.0	0.6	1.1		0.6	0.6
	σ_g	2.4	2.8	2.6	2.6	2.8	2.6		2.9	3.1
	% < .42 mm	2.6	6.4	4.1	3.4	8.6	4.9		9.8	10.2
	% < .125 mm	0.2	0.3	0.2	0.2	0.8	0.5		1.2	1.7
	% < 1.0 mm	13.8	22.8	16.0	16.5	28.0	15.5		27.2	28.0

Where applicable dimensions are in millimeters.

TABLE A1:3 Third Series of Experiments

		E0		E1		E2		E3		E4		E5	
		A	B	A	B	A	B	A	B	A	B	A	B
PAVEMENT	D_{50}	3.4	4.0	4.3	5.7	5.7	5.0	5.4	5.6	5.0	6.0	5.0	5.5
	D_{84}	6.8	6.3	7.4	8.3	8.6	7.8	8.2	9.0	7.8	9.1	8.7	8.4
	D_{16}	1.4	1.8	2.2	1.8	1.5	1.3	1.7	1.3	1.4	1.0	1.8	1.4
	σ_g	2.2	1.9	1.8	2.1	2.4	2.5	2.2	2.7	2.4	3.1	2.2	2.5
	% < .42 mm	2.1	2.2	1.4	4.6	2.3	2.6	1.0	4.1	1.2	4.2	1.6	2.9
	% < .125 mm	1.7	1.4	1.1	3.0	1.0	1.2	0.8	1.3	0.9	1.2	1.2	1.3
	% < 1.0 mm	10.0	5.8	2.0	10.0	11.0	12.0	5.7	13.5	8.3	16.3	4.0	11.0
SUBPAVEMENT	D_{50}	1.9	2.2	3.3	2.8	1.9	2.9	2.1	2.0	2.6	1.7	2.3	2.0
	D_{84}	4.8	5.4	6.8	6.5	5.3	6.2	6.0	5.2	6.5	5.4	6.0	5.4
	D_{16}	0.6	0.8	1.4	0.8	0.6	0.7	0.6	0.6	0.6	0.5	0.5	0.5
	σ_g	2.7	2.6	2.2	2.9	3.0	3.0	3.2	2.9	3.3	3.4	3.6	3.4
	% < .42 mm	5.7	4.3	3.3	5.7	7.1	6.7	7.2	9.2	8.9	13.3	13.4	12.8
	% < .125 mm	0.3	0.2	0.1	0.1	0.8	0.7	1.7	2.2	3.8	3.9	7.0	6.8
	% < 1.0 mm	27.2	21.3	11.3	20.2	28.5	22.0	27.0	24.0	23.2	35.5	28.0	27.6
BOTTOM LAYER	D_{50}	2.3	2.6	2.1	2.1	1.6	2.4	2.2	2.2	2.7	2.0	2.2	2.0
	D_{84}	6.2	6.4	5.5	5.5	4.6	5.4	5.6	5.6	6.4	5.8	5.7	4.3
	D_{16}	0.7	0.8	0.7	0.6	0.5	0.8	0.6	0.8	0.8	0.5	0.6	0.7
	σ_g	3.0	2.8	2.8	3.1	3.0	2.7	3.0	2.7	2.9	3.4	3.2	2.5
	% < .42 mm	6.4	5.5	5.9	9.0	9.6	6.0	7.6	5.1	6.8	11.6	11.0	6.5
	% < .125 mm	0.5	0.4	0.2	0.6	1.1	0.6	1.6	0.8	2.3	2.2	4.3	1.9
	% < 1.0 mm	23.3	19.7	22.2	27.0	30.8	20.0	22.7	20.1	19.3	28.5	26.0	24.5

Where applicable, dimensions are in millimeters.

TABLE A1:4 Fourth Series of Experiments

		E0		E1		E2	E3		E4		E5		E6	
		A	B	A	B		A	B	A	B	A	B	A	B
PAVEMENT	D_{50}	4.4	5.2	4.9	4.4		4.8	5.4	4.8	4.9	4.1	3.5	2.8	4.0
	D_{84}	7.4	8.4	8.5	7.8		8.2	8.0	8.5	8.3	8.0	7.0	6.4	7.1
	D_{16}	1.8	2.5	1.6	1.5		1.9	2.0	1.6	1.9	1.5	1.0	0.5	1.4
	σ_g	2.1	1.9	2.3	2.3		2.1	2.0	2.3	2.1	2.3	2.7	3.8	2.2
	% < .42 mm	1.3	0.6	1.0	1.1		1.1	0.9	1.6	1.6	5.4	9.4	15.2	10.4
	% < .125 mm	1.3	0.4	0.8	0.7		0.9	0.9	1.1	1.0	3.6	5.8	10.0	6.8
	% < 1.0 mm	3.8	1.8	7.0	7.1		4.0	2.6	7.0	3.6	10.2	16.0	20.8	13.2
SUBPAVEMENT	D_{50}	2.5	2.2	2.2	2.7		2.1	2.8	1.9	2.5	2.1	2.3	2.7	2.0
	D_{84}	6.2	5.6	6.8	5.9		5.7	6.0	5.5	6.1	5.9	6.9	6.0	6.2
	D_{16}	0.8	0.8	0.6	1.3		0.7	0.9	0.5	0.7	0.5	0.5	0.5	0.3
	σ_g	2.9	2.7	3.3	2.2		2.8	2.6	3.2	3.0	3.6	3.9	3.5	4.3
	% < .42 mm	4.5	4.7	7.3	1.2		6.8	5.2	10.9	8.5	14.9	15.2	13.3	19.2
	% < .125 mm	0.1	0.1	0.3	0.2		1.9	2.4	4.9	5.1	6.7	7.7	7.7	11.2
	% < 1.0 mm	21.0	20.7	24.8	11.4		21.4	18.0	28.0	22.5	29.0	28.4	23.5	31.0
BOTTOM LAYER	D_{50}	2.4	2.2	2.0	3.2		1.9	2.9	1.7	3.0	2.0	1.8	3.0	2.4
	D_{84}	5.8	6.0	5.4	6.4		5.3	6.1	4.7	6.2	5.7	5.3	6.4	6.6
	D_{16}	0.7	0.7	0.6	1.5		0.6	1.2	0.5	1.0	0.6	0.5	1.0	0.6
	σ_g	2.9	3.0	3.1	2.1		2.9	2.3	3.1	2.6	3.2	3.4	2.6	3.5
	% < .42 mm	6.0	7.0	9.5	3.9		6.9	5.1	11.8	6.1	9.7	13.0	6.7	10.8
	% < .125 mm	0.2	0.4	0.5	0.3		1.0	1.1	2.7	1.5	1.4	2.0	1.9	2.4
	% < 1.0 mm	21.5	22.0	27.2	10.0		25.0	14.5	34.6	16.5	26.2	32.0	16.3	26.0

Where applicable dimensions are in millimeters.

TABLE A1:5 Fifth Series of Experiments

		E0		E1		E2	E3		E4		E5	E6	
		A	B	A	B		A	B	A	B		A	B
PAVEMENT	D_{50}	3.8	4.7	4.8	5.1		4.3	3.7	4.5	4.7		4.6	4.6
	D_{84}	6.4	7.6	7.4	8.0		7.9	7.4	8.5	8.8		8.0	8.0
	D_{16}	2.0	2.0	1.8	1.7		1.9	1.7	2.0	2.0		1.6	1.5
	σ_g	1.8	2.0	2.0	2.2		2.0	2.1	2.1	2.1		2.3	2.3
	% < .42 mm	0.5	0.8	1.1	0.8		0.3	0.5	0.4	1.9		8.6	9.6
	% < .125 mm	0.5	0.8	0.6	0.6		0.3	0.3	0.4	1.3		6.4	6.7
	% < .177 mm						0.3	0.3	0.4	1.7		8.3	9.1
	% < 1.0 mm	1.0	2.0	4.2	5.6		1.0	3.0	0.6	4.0		10.4	12.0
SUBPAVEMENT	D_{50}	2.1	2.3	2.1	1.9		2.3	2.7	2.1	2.9		2.2	2.3
	D_{84}	5.8	5.8	5.2	5.4		5.9	5.4	5.6	6.5		6.1	5.8
	D_{16}	0.7	0.9	0.8	0.6		0.6	1.3	0.5	1.0		0.1	0.2
	σ_g	2.9	2.6	2.5	2.9		3.2	2.1	3.3	2.6		6.4	6.2
	% < .42 mm	5.5	3.5	4.5	4.0		8.3	3.0	10.8	6.3		19.4	19.8
	% < .125 mm	0.2	0.2	0.5	0.2		2.1	1.1	4.1	3.3		12.6	11.5
	% < .177 mm						2.6	1.2	5.6	4.4		18.1	18.4
	% < 1.0 mm	23.8	19.8	20.0	27.0		26.0	12.5	27.3	16.6		28.2	29.0
BOTTOM LAYER	D_{50}	2.1	2.4	1.7	2.0		2.4	3.0	1.9	2.9		1.7	1.4
	D_{84}	5.1	6.0	5.4	5.8		5.8	5.6	5.4	6.6		5.2	4.2
	D_{16}	0.6	0.8	0.5	0.5		0.6	1.6	0.5	1.0		0.4	0.4
	σ_g	2.8	2.8	3.3	3.3		3.0	1.9	3.3	2.6		3.6	3.1
	% < .42 mm	7.2	6.0	11.0	10.6		7.7	3.1	11.2	5.1		16.6	16.3
	% < .125 mm	0.5	0.5	0.9	0.7		1.6	1.1	1.8	1.9		6.2	6.0
	% < .177 mm						2.0	1.4	2.4	2.4		8.4	7.9
	% < 1.0 mm	25.8	20.0	34.0	31.5		22.7	7.0	32.0	16.3		37.0	40.8

Where applicable dimensions are in millimeters.

TABLE A1:6 Sixth Series of Experiments

		E0		E1	E3	
		A	B		A	B
PAVEMENT	D_{50}	5.2	5.2	6.1	3.1	2.5
	D_{84}	8.4	7.8	8.3	6.9	7.0
	D_{16}	2.5	3.0	1.3	0.1	
	σ_g	1.8	1.6	2.5	9.17	
	% < .42 mm	0.6	0.4	2.2	26.2	23.9
	% < .177 mm	0.6	0.4	0.5		
	% < .125 mm	0.6	0.4	0.5	24.9	22.1
	% < 1.0 mm	0.6	0.5	13.0	29.6	29.0
SUBPAVEMENT	D_{50}	2.0	2.1	2.2	2.3	2.5
	D_{84}	5.8	5.6	6.1	6.7	6.4
	D_{16}	0.7	0.7	0.6	0.1	0.2
	σ_g	2.8	2.9	3.2	7.9	5.6
	% < .42 mm	5.7	7.3	7.1	21.2	18.1
	% < .177 mm	0.5	0.6	0.7		
	% < .125 mm	0.3	0.4	0.4	17.9	14.4
	% < 1.0 mm	22.3	25.3	27.0	31.0	26.0
BOTTOM LAYER	D_{50}	2.3	1.9	2.2	1.7	1.9
	D_{84}	6.1	5.3	5.8	5.0	5.4
	D_{16}	0.7	0.6	0.6	0.5	0.5
	σ_g	2.9	2.9	3.2	3.2	3.2
	% < .42 mm	6.5	8.0	8.8	13.3	11.4
	% < .177 mm	0.6	0.8	1.0		
	% < .125 mm	0.4	0.6	0.6	2.5	1.4
	% < 1.0 mm	22.0	25.5	25.4	33.2	29.5

Where applicable, dimensions are in millimeters.

TABLE A1:7 Seventh Series of Experiments

		E0		E1					E2				E3				
				Bar Tail	Bar Mid.	Bar Head	Pool		Bar Tail	Bar Mid.	Bar Hear	Pool	Bar Tail	Bar Mid.	Bar Head	Pool	
		A	B				A	B								A	B
PAVEMENT	D_{50}	5.7	5.4	4.7	6.8	7.2	6.4	2.6	5.5	6.2	6.2	6.6	5.2	5.8	5.9	6.4	6.3
	D_{84}	7.9	7.9	6.5	8.4	9.0	8.4	5.7	8.2	8.5	8.2	8.5	7.8	7.9	8.2	8.7	8.4
	D_{16}	2.1	2.3	2.0	3.8	3.8	2.2	1.4	2.2	2.4	3.7	3.8	1.8	1.9	1.6	1.9	1.6
	σ_g	1.9	1.9	1.8	1.5	1.5	2.0	2.1	2.0	1.9	1.5	1.5	2.1	2.1	2.3	2.1	2.3
	% < 1.0 mm	2.2	2.0	10.0	4.2	2.0	7.3	10.0	8.0	5.0	1.9	0.4	11.7	7.8	9.5	8.8	13.2
	% < .42 mm	1.0	1.3	5.0	2.3	1.0	2.5	2.4	4.1	1.8	0.9	0.3	6.9	3.1	2.3	3.5	9.2
	% < .177 mm	0.9	0.9	2.5	1.8	0.8	1.1	1.6	2.2	1.0	0.6	0.3	4.2	1.7	1.5	1.9	7.2
SUBPAVEMENT	D_{50}	2.5	2.4	2.7	3.0	2.2	2.7	2.3	2.2	2.0	2.0	2.4	2.0	2.3	2.3	2.1	2.0
	D_{84}	6.6	6.0	6.0	6.7	5.1	6.3	5.4	5.2	4.5	6.6	6.6	5.4	5.4	6.6	5.7	7.0
	D_{16}	0.9	0.9	0.5	0.6	0.6	0.6	0.9	0.5	0.5	0.4	0.5	0.5	0.5	0.5	0.4	0.3
	σ_g	2.7	2.6	3.5	3.3	3.1	3.1	2.4	3.2	3.0	3.9	3.7	3.5	3.2	3.8	3.9	4.7
	% < 1.0 mm	18.0	18.7	25.0	22.2	26.0	23.5	17.5	28.2	31.0	33.0	28.0	29.7	26.7	28.8	34.5	33.8
	% < .42 mm	4.2	4.0	12.0	8.0	9.0	6.9	3.0	13.4	13.3	14.9	13.3	15.3	13.1	13.7	17.3	19.4
	% < .177 mm	0.3	0.2	0.7	0.6	0.5	0.3	0.3	5.7	4.8	0.3	6.0	4.4	4.7	5.9	9.4	9.6
BOTTOM LAYER	D_{50}	2.3	2.3	2.2	2.3	2.2	1.9	4.3	2.4	2.4	2.1	3.1	2.4	2.3	2.3	3.0	1.9
	D_{84}	6.1	6.6	5.4	5.8	6.3	5.1	8.4	5.7	5.4	6.0	7.0	5.8	5.2	5.7	6.6	6.0
	D_{16}	0.7	0.7	0.5	0.6	0.5	0.6	1.6	0.7	0.7	0.5	0.7	0.5	0.7	0.5	1.3	0.4
	σ_g	3.0	3.0	3.3	3.2	3.7	3.0	2.3	2.9	2.8	3.6	3.2	3.3	2.7	3.3	2.2	3.7
	% < 1.0 mm	23.0	21.8	27.5	26.2	31.0	29.5	8.6	21.8	21.5	31.5	22.3	24.0	20.0	26.0	12.2	34.5
	% < .42 mm	6.5	6.0	15.0	10.0	13.0	8.9	1.7	8.2	9.5	13.6	9.3	11.8	9.4	10.2	4.4	15.3
	% < .177 mm	0.5	0.4	1.2	0.3	0.3	0.3	0.3	1.5	2.0	1.5	3.1	1.2	1.2	0.8	1.4	2.2

Where applicable, dimensions are in millimeters. Table continued on next page.

TABLE A1:7 Seventh Series of Experiments

		E4			E5			E6					E7	
		Bar Tail	Bar Head	Pool	Bar Tail	Bar Head	Pool	Bar Tail	Bar Mid.	Bar Head	Pool A	Pool B	A	B
PAVEMENT	D_{50}	5.5	5.2	7.8	6.2	6.5	6.2	4.7	6.7	7.3	6.7	7.3	5.4	7.0
	D_{84}	8.2	7.9	8.7	8.4	8.4	8.7	7.6	8.5	8.4	8.5	8.6	8.5	8.4
	D_{16}	1.7	1.3	3.7	3.8	2.0	2.0	1.5	2.1	3.8	1.2	2.5	1.5	3.0
	σ_g	2.2	2.4	1.5	1.5	2.0	2.1	2.2	2.0	1.5	2.7	1.9	2.4	1.7
	% < 1.0 mm	12.6	13.8	4.3	4.7	7.3	8.3	11.0	8.7	5.5	14.5	4.0	9.0	7.3
	% < .42 mm	8.9	7.7	2.9	3.3	3.0	3.8	3.7	3.4	2.5	3.9	1.7	1.2	4.0
	% < .177 mm	6.9	6.1	2.1	3.0	1.6	2.4	2.1	0.6	1.4	1.1	1.3	1.0	1.4
SUBPAVEMENT	D_{50}	2.1	2.4	2.3	2.1	2.1	2.3	3.3	2.1	2.2	2.1	2.3	2.1	2.4
	D_{84}	4.7	6.8	6.0	4.9	6.2	6.6	7.7	7.9	7.4	6.7	8.0	6.1	7.0
	D_{16}	0.4	0.6	0.4	0.4	0.5	0.4	1.1	0.6	0.5	0.5	0.6	0.5	0.5
	σ_g	3.4	3.5	4.1	3.4	3.6	3.9	2.7	3.8	3.8	3.7	3.8	3.7	3.8
	% < 1.0 mm	29.2	26.5	30.0	30.0	30.3	30.0	14.3	28.3	30.0	31.0	28.0	32.0	29.0
	% < .42 mm	15.9	11.4	17.0	15.4	13.5	15.9	3.2	10.1	11.1	12.1	8.5	14.3	13.3
	% < .177 mm	5.1	5.5	11.4	7.6	6.1	9.4	1.0	1.3	0.9	3.3	0.6	1.1	1.4
BOTTOM LAYER	D_{50}	2.2	2.5	1.8	2.0	2.3	2.8	2.2	2.2	2.0	2.5	2.3	2.0	2.2
	D_{84}	5.2	6.3	4.1	4.4	6.0	6.4	5.4	5.6	6.3	6.6	6.4	5.8	6.6
	D_{16}	0.5	0.7	0.3	0.6	0.5	1.0	0.5	0.5	0.4	0.5	0.6	0.4	0.4
	σ_g	3.2	3.0	3.7	2.8	3.3	2.6	3.4	3.5	3.9	3.6	3.2	3.7	3.9
	% < 1.0 mm	26.7	22.0	36.3	25.0	27.0	27.0	28.5	31.4	35.0	28.0	24.2	33.4	30.0
	% < .42 mm	13.1	8.0	19.5	12.0	11.2	5.4	14.0	14.1	16.0	11.7	9.6	15.1	15.7
	% < .177 mm	3.1	2.0	11.5	1.9	3.7	1.8	5.9	6.0	4.9	2.4	3.7	3.0	2.9

Where applicable, dimensions are in millimeters.

APPENDIX 2

Some characteristics of bedload samples obtained during the present experiments are included in the following two tables. The values of W_i^* and τ_i^* listed in Table A2:2 are those used in Section 7, where the bedload transport rate from Oak Creek and the present study are examined.

Table A2:1

Range (mm)	D_i (mm)	Percentage of Bedload Material in Each Size Range										f_i value for two representative subpavement samples	
		S1:E2	S1:E3	S1:E6	S3:E3	S3:E4	S3:E5	S4:E2	S4:E5	S5:E3	S6:E1		
9.0-6.68	7.84	2.2	2.5	0.0	7.7	2.1	2.1	0.6	1.2	10.0	5.4	8.6	5.8
6.68-4.7	5.69	11.9	9.0	5.6	17.1	18.7	8.5	4.6	13.6	20.8	18.7	10.7	15.2
4.7-3.36	4.03	20.4	11.3	7.6	15.5	18.5	9.9	16.8	20.9	18.9	18.2	11.7	8.0
3.36-2.36	2.86	28.1	18.0	18.8	22.2	24.5	15.4	34.5	30.8	25.6	23.6	13.3	14.6
2.36-1.41	1.89	34.6	33.5	51.1	28.2	31.4	40.3	39.9	30.9	21.7	30.1	18.9	21.4
1.41-0.71	1.06	2.4	22.7	16.7	9.0	4.5	23.5	2.6	1.75	2.3	3.4	13.3	12.7
0.71-0.42	0.57	0.2	3.1	0.0	0.2	0.2	0.1	0.4	0.7	0.7	0.1	13.0	9.8
0.42-0.125	0.27	0.2	0.1	0.0	0.1	0.0	0.0	0.4	0.3	0.0	0.0	9.8	6.9

D_i is the arithmetic mean diameter for the ith grain size range; f_i is the fraction of the subpavement - is the ith grain size.

Table A2:2

Experiment	q_B (cm^2/sec)	$Sx10^2$	d' (cm)	D_i = 7.84 mm		D_i = 5.69 mm		D_i = 4.03 mm		D_i = 2.86 mm		D_i = 1.89 mm		D_i = 1.06 mm	
				W_i^*	τ_i^*	W_i^*	τ_i^*	W_i^*	τ_i^*	W_i^*	τ_i^*	W_i^*	τ_i^*	W_i^*	τ_i^*
S1:E2	.01441	0.4	6.2	.05863	.01917	.12102	.02642	.39419	.0373	.29752	.05255	.24993	.07953	.029213	.1418
S1:E3	.0118	0.44	6.17	.047858	.02099	.065742	.02892	.156831	.04083	.136887	.05753	.17381	.08705	.19758	.15522
S1:E6	.01489	0.41	6.54			.05298	.02856	.13661	.04032	.18517	.05682	.34337	.08598	.18909	.15331
S3:E3	.02254	0.41	7.81	.21497	.02475	.18217	.03411	.31374	.04816	.24622	.06786	.21338	.10268	.11475	.18308
S3:E4	.02752	0.45	7.82	.06319	.0272	.21472	.03748	.40361	.05292	.29288	.07457	.25609	.11284	.061842	.2012
S3:E5	.02096	0.43	8.13	.04883	.02702	.07541	.03724	.16688	.05257	.14224	.07408	.25395	.1121	.24953	.19988
S4:E2	.00629	0.28	9.4	.00564	.02035	.016512	.02803	.11458	.03958	.12893	.05577	.10173	.0844	.01117	.15049
S4:E5	.00655	0.26	9.36	.012991	.018813	.056182	.02592	.164043	.0366	.132465	.05157	.090667	.07804	.00865	.13914
S5:E3	.03931	0.24	9.7	.60584	.018	.48084	.0248	.83015	.03501	.61613	.04933	.35631	.07465	.063637	.1331
S6:E1	.02883	0.27	10.7	.18405	.02194	.2432	.03023	.44972	.04268	.31954	.06014	.27805	.09101	.05292	.16227

$q_B = Q_B/24$, where 24 cm is considered to be part of the channel width over which bedload motion takes place; d' is the effective depth calculated from the Vanoni and Brooks method; the effective depth is used for the W_i^* and τ_i^* calculations. For the experiments S1:E2, S1:E3 and S1:E6 the f_i values used to calculate W_i^* are taken from the 13th column of Table A2:1; for the rest of the experiments, the f_i values used to calculate W_i^* are taken from the 14th (last) column of Table A2:1.